

The Design of an Improved Hybrid III Six-Year Old Neck

Team SQUAD: Jacob Ruprecht, Drew Freyberger, Michael Sutton, and
Andrew Method

BME 432L: Biomechanics and Vehicle Safety Engineering
Instructor: Roger Nightingale
TA: Maria Ortiz
December 4, 2015



Abstract

The purpose of this project, “The Design of an Improved Hybrid III Six-Year Old Neck,” was to formulate performance specifications of an average six-year old neck, to create a more biofidelic neck, and to evaluate the validity of the model. Auto manufacturers are required by law to adhere to certain standards that “aim to reduce the number of children killed or injured in motor vehicle accidents” (FMVSS 213). Moreover, included in the Hybrid III family is a 50th percentile, 21 kg six-year old (Figure 1, far left). Specifically, pediatric head injury in car crashes is the top cause of death and disability for children under eighteen years old [1]. Additionally, car crashes are responsible for 30% of all childhood injuries, 500,000 trips to hospitals annually, and cost \$10 billion dollars per year [1]. Thus, there is a critical need for an anthropomorphic, biofidelic six-year old dummy neck that can consistently model accurate responses to automotive crash tests. If the neck model is not realistic, auto manufacturers will design safety features that are not ideal. To improve upon the current Hybrid III six-year old neck model, the body of the neck was redesigned as seven chloroprene rubber 25% carbon (visco) rods that could be fine tuned to meet the set performance corridors. Additionally, a slider attached to an acrylate-butadiene rubber (ABR) spring was added at the base of the neck in order to tune the neck lag characteristic of an average six-year old. The final neck model, named “Spaghetti Neck V36,” was subjected to a variety of finite element analysis tests, and a statistical analysis was used to objectively rank the results. The statistical analysis evaluating how well the results fit the performance specifications returned an overall score of 53/100 for the final model. This was one of the highest scores obtained during the design process, but it leaves room for continued design improvements.



Figure 1: The Hybrid III crash test dummy family [1].

Table of Contents

1. Introduction.....	3
a. Customer and Clinical Need.....	3
b. Standards and Regulations.....	3
c. Design Constraints.....	4
d. Performance Specifications.....	5
2. Methods.....	11
a. Initial Designs.....	11
b. Design Iterations.....	12
c. Criteria for Design Acceptance.....	31
3. Results and Discussion.....	36
a. Final Design.....	36
b. Convergence Study.....	42
c. Final Testing Methods.....	44
d. Final Testing Results.....	46
e. Stress Failure.....	54
f. Ethical Concerns.....	55
4. Conclusion.....	55
a. Limitations.....	55
b. Next Steps and Final Remarks.....	55
5. References.....	57
6. Appendix.....	59
a. Engineering Drawings.....	59
b. Convergence Study Plots.....	71
c. FitMetric MATLAB Code.....	75
d. Final FitMetric Results.....	84
e. Cfiles.....	86

Introduction

a. Customer and Clinical Need

Even before the first documented fatality of Mary Ward in 1869 when she was ejected and run over by a steam-powered car, there has been a need to regulate and ensure the safety of passengers in motor vehicles [1]. In 1940, the first motor vehicle safety regulation in the US required two headlights on all vehicles [1], and in 1979, the National Highway Traffic Safety Administration (NHTSA) began crash testing in accordance with Federal Motor Vehicle Safety Standard 208 (FMVSS 208). This standard originally specified the type of occupant restraints (i.e., seat belts) required; it was later amended to specify performance requirements for anthropomorphic test dummies. Furthermore, FMVSS 213 specifies the standards “to reduce the number of children killed or injured in motor vehicle crashes by restricting the maximal forces allowed on anthropomorphic child crash dummies.”



Figure 2: Frontal crash test required by FMVSS 208 [1].



Figure 3: Hybrid III six year-old neck [1].

These current standards are based off of the Hybrid III six-year old child dummy neck molded out of butyl rubber (Figure 3). There are accurate features of it, such as its flexion and extension responses; however, the model as a whole is too stiff, leading to false head lag results as well as inaccurate tension and compression results. This has led to the misrepresentation of an average six-year old's head and neck performances during crash tests. Needless to say, this is problematic because manufacturers may, in fact, make a safe vehicle for the Hybrid III six-year old crash test dummy but an unsafe vehicle for an average six-year old. Thus, both the NHTSA and automobile manufacturers can benefit from an improved, biofidelic six-year old neck model. The NHTSA would be able to make more realistic and more appropriate regulations, and the automobile manufacturers would be able to design safer vehicles.

b. Standards and Regulations

The applicable standards and regulations for the neck model are governed by the NHTSA through the Code of Federal Regulations (CFR). As stated previously, the two applicable standards for this device would be FMVSS 208 and FMVSS 213. The former “specifies performance requirements for the protection of vehicle occupants in crashes” [16]. Its purpose is to reduce the number of deaths of vehicle occupants, and the severity of injuries, by specifying

vehicle crashworthiness requirements in terms of forces and accelerations measured on anthropomorphic dummies in test crashes. Thus, again, it is critical that the model responds as accurately as possible in order to be certain of the exact forces experienced in crash tests. FMV 213 is the second applicable standard, and it “specifies requirements for child restraint systems used in motor vehicles” [17]. Its purpose is to reduce the number of children killed or injured in motor vehicle crashes. It explains the procedures for testing the Hybrid III six-year old and thus, it is relevant for the performance of Spaghetti Neck V36.

Also found in a subsection of CFR Part 572, the NHTSA has described the regulations for anthropomorphic test devices. Subpart I, Section 572.73 describes the “neck assembly and test procedure” for a six-year old child. This includes the timing and positioning of the neck in response to a pendulum dropped onto the head from a constant height (Figure 4).

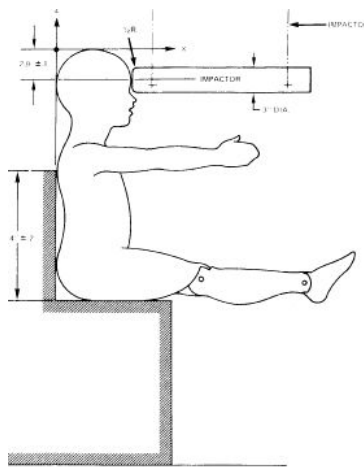


Figure 4: Depiction of neck testing procedure for six year-old [17].

c. Design Constraints

In order to meet the project goals of developing an improved neck for the Hybrid III six-year old crash test dummy, it was important to consider the testing environment throughout the design process. The final neck design will be tested by attaching it to the current H-III six-year old head and torso, meaning that its dimensions and attachments must match those currently used by this dummy. The design must span the distance from the lower neck bracket at the base of the neck to the base of the head, a total distance of 109 mm [2]. The other dimensions of the neck apart from length were not constrained. The current H-III neck has a weight of 1.7 kg [2]; however, it was decided that weight was not significant enough in performance or attachment to consider it a design constraint. When testing the final design, it is important to ensure that it is fully constrained in the same manner as the previous neck such that no uncertainty is introduced from the attachments loosening or moving. In order to achieve this, the dimensions and screw holes on the top and bottom portions of the design are constrained to match those of

the head base and nodding joint of the current H-III six-year old dummy. Engineering drawings of these two pieces showing their proportions, locations, and threadings of the screw holes can be found in Appendix A.

d. Performance Specifications

Once the design constraints were established, Team SQUAD defined performance specification corridors to evaluate the responses of the new neck model. These specifications can be broken into two groups: one based on kinetics, such as tension and compression, and the other based on kinematics, such as head/neck position and angle over the time for a frontal impact. The final performance specifications that were used to evaluate the biofidelity of the design are (in order of importance): head center of gravity (CG) x-displacement timing, head CG z-displacement timing, stiffness in tension, stiffness in compression, head CG x-displacement versus z-displacement (referred to as head CG), and head angle vs. neck angle (referred to as head lag) [2]. The timing corridors are the most significant because if the dummy does not accurately predict the location of the head over time, it will be impossible to reasonably assess the effectiveness of vehicle safety systems and how they interact with the dummy. For each of these criteria, a corridor of acceptable values were created and used to evaluate how well the model response matches the behavior of an actual six-year old neck. Additionally, injury assessment reference values (IARVs) were assigned for tension and compression, as these are the two primary modes for catastrophic injury [2]. These values are meant to serve as benchmarks for when injury will occur during these modes of loading the neck. It is important to note that the required testing data to develop these corridors for a pediatric neck is not currently available. This is largely because of the ethical concerns of using children in high-velocity frontal impact testing, as well as a lack of available cadaveric subjects. Additionally, it is difficult to assess the tensile and compressive properties of human tissue through cadaver studies because of the large scale physiological changes that occur after death, especially in skeletal muscle tissue.

Each group was asked to propose their own unique stiffness corridors and IARVs for tension and compression, as well as pathway corridors for head lag and head CG. The class then voted on which of the proposed corridors and IARVs everyone would aim to fit for their models. The idea was to do thorough research and statistical analysis in order to come up with these values and make them representative of what should be expected for the mechanical response of a six-year old neck. When creating the compression specification, Team SQUAD analyzed data from three research papers looking at correlations between peak force and injury force [3], and then peak force and age [4], to come to an analytically-sound IARV for that specification. For the stiffness corridor, Team SQUAD applied a logarithmic regression to stiffness versus age data for certain segments of the cervical spine [4,5]. Then, the team estimated the stiffness of the unknown segments using a weighted average from data already given, treating the cervical spine segments as springs in series. In order to account for errors inherent to the calculation methods, the group developed upper and lower bounds representing one standard deviation above and below this average.

When determining the tensile stiffness, a similar process was used. First, the relative contributions of bone and muscle to the overall adult neck stiffness were determined [7]. Then, it was found that bone and skeletal muscle max tensile strength scale differently from adults to children, so a unique scaling factor was developed for each component of the neck [9, 8]. These scaling factors were applied to the adult tensile injury thresholds for bone and muscle to develop an IARV for the six-year old neck in tension [7]. To calculate the tensile stiffness corridor, the tensile stiffness for each of the neck vertebrae were found for a six-year old [4]. The individual stiffnesses were added together as if the vertebrae were springs in series to calculate an overall stiffness of bone in the neck. Finally, this partial stiffness was used to calculate the overall tensile stiffness of the neck based on the relative contribution of bone and skeletal muscle [7]. The width of the corridor was established by researching the standard deviation observed in a whole, unconstrained neck [14].

When creating the head lag corridor, Team SQUAD made sure to capture the phenomenon of head lag (significant forward excursion of the head prior to any rotation) observed during full frontal impact testing [11]. Initially, the scaling was attempted through the low-velocity frontal impact data [12]. However, this data proved to be a poor representation of the impact behavior at high velocities. Because of this, the scaling was performed by utilizing head-to-neck girth ratio (HNGR), which has been shown to be a categorical predictor of age-dependent differences in neck kinematics [13]. For the initial portion, only the neck angle was scaled. Then, after head lag had ceased, both head and neck angle were scaled by the average HNGR ratio over the remainder of the corridor [12,13] .

The first step team SQUAD took in creating the head CG corridor was scaling down the entire corridor linearly to reflect the shorter neck of a six-year old [8]. Then, scaling factors in the x- and z-directions were developed based on the ratio of the average excursion of the head during low-velocity impact for adults versus children [12]. These scale factors were applied to the entire range of data simultaneously in a variety of ways, yet none of them yielded reasonable corridors. Thus, an inflection point was found to represent the endpoint of head lag in adult subjects and scaled by the neck length factor. Then, the x-direction scale factor was applied exclusively prior to the inflection point, and the z-direction scale factor was applied exclusively after the inflection point. This method better reflected the actual behavior of the head and neck in frontal impact and yielded Team SQUAD's final head CG corridor.

Some groups chose not to use this level of analytical and pathophysiological deduction to reach their conclusions. This was evident by specifications that were, for example, calculated based only on data from one resource or not accounting for the activation of muscle when applying a tensile force. The class as a whole almost unanimously decided to use the tensile stiffness, head lag, and timing corridors determined from a previous work published by Dr. Alan T. Dibb [6]. Given his extensive knowledge and computational resources used at the time, he arguably had the most accurate results for estimating these mechanical features for the six-year old neck response. One might assume that the same logic would be applied to how the remaining two corridors were chosen, but one would be incorrect in such thinking. Each group gave a

presentation on what their proposed corridors were and how they were reached. While some groups voted based on the methodology behind these decisions, the majority of groups voted based on more unorthodox means, giving such reasoning and justification as “We just picked the value that was in the middle of everyone’s values,” or, “It seemed like the easiest corridor to fit.” Not only can such nonchalance and insensitivity be quite disheartening for those who put a great deal of effort into their proposals, but also, more importantly, the conclusions voted upon are not necessarily representative of what is to be expected in terms of biofidelity. This both complicates the design process significantly and defeats the entire point of the design challenge, which is to create the most biofidelic dummy neck possible.

Ultimately, the class voted on a tensile stiffness of 85 ± 15 N/mm and a compressive stiffness of 155.4 ± 41.5 N/mm [6]. The class decided to use the tensile and compressive IARVs that the NHTSA recommends for a six-year old, which were 1,490 N and 1,820 N, respectively. The corridors for head timing, head CG, and head lag are more graphical, and can be seen below, along with the graphical representations of the compressive and tensile stiffness corridors [6]. One performance specification that became useful for evaluating the accuracy of the iterations was being able to use the IARVs to constrain the stiffness corridors. To be more specific, each corridor was originally extended to an arbitrary length of 20 mm. However, some of the groups’ iterations stayed within the corridors up to a certain displacement, then moved outside of them near the final value of 20 mm. Because Team SQUAD had little use for data being collected after injury, the group could ignore data after a certain length in the corridors. Specifically, a tensile force of 1,490 N applied to a neck with an average tensile stiffness of 85 N/mm corresponded to about 17.5 mm of elongation. Additionally, a compressive force of 1,820 N applied to a neck with an average compressive stiffness of 155.4 N/mm corresponded to about 11.7 mm of compression. Thus, these were the target values of focus for determining how well the iterations fit into the corridors.

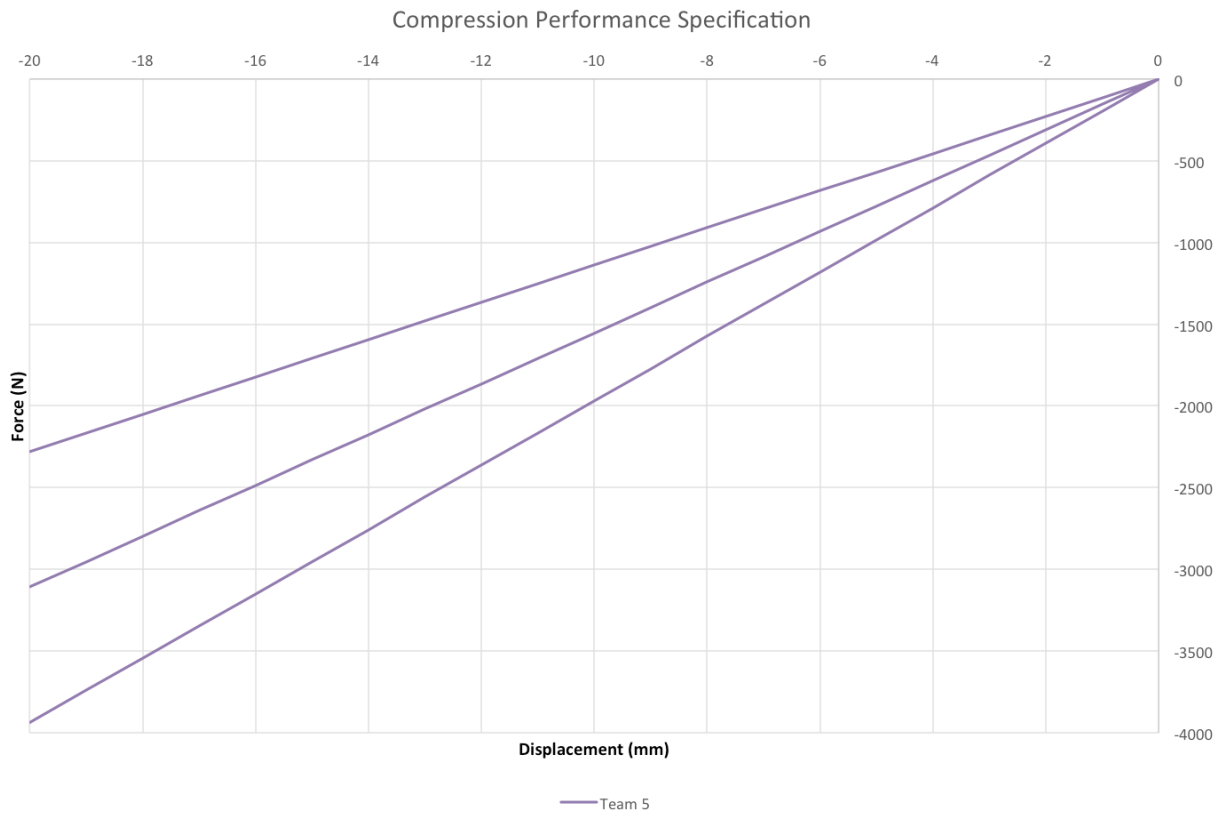


Figure 5: Compressive stiffness corridors created by Team 5.

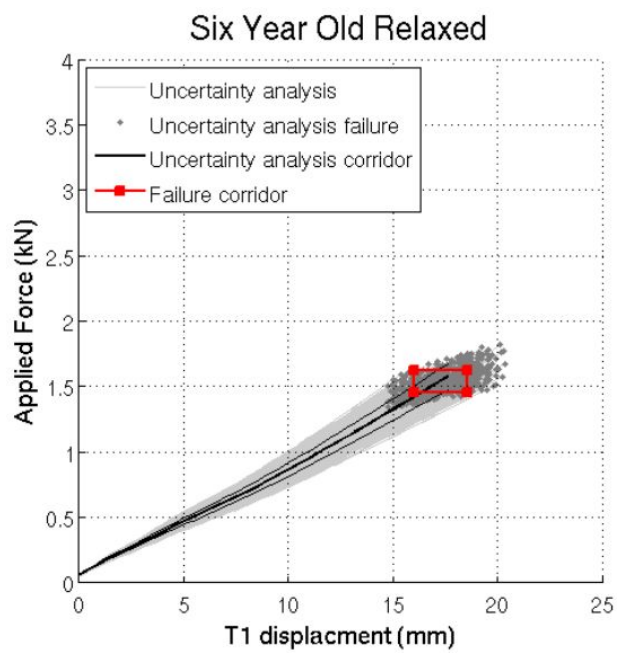


Figure 6: Tensile stiffness corridors created by Dibb [6].

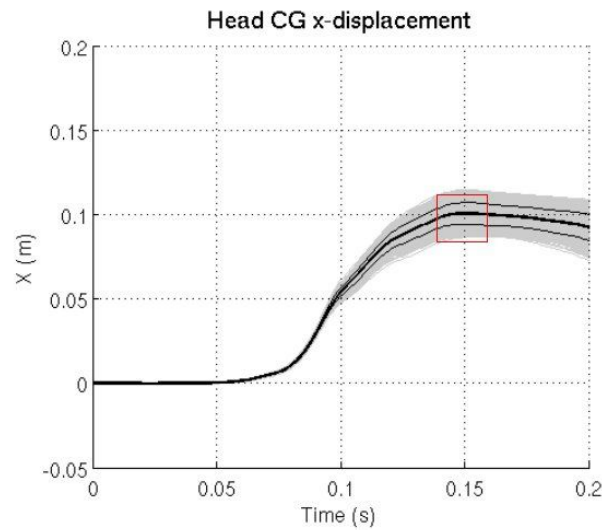


Figure 7: Timing corridor for head CG x-displacement [6].

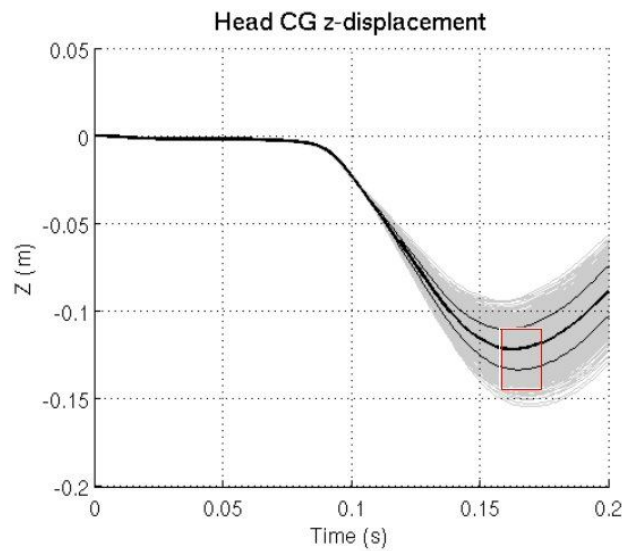
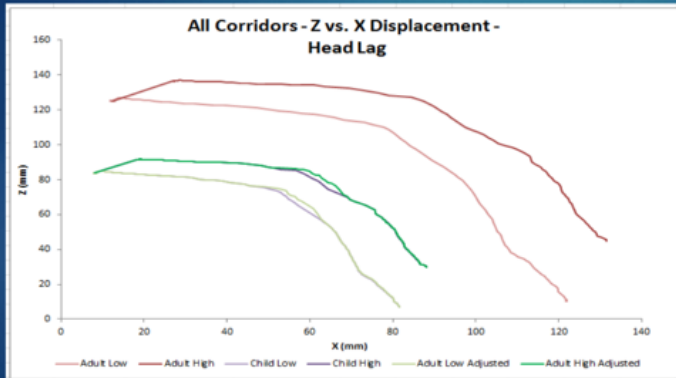


Figure 8: Timing corridor for head CG z-displacement [6].

Final Results – Head Location



Results

- Scale factor function applied along 40-60 mm range for lower corridor, 45-65 mm range for higher corridor
- Shows slight adjustment to account for more drastic head lag in 6 year-old

Recommendation

- Effective model of change in elongation/compression for neck would require more precise data/experimentation
- Due to minimal differences in corridors, we would recommend the **Length-Adjusted Corridor** (purple on graph)

Figure 9: Head CG corridors created by PLUM.

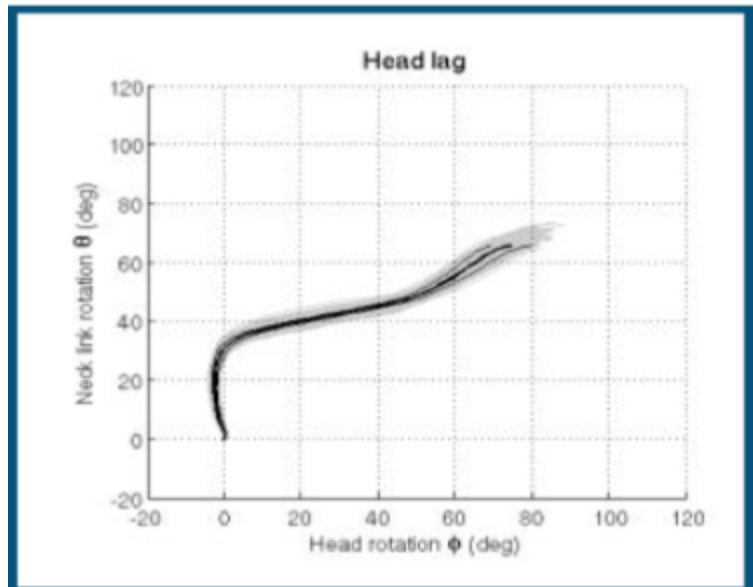


Figure 10: Head lag corridors created by Dibb [6].

Methods

a. Initial Designs

Team SQUAD knew that the success of the design would be judged based on how well the responses fit the four distinct corridors. In order to break everything up systematically, the team brainstormed a number of ideas, some of which focused solely on one performance specification, with the hopes that we could combine the characteristics of each into a single design (Figure 11).

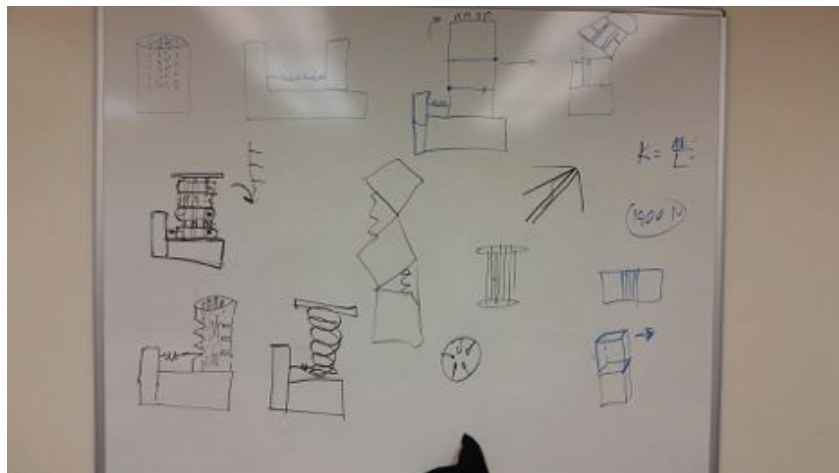


Figure 11: Design drawings from an initial group brainstorming session.

For compression, one group member had the idea of using a number of thin rods as the center of the neck design. Since the stiffness of an axial load can be approximated as $K=AE/L$, this performance specification would, in theory, be easy to tune by changing the cross-sectional area of contact as needed. For tension, another member thought about using rubber bands or some stretchy material to simulate the activation of muscle in tensile loading. The head lag and CG responses could have been matched using some sort of sliding track (to show the head's initial forward motion in the x-direction) in conjunction with a series of internal springs that would allow full downward motion (z-direction). The compromise reached was a general framework that integrated each of these parts. Rather than springs, whose use caused many concerns (primarily with circumventing the issue of oscillation and the need for dampening), the group decided that some type of rubber should be used instead. The design, moving forward, would have a central rod in the middle with rods on the outside, all made of rubber. In order to better tune the specifications as needed, it was ideal to isolate components of the design that were specific to certain specifications. This was done by removing any contact between the central rod and the top plate so that only the outer rods would be activated in tension. Thus, Team SQUAD could run different calculations and iterations that adjusted the diameter and material of the outer rods until the tensile response was an accurate fit for the corridor. Then, by only altering the central rod, the compressive stiffness could be tuned. Once this specification was met, the group could move on to the head lag and CG corridors, which could largely be dictated

by the characteristics of the slider. It was primarily this step-by-step sequence that guided Team SQUAD'S iteration process.

b. Design Iterations (Model Properties, LS-PrePost Modifications, Testing Results)

Assembly Attempt 1: Three Outer Rods

Team SQUAD originally thought butyl rubber would be an appropriate material to use for the rods. Running material comparison simulations in DYNA indicated that the estimated tensile and compressive stiffnesses for butyl rubber were 1 MPa and 1.6 MPa, respectively. The group plugged in the length of the neck (69 mm) to calculate what the total contact surface area needed to be (given the governing equation $K = (AE)/L$). But, the diameter of the rods required to reach the stiffness values far exceeded what could be structurally implemented given the size of the chest cavity of the dummy. Specifically, giving each rod a radius of 32 mm would have pushed them far over the bottom plate of diameter 60 mm. Please reference the calculations in Figure 12.

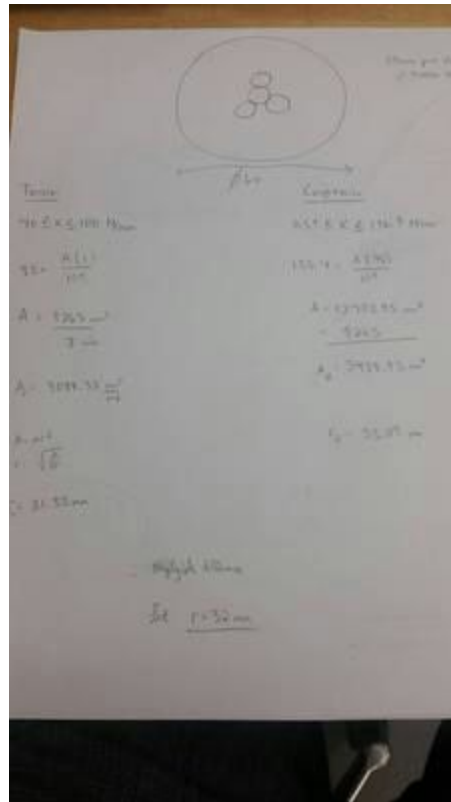


Figure 12: Initial stiffness calculations to determine arbitrary radii of rods.

Team SQUAD then decided to temporarily delay the prospect of knowing the exact material that would hit the stiffness corridors, but rather correct the model's material properties to fit those corridors later. The group defined each rod to have an arbitrary diameter of 15 mm (one central and three outer) with the top and bottom plates having diameters of 60 mm (Figure 13). Given

the length and stiffness values the group was trying to hit, Team SQUAD explored new material options with more ideal Young's Moduli. In particular, chloroprene rubber ended up being the team's rubber of choice.

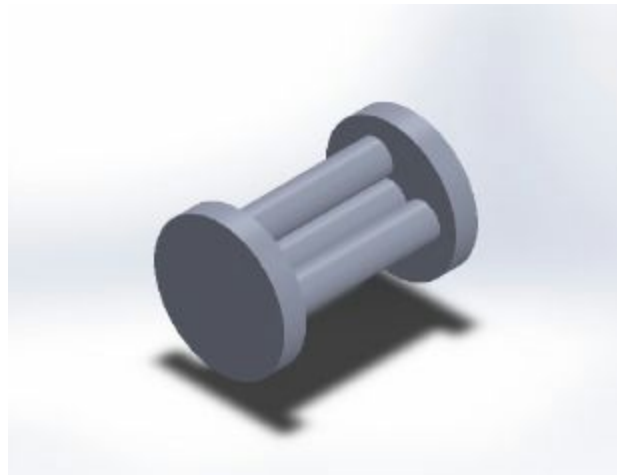


Figure 13: Image of first model design: central rod with three outer rods, all diameter of 15 mm.

The original design included an outer shell surrounding the internal rods with a truss system so that the structure would not buckle. However, because the rods covered such a large percentage of the plate's surface area, the group decided that such precautions might not be necessary. Team SQUAD opted to exclude them from early designs with the possibility of adding them later if needed.

As this was the first model that was successfully tested in LS-DYNA, it required a significant amount of alteration of the command files provided by Dr. Nightingale for automation of the meshing process. The first step was ensuring that the element size for the surface mesh was acceptable. An element size of 6 mm was used to allow for fast computation at this preliminary stage of the design process.

Next, it was ensured that these files accounted for the correct number of parts (6) and that all parts were labeled correctly. These files use a naming scheme where each part is numbered in the millions (1000000, 2000000, 3000000, ect.), with the associated nodes and elements numbered starting at the same millions value as the part. This allowed the user to easily associate a node or element with the part it to which it belonged. For example, any node or element numbered in the four millions was associated with part four. The exceptions to this were the top and bottom plates. Their nodes and elements were labeled as described above, but the part numbers were changed to 99 and 98, respectively. This is because the MATLAB script used to test the neck model attaches the design to the test apparatus using those part IDs for the top and bottom plates.

The next step in preparing this model for simulation was defining section properties, specifically the material's deformability. This was accomplished by altering the elform value in the Sections

portion of the keyword file, with a value of '1' indicating a rigid body and a value of '10' representing a deformable body. After the sections were defined, the relevant material properties had to be loaded from the materials database provided by Dr. Nightingale. For this model, the only two materials necessary were aluminum for the rigid bodies and chloroprene rubber for the deformable parts. After these materials were called, they were assigned to the appropriate parts, and the kfile was fully defined.

In order to prepare this model for simulation, the rods had to be constrained to the plates so it could be loaded. This was accomplished by defining two node sets, one containing the nodes on top of the three outer rods, and the other containing the nodes on the bottom of all four rods. Then, the `Extra_Nodes_Set` portion of the keyword file was modified so that the tops of the outer rods were connected to the top plate, and the bottoms of all the rods were connected to the bottom plate.

Once the model was fully constrained, the contacts had to be defined. For this design, these contacts were the center rod to the top plate and the center rod to the outer three rods. All four contacts were necessary at this stage, because the rods experienced a high degree of area expansion in compression. These contacts were defined as `Automatic_Surface_to_Surface` in the `Contacts` portion of the keyword file. For each case, the contact was defined between the corresponding two parts, and the coefficients of friction were imported from the material properties. At this point, the model was fully meshed, sectioned, defined, constrained, and ready for testing.

The first set of results for the four primary performance specification corridors can be found in Figures 14-17.

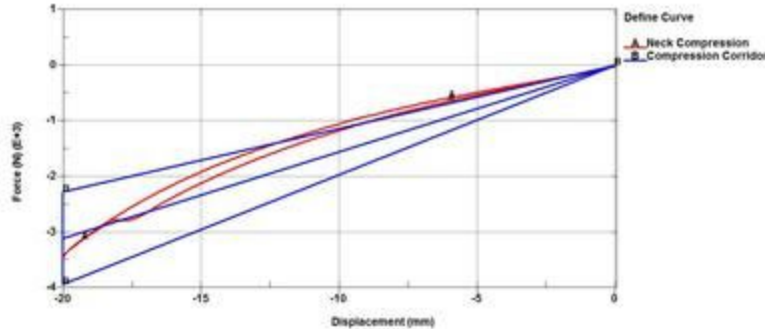


Figure 14: Compressive stiffness response for attempt 1.

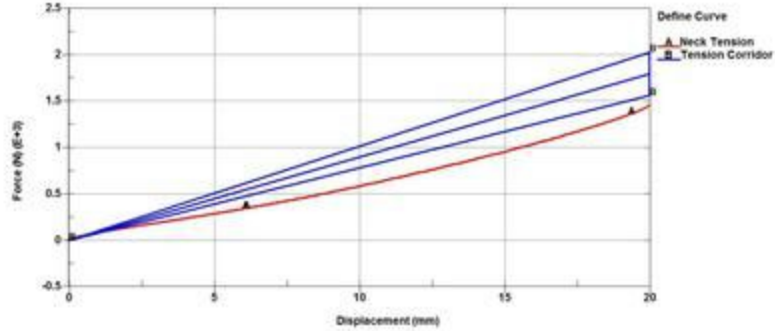


Figure 15: Tensile stiffness response for attempt 1.

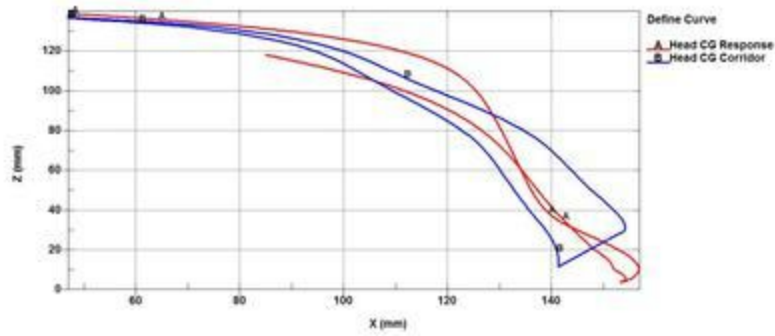


Figure 16: Head CG response for attempt 1.

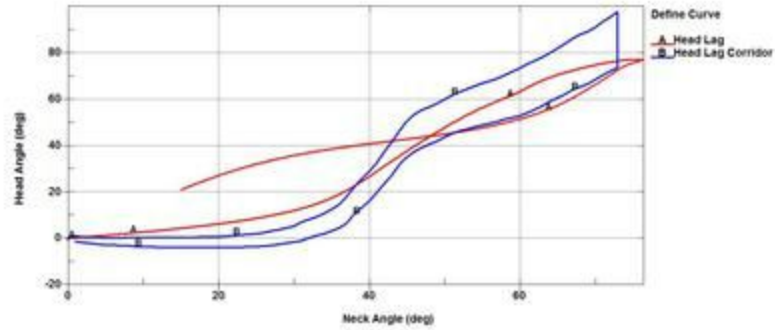


Figure 17: Head Lag response for attempt 1.

The initial results appeared quite good for a first try. The obvious specification to correct was tension. So, the group tried changing the radii of the rods to a number of different values in order to compensate. For future planning, the group had already created a slider base in SolidWorks but struggled with a way to constrain the distance the slider would move. The purpose of the slider was to hit the CG and lag corridors. Given the initial success hitting these corridors, the group noted that the slider may not have actually been needed.

Assembly Attempt 2: Three Outer Rods + Slider

As part of the design process, the group wanted to see what effect the slider might have on the model response. Specifically, prior to implementing the slider, any change to the rods would have resulted in a change to all of the responses. Keeping all other dimensions the same, the slider and dovetail set were added to the bottom of the neck (Figure 18).

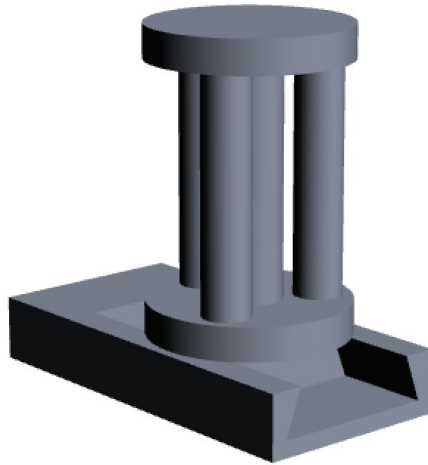


Figure 18: Image of neck model design attempt 2; outer rods have reduced diameter and slider added.

As an additional part of iteration for this design, the group also took this model as an opportunity to test the influence of varying the orientation of the three rods. Again, the radii of the four rods were altered to fit as much of the tensile and compressive responses within the corridors as possible.

When the slider was incorporated into the design, it added two new parts, bringing the total number to eight parts. This required the numbering system to be expanded to extend up to 8 million, and the other cfiles had to be modified to incorporate the two new parts (slider base and slider nub). The part numbering had to be modified so that the slider base was part 98, as it would attach to the base of the neck during simulation. The initial bottom plate was switched back to the traditional numbering scheme. Additionally, their section and material properties had to be defined so that both new parts were rigid bodies constructed of aluminum.

The constraints and contacts among the rods and plates could be defined as done previously; however, the slider must now be defined, and the bottom plate must be attached to the slider nub. The bottom plate was attached to the slider nub by adding a Rigid_Bodies constraint between the two parts. Initially the slider was defined by creating an Automatic_Surface_To_Surface contact between the slider nub and slider base, with frictional coefficients set to zero to simulate a free sliding joint. However, this did not accomplish the desired goal, as LS-DYNA has trouble working with contact between rigid bodies. The result

was a slider that did not engage at all, acting as if the nub was constrained to its starting point. The solution to this problem was provided by Dr. Nightingale in the form of the “jointsV2” Excel file, which allows the user to define a frictionless joint with a freedom of movement in only one direction. The user inputs the location of one node on the moving piece (the slider nub in this case), a vector describing the direction of translation, a vector orthogonal to the direction of translation, the part IDs of the two rigid bodies involved, and the Joint ID. The result is a piece of code that can be copied and pasted into the end of the completed kfile to define the translational joint. Once this code was added, the model was fully defined and ready for testing.

The computer simulations returned invalid results due to the slider nub ejecting from the slider base.

Assembly Attempt 3: Three Outer Rods + Slider + Spring

Although the group found a way to constrain the movement of the dovetail, it was still difficult to manually tweak as needed. Thus, the group added a rubber spring that would attach the dovetail to the back of the slider base. The characteristics of this spring (material properties, length, diameter) could all be modified to alter the head lag and CG responses as needed. All other design dimensions from the previous model were held constant (Figure 19).

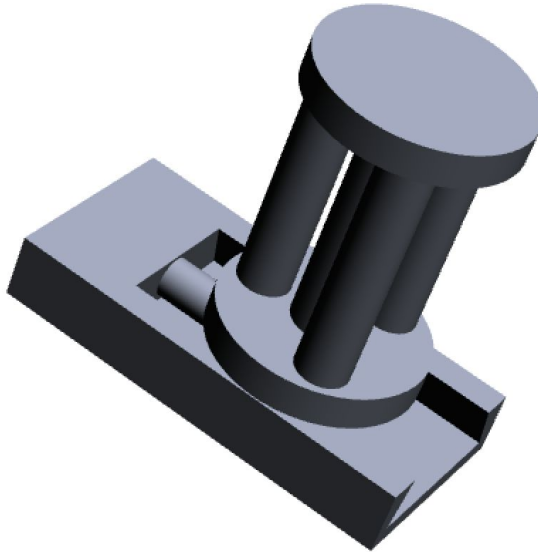


Figure 19: Image of neck model design attempt 3; added rubber spring to slider base.

The addition of a rubber spring connecting the slider base and the slider nub brought the total number of parts up to nine. As done previously, this required expanding the numbering system up to 9 million and modifying the other cfiles to account for nine parts. Additionally, the new part was a deformable rod made of chloroprene, so its section and material properties had to be

adjusted accordingly. This new spring had to be constrained to both the base of the slider and the slider nub to prevent the slider nub from flying out of the dovetail joint upon impact. Two new node sets were defined: one for the nodes on the front of the spring and one for the nodes on the back of the spring. The front node set was constrained to the slider nub, and the back node set was constrained to the slider base, both through modifying the `Extra_Nodes_Set` portion of the keyword. After these extra constraints were added, the model was ready for simulation.

In this stage of testing, multiple material types (chloroprene, butyl, and ABR rubbers) were tested for the spring. Each time a new material was tested it had to be loaded from the provided material database. Then the material category and properties had to be pulled up in LS Prepost and entered in the cfile with the correct spacing prior to running it, so that it was assigned a material ID. This was designed to ensure that the physical properties associated with the material ID were correct. This new material ID could be matched with the appropriate part. Additionally springs of different diameters were tested. Changing the diameter did not affect the meshing process except when the diameter was reduced below the element size. This resulted in LS-PrePost being unable to properly create a surface and, therefore, a tetrahedral mesh of the spring. This issue was resolved by modifying the element size of the rubber spring so that it is less than the diameter of the rubber spring.

The results from the model with the three outer rods plus the slider can be found in Figures 20-23.

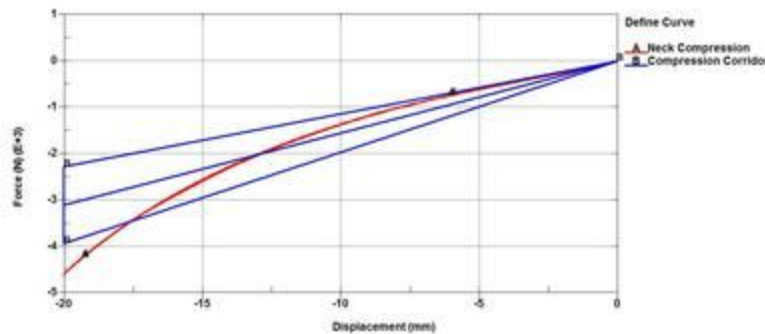


Figure 20: Compressive stiffness response for attempt 3.

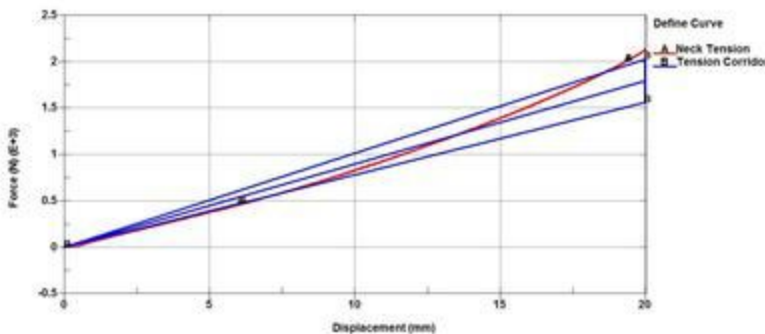


Figure 21: Tensile stiffness response for attempt 3.

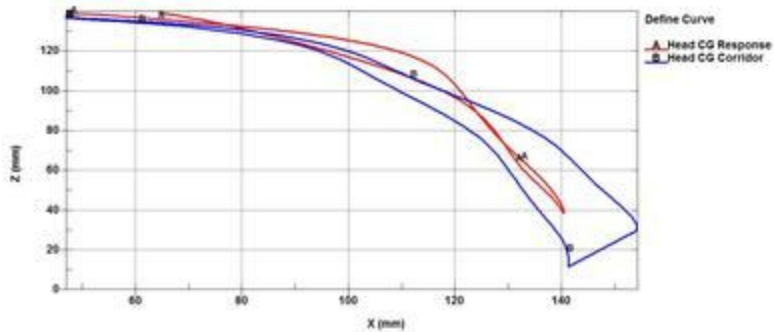


Figure 22: Head CG response for attempt 3.

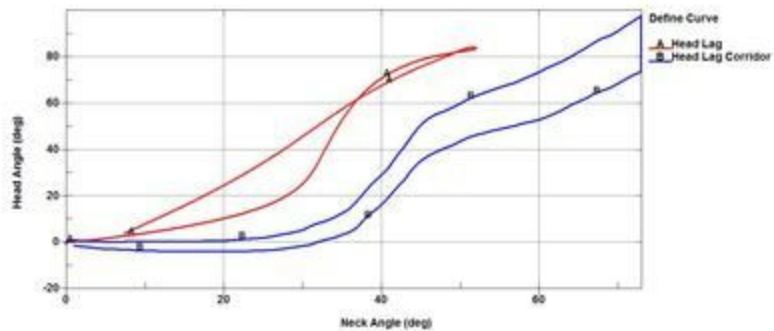


Figure 23: Head Lag response for attempt 3.

The end of the compressive trial indicated that the model behaved too stiffly, while tension hit the mark well. While the head CG stayed well within the corridors, the head lag response did not reach its mark for neck or head angle, indicating that more remodeling needed to be done.

Assembly Attempt 4: Six Outer Rods + Slider + Spring

After viewing relevant D3 plots and comparing common characteristics among the corridors through a number of trials, it seemed as though the outer rods and center rods were contacting when activated in compression. In addition, the models continuously obtained nonlinear responses, which was initially thought to be due to a lack of symmetry. In an effort to address this concern, the group went from three outer rods to six (keeping the same total surface area) and moving the rods slightly further away from the center (Figure 24).

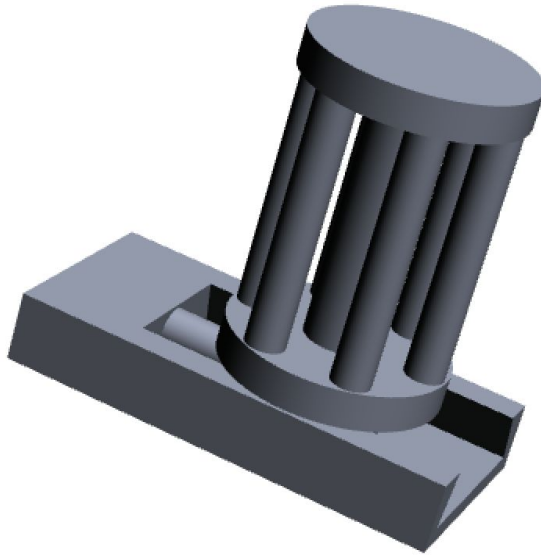


Figure 24: Image of neck model design attempt 4; converted outer three rods into six rods (maintaining cross sectional area of contact).

Changing from three rods to six rods brought the total number of parts to 12, which meant that large changes were needed in the numbering system. This was because, while the tetrahedral meshes were being created, each part was temporarily numbered in the hundred-thousands place (part 1 - 100000, part 2 - 200000, part 3 - 300000, etc.). So, when it was time to name the tetrahedral mesh for part 10, it was named part 1000000. Therefore, when the Sections and Materials cfile attempted to name part 1 as part 1000000, LS-PrePost determined that this part already existed and subsequently crashed. This was fixed by temporarily numbering the tetrahedral mesh for the parts numbered 10 or higher in the ten-thousands place (part 10 - 20000, part 11 - 30000, part 3 - 40000, etc.). Thus, there is no overlap between part names during the meshing process. Then, when it was time to rename the parts, nodes, and elements, the original naming scheme was used, with each part and its associated nodes and elements labeled in the millions. Once the numbering issue was resolved, there was still a consistent problem of LS-PrePost crashing when the Sections and Materials cfile was run. This was remedied by splitting it into two separate cfiles: one that renames the parts and defines their section properties and one that loads the material database and defines their material properties. The new rods had their section and material properties defined to match those of the original three deformable rods made of chloroprene rubber. After this step, the contacts and constraints were defined. This was done as in Assembly Attempt 4, except the node sets of the rod tops and bottoms now included all six of the outer rods. Additionally, three new Automatic_Surface_To_Surface Contacts were added to account for each of the three new rods contacting the center rod.

Although the exact responses were not all quite as good as some previous models, the group took solace in knowing that modifying each specification response in isolation could be easily completed with this newer model.

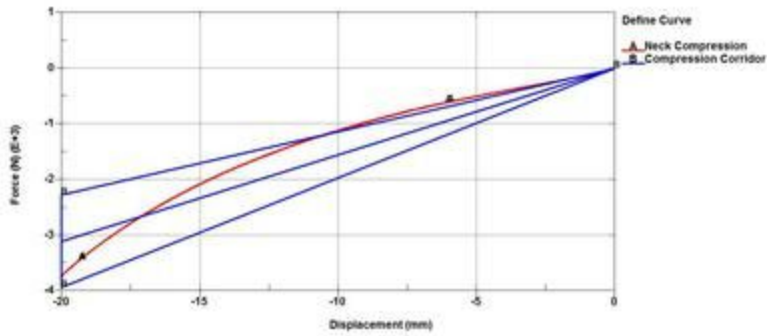


Figure 25: Compressive stiffness response for attempt 4.

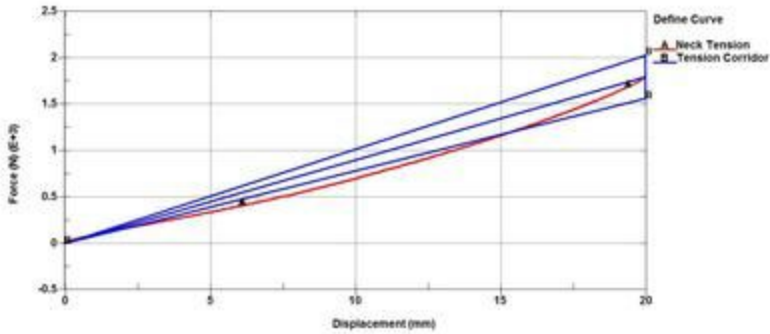


Figure 26: Tensile stiffness response for attempt 4.

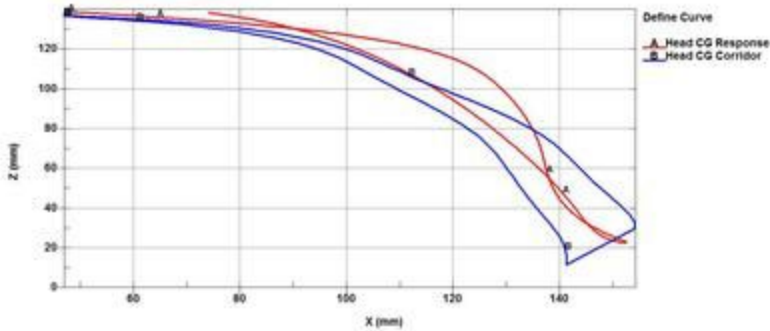


Figure 27: Head CG response for attempt 4.

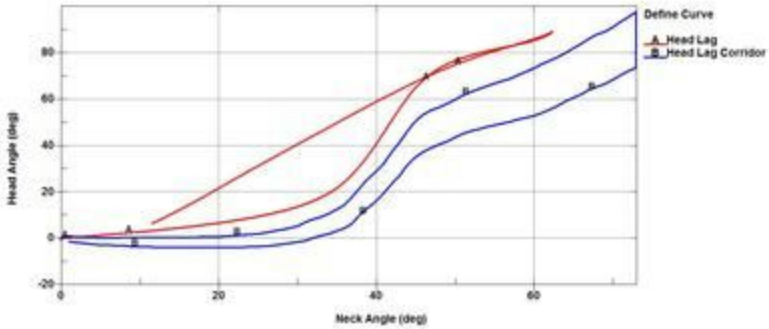


Figure 28: Head Lag response for attempt 4.

Measurement alterations were initially made to increase the tensile stiffness since it was still below the corridor. This required the area of the outer six rods to increase. However, the compressive stiffness corridor was fine, so the surface area of the central rod had to be subsequently decreased in order to compensate. Without this step, the model would have been too stiff in compression. With this model, the group also tried altering the dimensions of the rubber spring. While the CG response looked good, the head lag response needed to reach a greater neck angle before the head followed.

Assembly Attempt 5: Six Outer Rods + Slider + Spring/Bumper

One of the primary issues with this design from a simulation perspective was that for various measurement combinations of the circular spring (diameter and length), the slider was inadvertently activated in compression (the neck translated backwards). To correct for this effect, a damper was inserted to fill the space around the spring, between the front of the base and the back of the dovetail (Figure 29).

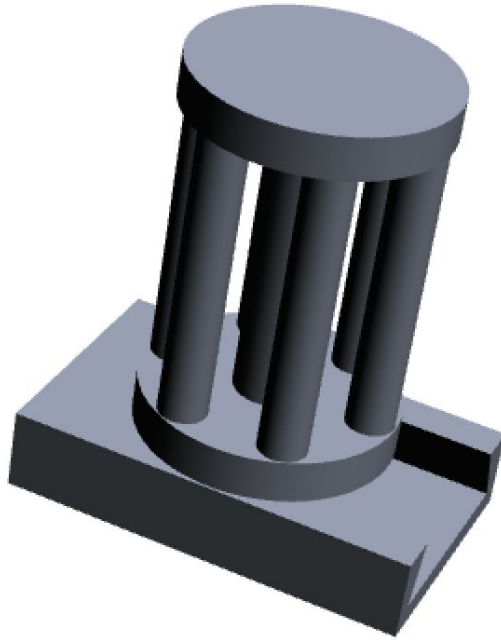


Figure 29: Image of neck model design attempt 5; created contact to fill space around spring to avoid activation in compression.

The thin bumper was added using the numbering system described in Assembly Attempt 4, with it being assigned as the last part. The issue discussed in Assembly Attempt 4 of the part being smaller than the node size was also encountered here. It was resolved by setting the element size of the thin bumper to 2mm. The bumper was not constrained. However, Automatic_Surface_To_Surface Contacts had to be defined between this part and both the slider base and the slider nub so it could perform its function. Aside from these two new contacts, all other constraints, contacts, and joints were defined as done previously.

The NBDL results from this model are included below (Figures 30-33). This was also the first model for which the group was encouraged to account for CG timing in both the x- and z-directions, noting the importance of the timing that the maximum displacement occurs (compression and tension simulations were omitted).

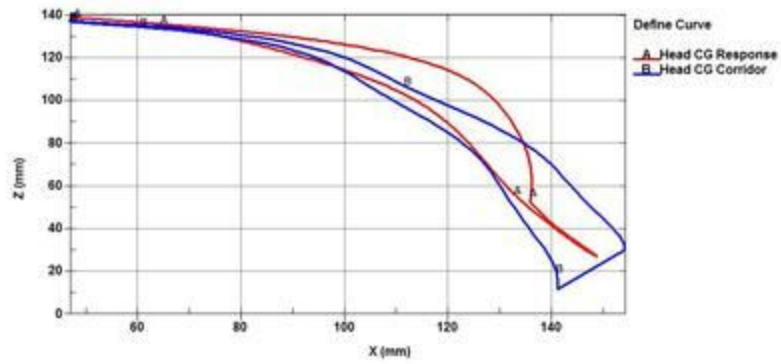


Figure 30: Head CG response for attempt 5.

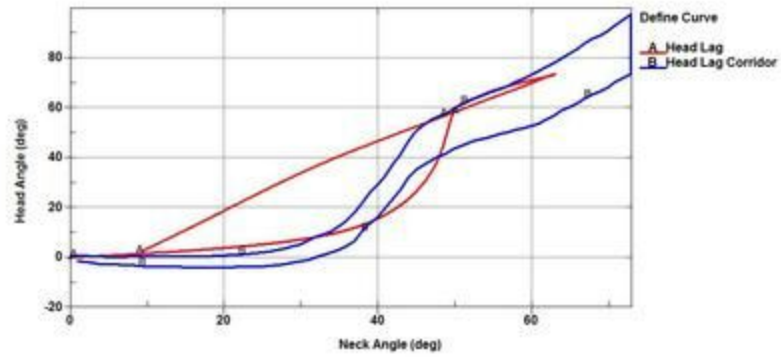


Figure 31: Head Lag response for attempt 5.

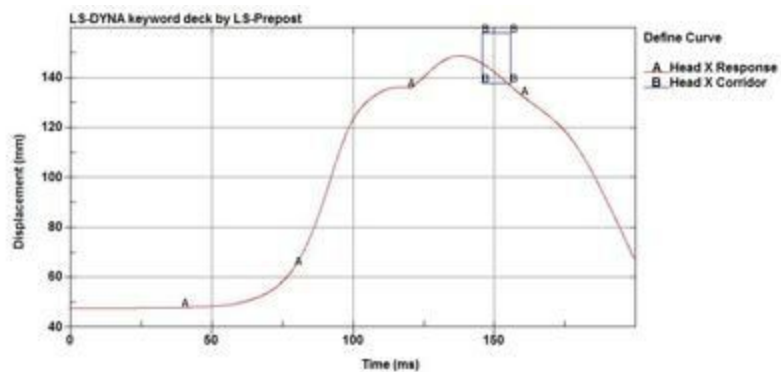


Figure 32: Head CG x-displacement relative to time for attempt 5.

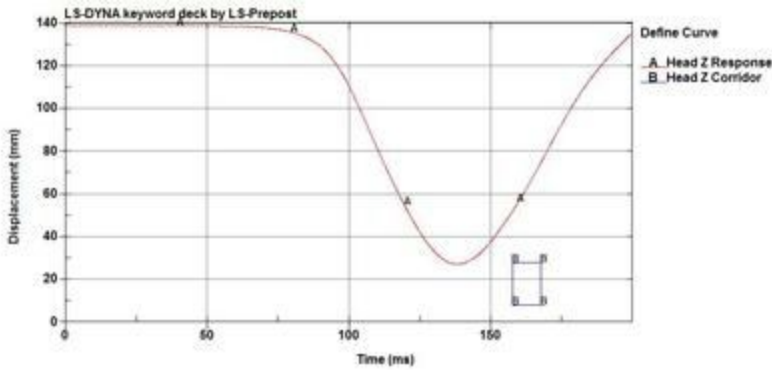


Figure 33: Head CG z-displacement relative to time for attempt 5.

Because this was the first time that the group learned that timing was something that was necessary to model, future brainstorming included how to correct for this as well.

Assembly Attempt 6: Altering Moment of Inertia

The group noted that the key to tuning bending stiffness was altering the moment of inertia. Because of the design of the model ("the spaghetti neck approach"), this could be easily accounted for by moving some of the rods closer to or farther from the center, which would allow more or less rotation in the z-direction. Specifically, the group moved only the front and back rods towards the center by varying distances and observed how the resulting responses were affected. Note that in the diagram of one model iteration below, although the rods appear to be equidistant from the center, the front and back rods have a larger diameter than the outer four rods and are therefore closer to the center.



Figure 34: Image of neck model design attempt 6; place front and back rods on circle of smaller radius to bring them closer to the center of the neck.

Because the moment of inertia was altered by changing the position of the rods and not their material properties or dimensions, the procedure for meshing these models and preparing them for simulation was identical to the process used in Assembly Attempt 5.

To get an idea of specific values up to this point in the iteration phase, the front and back rods (diameter 13.78 mm) were on a circle of radius 21 mm, and the outer 4 rods (diameter 11 mm) were on circle of radius 23 mm. The center rod had a of diameter 20 mm. The results of this simulation can be found in Figures 35-40. Other values of the diameter of the circle on which the front and back rods lie were simulated as well.

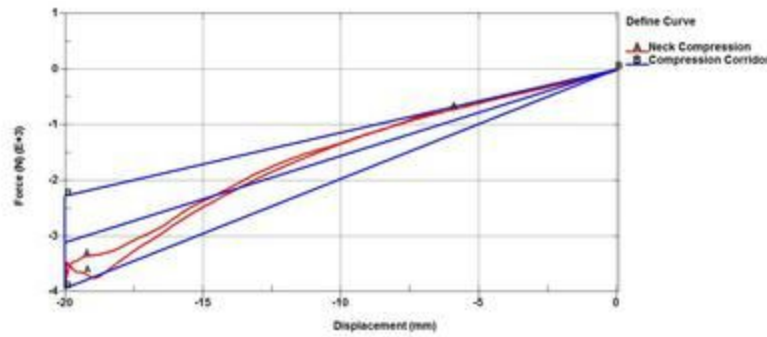


Figure 35: Compressive stiffness response for attempt 6.

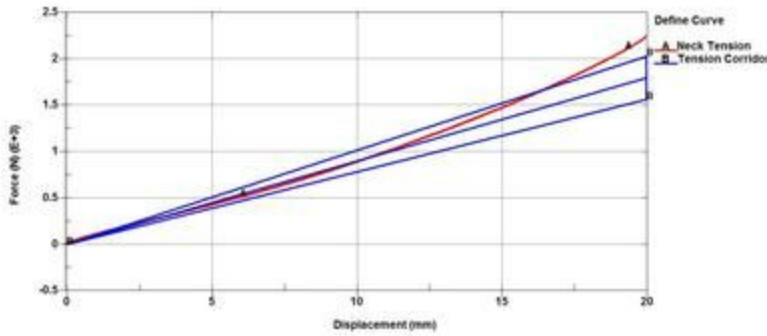


Figure 36: Tensile stiffness response for attempt 6.

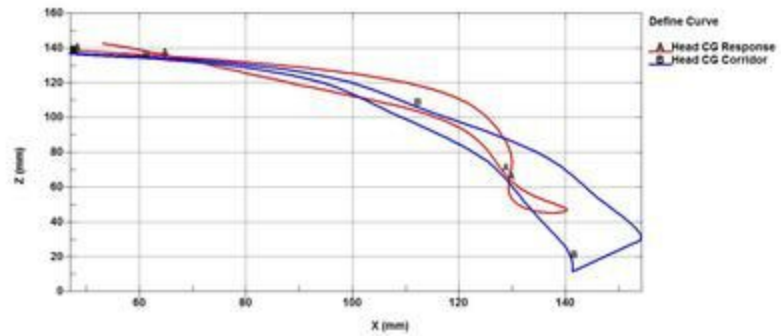


Figure 37: Head CG response for attempt 6.

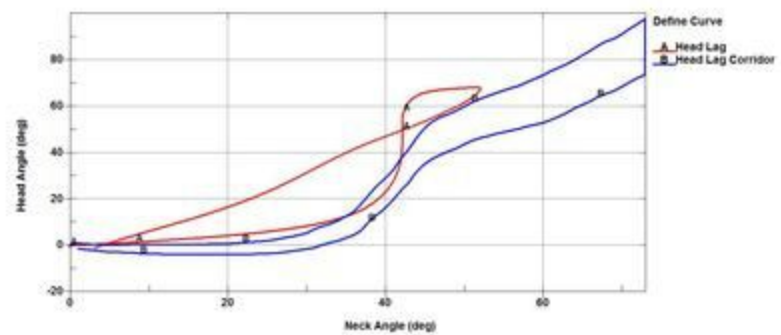


Figure 38: Head Lag response for attempt 6.

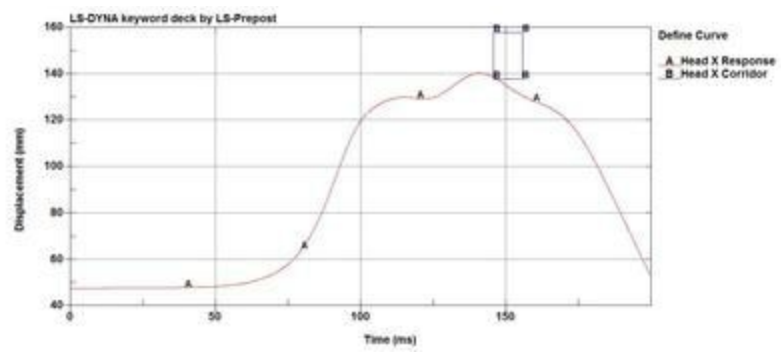


Figure 39: Head CG x-displacement relative to time for attempt 6.

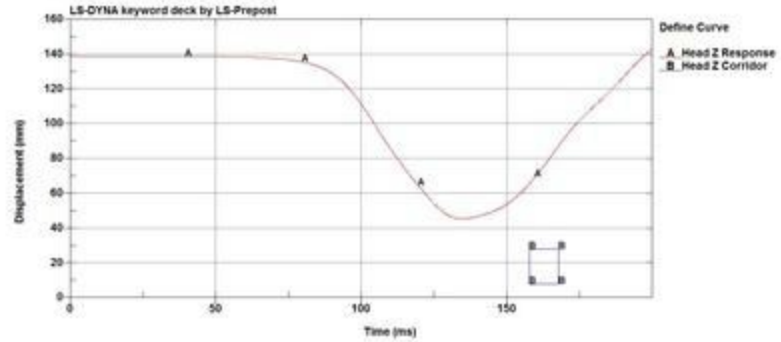


Figure 40: Head CG z-displacement relative to time for attempt 6.

Assembly Attempt 7: Incorporating Failure Analysis

As the deadline of the project approached, the group looked at the stress analysis of the model for the first time. The purpose was to hopefully conclude, after designing according to the performance specifications, that the model would not fail in any of the primary testing modes (tension, compression, NBDL). Team SQUAD was not concerned with the rigid parts on the assembly since only the rubber ones were activated (the seven rods, the damper, the spring). Both chloroprene rubber and ABR rubber have an ultimate stress of about 15 MPa. For the compression and tension tests, the stress levels in the rods fell well under this threshold, around 5.5 MPa and 6.6 MPa, respectively (Figures 41 and 42). However, the maximum stress recorded in the frontal impact test was about 64 MPa, which meant that the spring would break.

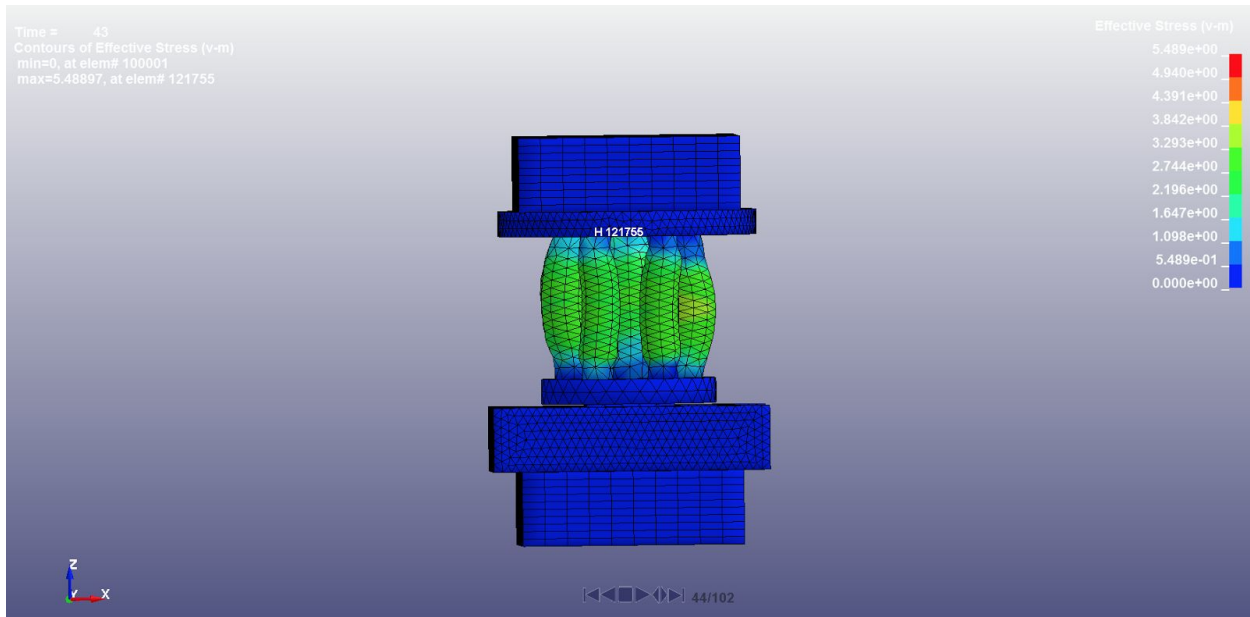


Figure 41: Von mises stress (max) for compression test of attempt 6.

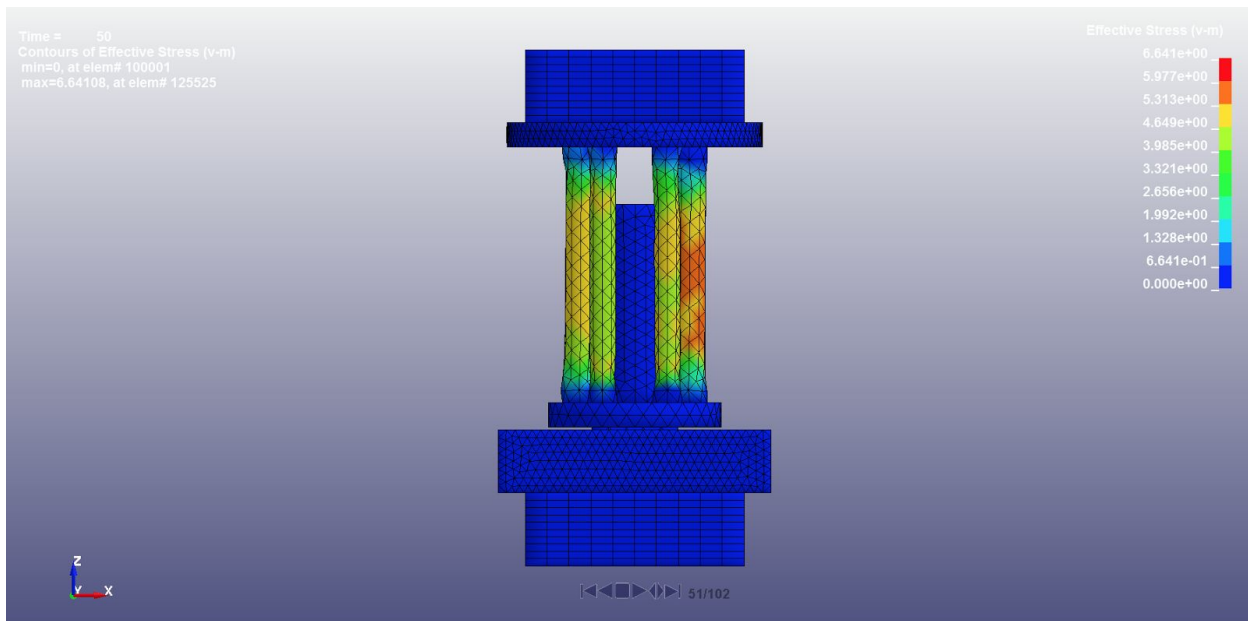


Figure 42: Von mises stress (max) for tension test of attempt 6.

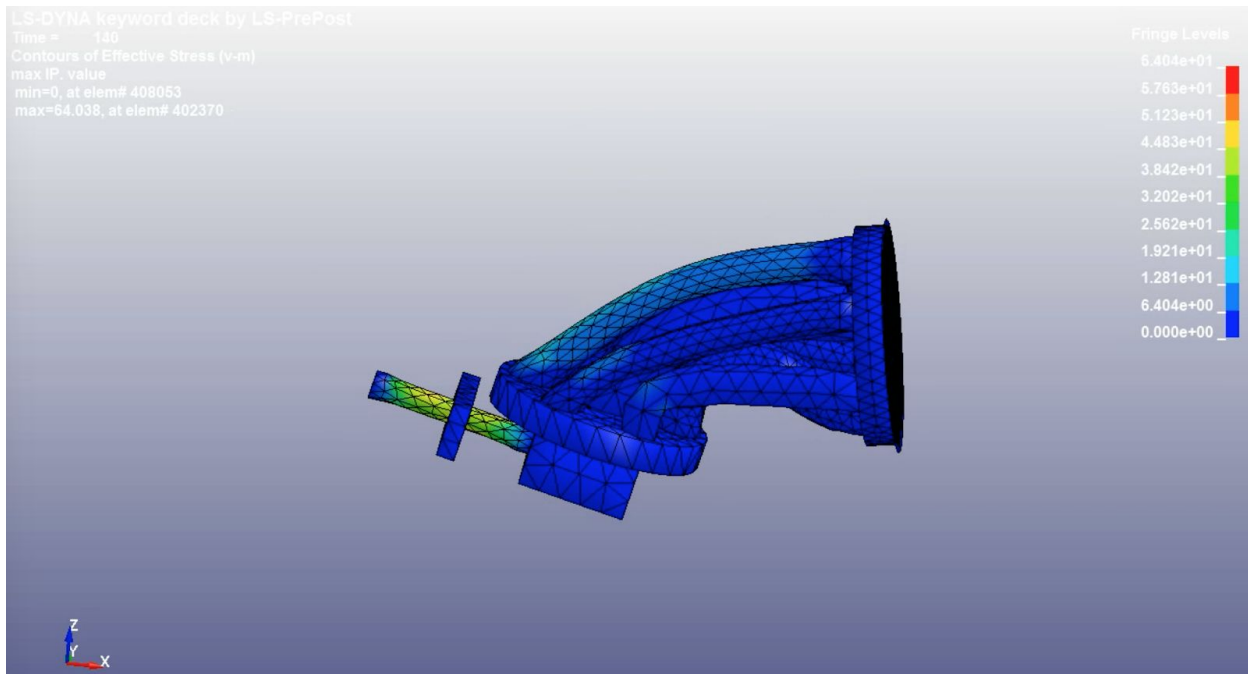


Figure 43: Von mises stress (max) for frontal impact test of attempt 6.

The group decided that there were two ways to correct for this failure: changing the material properties (e.g. use a stiffer rubber) and/or changing the structural properties (e.g. increase the cross sectional area). This would be the final step of the iterative process. Figure 44 below is the first attempt at increasing the cross sectional area and the Figure 45 is the final design.

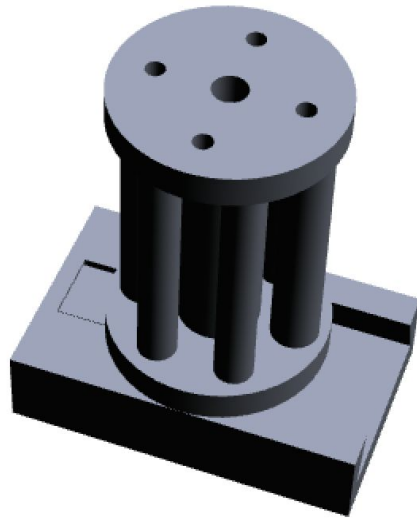


Figure 44: Image of neck model design attempt 7; increased area of spring.

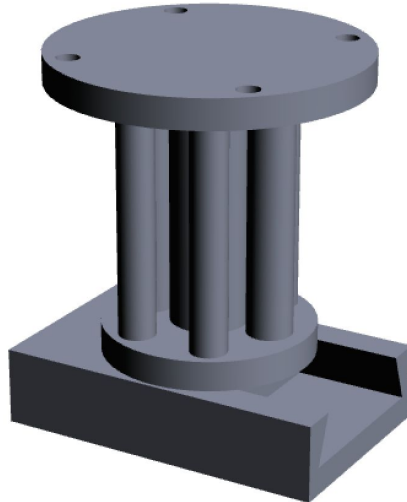


Figure 45: Final model design - Spaghetti Neck V36

During the incorporation of failure analysis, the two major changes that were made to the model were changing the dimensions and materials used for the slider. These processes were accomplished using the procedure described in Assembly Attempt 3.

The results of the final model maintained fitting the tension and compression corridors as expected. The head CG response also fit in the corridor rather well, but did not travel quite as far as the group may have hoped. The head lag response had a decent rise but flatlined early due to chin-to-chest contact (a recurring problem for most of the model attempts). The peak of the head CGx timing fell within the box, but the head CGz timing was still far from the mark. Details of this final model's analysis are explored in greater detail in the results and discussion section (note in particular figures 51-56).

c. Criteria for Design Acceptance

A fit metric program was developed using MATLAB to perform a statistical hypothesis test on the resulting data from each design iteration. The program is called FitMetric, and the MATLAB code used in the program can be found in Appendix C. This program was created to provide an objective way to analyze the results from each design, thereby enabling more informed decisions to be made throughout the design process. The resultant data for each of the six corridors was analyzed with the FitMetric program, and a score out of 100 was produced for each corridor. This scoring system provided the basis for objective comparisons between trials.

As mentioned previously, the performance specifications of importance to the design included tension, compression, head CG, head lag, x-displacement timing, and z-displacement timing. First, the fit metric analysis of the tension results was developed. The output data from the simulations for each trial took the form of a spreadsheet containing two columns of data: the first column containing all of the displacement steps, and the second column containing all of the force values at each displacement value. This data was read into the MATLAB script and separated into two different arrays. Then, the displacement array was used to create lines for the upper, middle, and lower bounds of the tension corridor using the slopes of each line in the corridor. By doing this, each displacement value then had a corresponding response force value and corresponding upper, middle, and lower corridor force values.

Then, a *for* loop was used to loop through the entire data and determine whether or not each force response value was within the corridor. The force response value was within the corridor only if it was greater than the lower bound value and less than the upper bound value at that specific displacement point. By looping through the data, the program was able to determine at which displacement values the force response curve was within the tension corridor.

One factor that was considered in the prior development of the tension corridor was that it was more important to be within the corridor for higher displacement values than it was for lower displacement values. As such, the corridor was split up into four equal regions along the range of displacement values. For example, region 1 ranged from 0 mm to 4 mm of displacement. Then, each of the four regions was assigned a weighting factor. The various weighting factors are summarized in Table 1. These factors were determined by the group at the beginning of the design process, and were chosen to represent the fact that in a motor vehicle accident, force

and displacement values near the upper end of the corridor would be much more important than the lower force and displacement values.

Table 1: The weighting values for each region in the tension corridor

Region	Approx Displacement Range (mm)	Weighting Factor
1	0 to 4	0.00
2	4 to 8	0.10
3	8 to 12	0.15
4	12 to 16	0.75

As the program looped through the data, a point value equivalent to the respective weighting factors was added to a running total based on which region was being analyzed. This resulted in a weighted score for how much of the response curve was within the tension corridor. Then, by knowing how many displacement points were within each region, a total possible score was calculated. The weighted score was divided by the total possible score, and then multiplied by 100 to yield a corridor fit score out of 100.

Another aspect of the tension response that was analyzed was how closely the response resembled the middle line in the center of the corridor. To objectively determine this goodness of fit, a linear regression statistical analysis was performed, where the response represented the data points and the center line represented the regression line. An r-squared value was calculated from the regression analysis, and used to determine a regression score. An r-squared value closer to 1 was desirable, so a calculation was performed to yield higher scores for r-squared values closer to 1. Equation 1 was used to perform this calculation, and the result was a score on a scale from 0 to 100. Any resultant calculation from Equation 1 of more than 100 was simply assigned a regression score of 100.

$$\text{Regression Score} = \frac{1}{1-R^2}, \text{ max score} = 100 \quad (1)$$

After performing this analysis, two scores out of 100 were obtained: a corridor fit score and a regression score. It was determined that being within the corridor was twice as important as closely fitting the center line in the corridor, so the corridor score was multiplied by two and then added to the regression score. This resultant score was then divided by a total possible score of 300 to yield an objective final tension fit score ranging from 0 to 100.

Next, a similar analysis was performed for the resultant compression data from the simulations. The data was read into the program and the upper, middle, and lower corridor lines were calculated using the displacement data. Then, a similar weighting scheme, which can be seen in Table 2, was used to determine a corridor score out of 100. A linear regression analysis was

also performed on the data to determine how well the force-displacement results fit the middle line of the corridor, and Equation 1 was used to calculate a regression score out of 100. Then, the resultant scores were combined with the same weighting factors as for the tension analysis, and a final compression fit score ranging from 0 to 100 was determined.

Table 2: The weighting values for each region in the compression corridor

Region	Approx Displacement Range (mm)	Weighting Factor
1	0 to -3	0.00
2	-3 to -6	0.10
3	-6 to -9	0.15
4	-9 to -12	0.75

Moving forward, a fit metric analysis was developed for the head lag data. The resultant head-neck angle data from the simulations was read into the script, and the neck angle (x-axis) data points were used to make a lag corridor with points corresponding to every neck angle point in the data. To create a lag corridor in MATLAB that had the same neck angle values as the data, the corridor was approximated with eight line segments: four representing the upper side of the corridor and four representing the lower side of the corridor. This approximated corridor can be found in Figure 46.

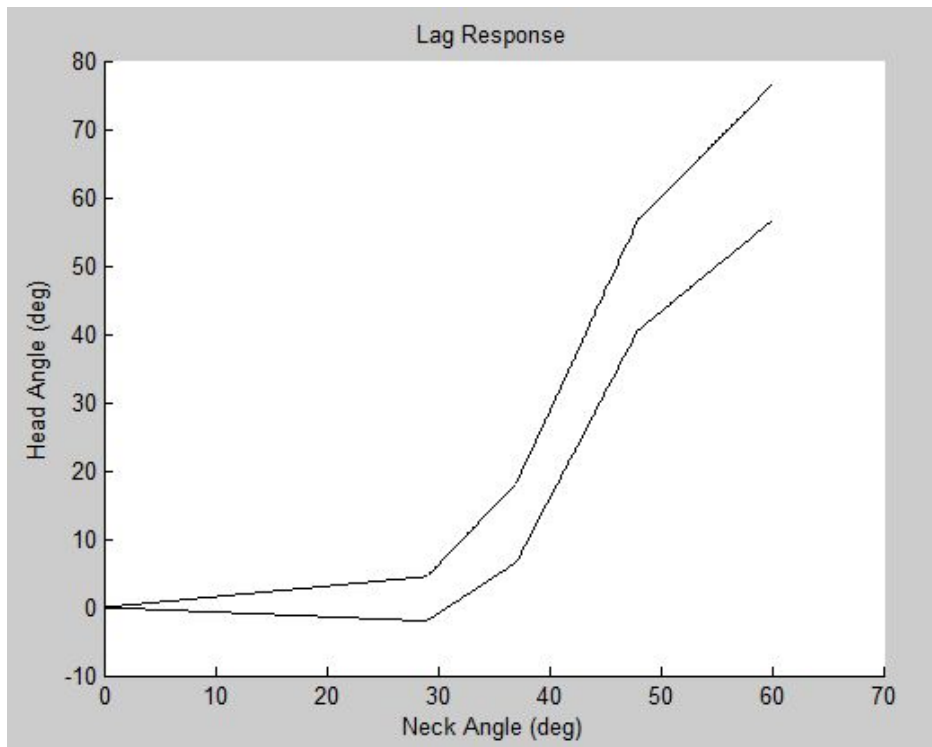


Figure 46: The eight lines used to approximate the head lag corridor in the FitMetric program.

Once the corridor was approximated in MATLAB, a *for* loop was used to loop through the simulation data and determine for which neck angle points the response was within the corridor. It was determined that being within the corridor was equally important at all points, so unlike for tension and compression, a weighting scheme was not implemented for the corridor score. Rather, one point was added to the running total for each data point that was within the corridor. At the end of the loop, this running total was divided by the total number of possible points and multiplied by 100 to yield a lag corridor score ranging from 0 to 100.

Next, using a very similar strategy, a fit metric for the head CG data was developed. The resultant head displacement data from the simulations was read into the script, and the x-displacement values were used in the construction of a head CG corridor. Like the head lag corridor, the head CG corridor had to be linearly approximated in order to assign values for each of the x-displacement data points. Six lines were used to approximate the corridor, with three lines representing the upper bound and three lines representing the lower bound. The approximated corridor can be seen in Figure 47.

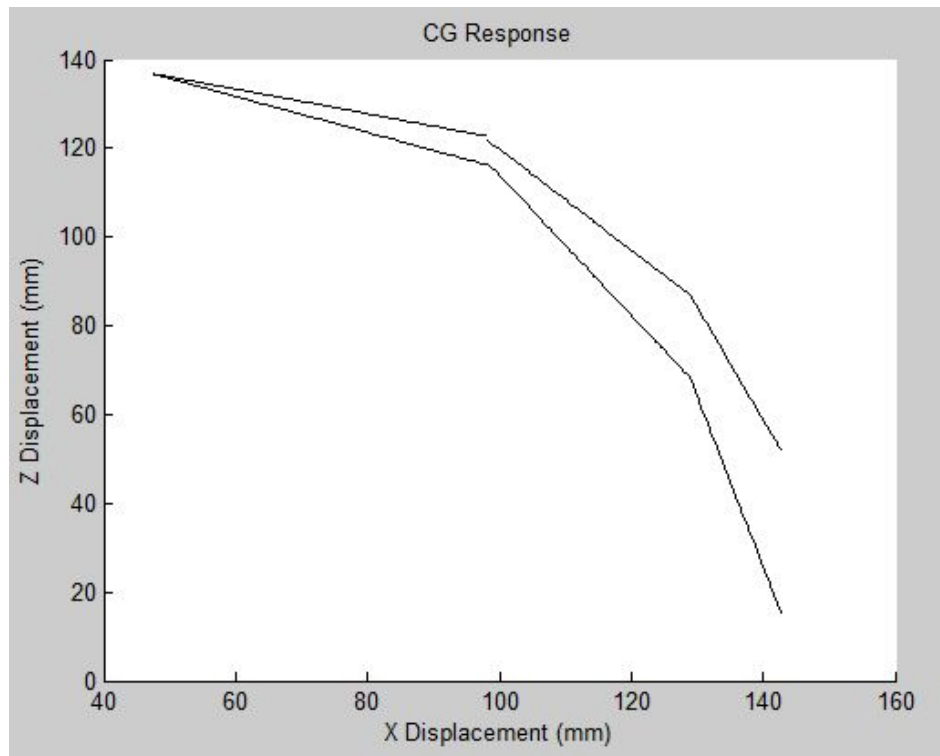


Figure 47: The six lines used to approximate the head CG corridor in the FitMetric program.

The entire head CG corridor was also weighted evenly, so the program looped through the data set and added one point to a running total for every data point that was within the corridor. After the loop, this total was divided by the total possible number of points and then multiplied by 100 to yield an objective head CG corridor score ranging from 0 to 100.

Next, a fit metric was developed for the x-displacement timing corridor. The simulation data was first read into the MATLAB script. The analysis was then performed by determining the time and

magnitude of the maximum x-displacement, and then finding the distance from that point to the center of the predetermined corridor. The center of the corridor had a magnitude of 148 mm at a time of 151 ms. Using the distance formula in Equation 2, the magnitude of the distance from the resultant peak to the center was calculated. Then, this value was subtracted from 100 to yield a score ranging from 0 to 100. If the calculated distance was greater than 100, then a score of 0 was assigned to that trial. This resulted in an objective score for the x-displacement timing data.

The fit metric for the z-displacement timing corridor was developed in a very similar manner. The simulation data was first read into the MATLAB script, and then the magnitude and timing of the absolute minimum of the data was determined. Then, the distance between this point and the center of the corridor was calculated using Equation 2. The center of the corridor had a magnitude of 18 mm at a time of 163 ms. The calculated distance was then subtracted from 100 to yield an objective score ranging from 0 to 100 for the z-displacement timing data. Again, if the distance was greater than 100, then a score of 0 was assigned to that trial.

$$Distance = \sqrt{(x, z_{resultant} - x, z_{center})^2 + (t_{resultant} - t_{center})^2} \quad (2)$$

These six fit metric analyses were applied to each design iteration, resulting in six scores ranging from 0 to 100 for each simulation trial. These scores were then added up, divided by 600, and then multiplied by 100 to get a final, overall score ranging from 0 to 100. In this portion of the analysis, each of the six corridors were weighted evenly with respect to one another. The final score, as well as the individual scores, were then compared to the previous design iterations to provide an objective determination of if a design change yielded improved results. When a design change was made, a hypothesis was established stating that the design change would yield a higher fit metric score. If the total score, or a targeted individual score, increased after a design change, then the hypothesis was accepted and the design change was implemented. On the other hand, if the scores decreased, then the hypothesis was rejected and a new, informed design change was made using the simulation data. The use of this fit metric program provided the team with a defined verification tool that could be applied uniformly across every simulation and design iteration.

Results and Discussion

a. Final Design

Features

After more than 30 unique design iterations tested over the course of the semester, the final Spaghetti Neck V36 six-year old crash dummy neck was developed. A CAD version of this product can be found in Figure 48, and the complete engineering drawings can be found in Appendix A. The final version is composed of the various elements that were determined to best contribute to the fit within each performance specification corridor. A general overview of the beneficial features of the design will be discussed now, and a complete list of parts included in the final design can be found following this discussion.



Figure 48: The CAD model of the Spaghetti Neck V36.

There are two major features in the final design that distinguish it from other designs, enabling it to achieve elevated performance levels in the various FEA tests. The first major design feature is the implementation of slender rods, which make up the bulk of the neck. There are six equally spaced rods arranged in a circular pattern on the bottom plate and one rod in the center of the bottom plate. The six outer rods are all firmly secured to both the top and the bottom plate, whereas the center rod is secured to the bottom plate, but not to the top plate. This orientation and connection of the rods within the neck is excellent because it allows the neck to be stiffer in compression than in tension, which is a major physiological aspect of the human neck.

Additionally, the use of equally spaced rods in the neck enabled the design group to slightly alter the compressive and tensile stiffnesses of the neck by simply increasing or decreasing the diameter of the rods. This design feature, which resulted a final product that excelled in many of the performance specification corridors, also enabled the team to use and understand the iterative design process to a greater degree. Once this basic design was implemented, only slight changes were required between iterations in order to tweak the specifications of the neck.

In addition to allowing the team to fine tune the compression and tension responses of the neck, the slender rods allowed the team to more closely model the head position corridors. The bending stiffness and area moment of inertia were vital factors to consider when designing for the NBDL corridors. Since the rods were spaced out on the bottom plate, their positions could be slightly altered between design iterations to change the bending stiffness and area moment of inertia, allowing the team to once again execute finely tuned iterative changes during the design process. The variable placement of the slender rods enabled the design team to orient the components in such a way that the product exceeded the goals for the NBDL corridors.

Various materials for the rods were experimented with during the design process. The final product uses chloroprene rubber 25% carbon (visco), which is a material available in the database provided by Dr. Nightingale for use with LS-DYNA. This material has an elastic modulus of approximately 22 MPa, allowing rods of reasonable diameter to be used to yield the desired tensile and compressive stiffnesses. Furthermore, the use of a rubber for the rods allowed the rods to bend sufficiently during a frontal impact test to satisfy the NBDL corridors. Even though this material is viscoelastic, the degree of nonlinearity of the response was small enough to the point where the tension and compression response curves could still fit within the corridors.

The dimensions and placements of the seven different rods are specified in the final engineering drawings, which can be found in Appendix A.

The second major design feature that makes the final product superior to other artificial necks is the implementation of a slider component. One of the main drawbacks of the current Hybrid III neck is that it fails to accurately model the severe degree of head lag experienced with six-year olds. The performance specification corridor for head lag portrays the idea that at the beginning of a frontal impact, the head translates forward without rotating until it hits a certain point. Then, the neck stops extending and the head rotates down towards the chest. To best model this feature, the design team settled upon using a dovetail slider. A spring is anchored to both the slider and the slider base to control the translational movement of the neck through the dovetail slider.

The implementation of the slider proved to be a valuable feature as it effectively enabled the head to translate forward prior to rotating towards the chest. As a result, the model was able to closely follow the head lag corridor, making it far superior in that aspect compared to the existing Hybrid III neck. Additionally, the implementation of the slider made it so the motion of

the center of gravity of the head during a frontal impact closely resembled the head CG corridor. Without the use of the dovetail slider, the head would have rotated immediately upon impact, thereby deviating from both the head lag and CG performance specification corridors. Significant design changes would have been necessary to achieve the performance specifications required to hit the head lag and CG corridors.

Furthermore, the x-displacement and z-displacement timing corridors could be finely tuned for by altering the properties of the spring connected to the slider, thereby influencing both the magnitude and time of the maximum x- and z-displacements. This enabled the design team to iteratively design for the timing corridors without changing any of the rods, thereby preserving the ideal tension and compression responses.

The implementation of the slider also provided valuable insight into the design process. The human neck does not have a mechanism that even closely resembles a dovetail slider. Therefore, the implementation of such a component is a huge deviation from physiological components in the human body. However, this design proved superior for modeling the NBDL corridors. The use of a slider clearly demonstrated that when designing a product or system, the only real concerns are the performance specifications, not the mechanisms used to achieve those specifications. The team was not burdened with a design constraint requiring a product that closely resembles the mechanical components in the human neck. Therefore, during the brainstorming process, the team was free to “think outside of the box” and consider mechanical systems that would enable the design to achieve the performance specifications in the best possible manner. Achieving the performance specifications was the highest goal for the team, and as a result, took priority over concerns such as designing a system to closely resemble the appearance of a human neck.

The slider system in the final product is composed of an aluminum base, an aluminum slider nub, a chloroprene rubber 25% carbon (visco) bumper, and an ABR rubber spring anchored to the base and the nub. As with the rods, various materials were experimented with for the assembly. The most effort during this material experimentation was spent on the slider spring. In the end, ABR rubber, which has an elastic modulus of approximately 20 MPa, was selected because it provided the best material properties for the size constraints of the spring in the assembly. The chloroprene bumper was included as a design feature because it acted as an interface between aluminum slider nub and slider base, and it stabilized the motion of the slider assembly during compression tests.

Aside from the use of slender rods and a slider assembly, the final product contains a number of minor features that enable it to function properly and that will increase its likelihood of acceptance into the crash test dummy market. First, the entire assembly has a length of 109 mm, which is equal to the length of the Hybrid III neck assembly. Additionally, the slider base of the final model screws directly into the existing lower neck bracket. Finally, the top plate on the final model screws directly into the base of the six-year old crash test dummy head. These

design features are not only important for modeling the accurate length of a six-year old neck, but also for increasing the ease of implementation of the new neck with existing dummies.

Drawbacks

Due to the relatively short amount of time allocated for the design of this product, there are a few notable drawbacks and flaws that need to be addressed prior to its introduction into the crash test dummy market. A major design flaw, which is discussed in detail later in this report, is that the stresses experienced by the back outer rod and the slider spring exceed the ultimate tensile stresses of the materials used for those components. The maximum Von-Mises stresses during a frontal impact are approximately twice the ultimate tensile stresses for the rod and the slider spring.

The reason this design flaw has not been accounted for is because the stress analysis was not performed until late in the design process. As a result, when it was determined that the stresses were too large, there was not sufficient time to make the necessary design changes to decrease the stresses to acceptable levels.

Another drawback of the final design is that it does not allow the head to extend far enough away from the chest of the dummy to allow for full head rotation and proper timing of that rotation. The x- and z-displacement timing corridors were introduced later in the design process than the rest of the performance specifications. As a result, the team was able to spend less time designing around these parameters. The current model yields acceptable results for the NBDL corridors, but improved head rotation would be necessary for this product's success and viability.

Furthermore, the use of a rubber spring in the slider system results in minor negative impacts on the performance of the neck. The ABR rubber is a viscoelastic material and acts a spring to constrain the translational motion of the slider. However, the material quickly responds after being elongated. As a result, when the slider translates all the way forward, the spring is stretched significantly, at which point it begins to rebound. This elastic rebound causes the spring to oscillate slightly as the head rotates forward during the impact. Although this drawback does not drastically affect any of the corridors, its effects are evident and should be addressed to yield more robust and consistent responses from the slider system.

Another drawback of the final design, especially when compared to the Hybrid III, is the large number of individual parts and the complex assembly procedure. The final model is composed of 13 separate parts and requires 21 screws for its full assembly. Not only would this assembly process take much longer and require significantly more documentation than the Hybrid III model, but it would also be more difficult to manufacture. The up front cost associated with creating the molds for the various parts required in the final model would be significant and could have been avoided with a design composed of fewer individual parts. The increased difficulty, time, and cost associated with manufacturing and assembly could be prohibitive for this product's entry into the market. This was a valuable failure in that it demonstrated an aspect

of the design phase to Team SQUAD that was not emphasized during the course of the project. Manufacturing needs to be valued and taken into consideration during all phases of design in order for a product to truly be engineered well.

There are a number of reasons why this drawback was not addressed during the design of the final model, but the main reason is that the team did not focus on “design for manufacturing.” The design team was so focused on hitting the various performance specification corridors that the negative impacts of the high complexity of the model were not largely considered during the process. Likely, the assembly and manufacturing processes would need to be greatly simplified prior to this model becoming a viable product.

Parts List

The final neck model is composed of 13 different parts, and the assembly is connected using 21 screws. Engineering drawings for each of the 13 parts, as well as for the assembly as a whole, can be found in Appendix A. Table 3 lists the part names, the part numbers, and the respective materials they are composed of, and summarizes the components used to make the final neck model.

Table 3: A summary of the parts composing the final model

Part Name	Part Number	Material	Figure No. in Appendix A
Slider Base	98	Aluminum	A.2
Slider Nub	2000000	Aluminum	A.6
Thin Bumper	13000000	Chloroprene	A.5
Slider Spring	3000000	ABR Rubber	A.9
Bottom Plate	4000000	Aluminum	A.3
Center Rod	5000000	Chloroprene	A.4
Outer Rod 1	6000000	Chloroprene	A.7
Outer Rod 2	7000000	Chloroprene	A.8
Outer Rod 3	8000000	Chloroprene	A.8
Outer Rod 4	9000000	Chloroprene	A.7
Outer Rod 5	10000000	Chloroprene	A.8
Outer Rod 6	11000000	Chloroprene	A.8
Top Plate	99	Aluminum	A.10

Budgets

Seed money would be required to continue to develop this neck past the scope of this course. After addressing the aforementioned drawbacks with design changes, the next steps would be to create a prototype using the actual required materials. Low volume prototyping with the actual materials would be an expensive phase in the process, but a very necessary one to prove the functionality of the neck. Then, after thorough testing with actual models, investment money would be needed for the front-end costs associated with large-scale manufacturing processes.

Ideally, each one of the parts would be injection molded, which would allow for efficient production of the individual components. The injection molding process is relatively cheap, as it does not cost much more than the price of the materials. The cost-prohibitive step, however, is having the molds made for each of the parts. Injection mold dies typically cost anywhere from \$8-20k [25]. Since four of the rods are identical to one another, and the two other outer rods are identical, only nine dies would need to be made. As a result, a rough estimate of the startup cost for the large-scale manufacturing process is approximately \$100,000. This money would need to be paid upfront, prior to the sale of any products.

After establishing the groundwork, however, the parts could be made quickly and cheaply. A cost analysis of the various materials and amounts of materials required for each part was carried out and can be found summarized in Table 4 [18-23]. The estimated cost of the materials per neck model was determined to be \$14.04. However, the actual costs of the dies would need to be distributed amongst the estimated number of parts that could be made using the die to yield a more accurate cost analysis.

Table 4: A cost analysis of the materials for the parts in the Spaghetti Neck V36 model

Material	Part(s)	Bulk Pricing (\$)	Amt. of Material per Model	Total Cost of Material per Model (\$)
Aluminum 6061	Slider base Slider nub Bottom plate Top plate	30.86/ft [M1] 10.98/ft [M2] 34.01/ft [M3] 72.07/ft [M4]	0.312ft 0.098ft 0.028ft 0.028ft	13.68
Chloroprene	Rods (7) Damper	3/kg [M5] 3/kg [M5]	0.066kg 0.003kg	0.21
ABR Rubber	Slider spring	1.66/ft [M6]	0.090ft	0.15

*The density of chloroprene is 960kg/m³

In addition to the costs of manufacturing each part, the cost of labor necessary to assemble each model would need to be determined. After performing this analysis, a sound estimate of the cost of an entire model could be generated, providing a better idea of how much the model would cost to customers, and if that price point would be competitive with the Hybrid III and other necks in the crash test dummy market.

b. Convergence Study

A convergence study, which compared computer processing unit (CPU) time and maximum tensile force, was performed in order to determine an element size to be used for each part of the model. This study was necessary to ensure accurate results in a timely manner. An element size that is too large will take minimal CPU time but will return inaccurate model measurements. An element size that is too small will return accurate model measurements but will take so much CPU time that the design can not be iterated for further improvements.

To begin the study, the maximum element size for each of the model's 13 parts was determined by finding the largest size LS-DYNA could make into a 3D tetrahedral mesh. These element sizes were halved, and these values were called the 'default element sizes' (Table 5). It should also be noted that rigid parts do not contribute to the CPU time. These parts were given element sizes of '6' for all convergence study iterations. It was decided that "ChloroRub_Slider_6rods_Stopper_FB7" would be the model used for the convergence study because this was the newest model at the time, and Team SQUAD had finalized the dimensions of the seven rods that would contribute to the tensile response.

Table 5: Default element sizes for the convergence study.

Part Name	Type	Default Element Size
Slider Base	Rigid	6
Dovetail	Rigid	6
Slider Spring	Deformable	4.5
Bottom Plate	Rigid	6
Center Rod	Deformable	4.5
Rod 1	Deformable	4.5
Rod 2	Deformable	4.5
Rod 3	Deformable	4.5
Rod 4	Deformable	4.5
Rod 5	Deformable	4.5
Rod 6	Deformable	4.5
Top Plate	Rigid	6
Thin Bumper	Deformable	2

The deformable parts' element sizes were then scaled by 0.50, 0.75, 1.00, 1.25, 1.50, and 2.00 in the 'CFASurfaceImportAndShells.cfile', and the tension test was run on the model. Note that the tension response corridor for each element size can be found in Appendix B. The corresponding CPU time was recorded from the message file, and the maximum tensile stress was found by copying the values from the .crv file into excel and using the 'MAX' function. The results are tabulated and graphed in Table 6 and Figures 49 and 50.

Table 6: Convergence study results.

Scale	Time (s)	Max Tensile Force (N)
2.00	54	1359.37
1.50	158	2209.33
1.25	242	2226.18
1.00	291	2255.51
0.75	1220	2283.41
0.50	4400	2100.04

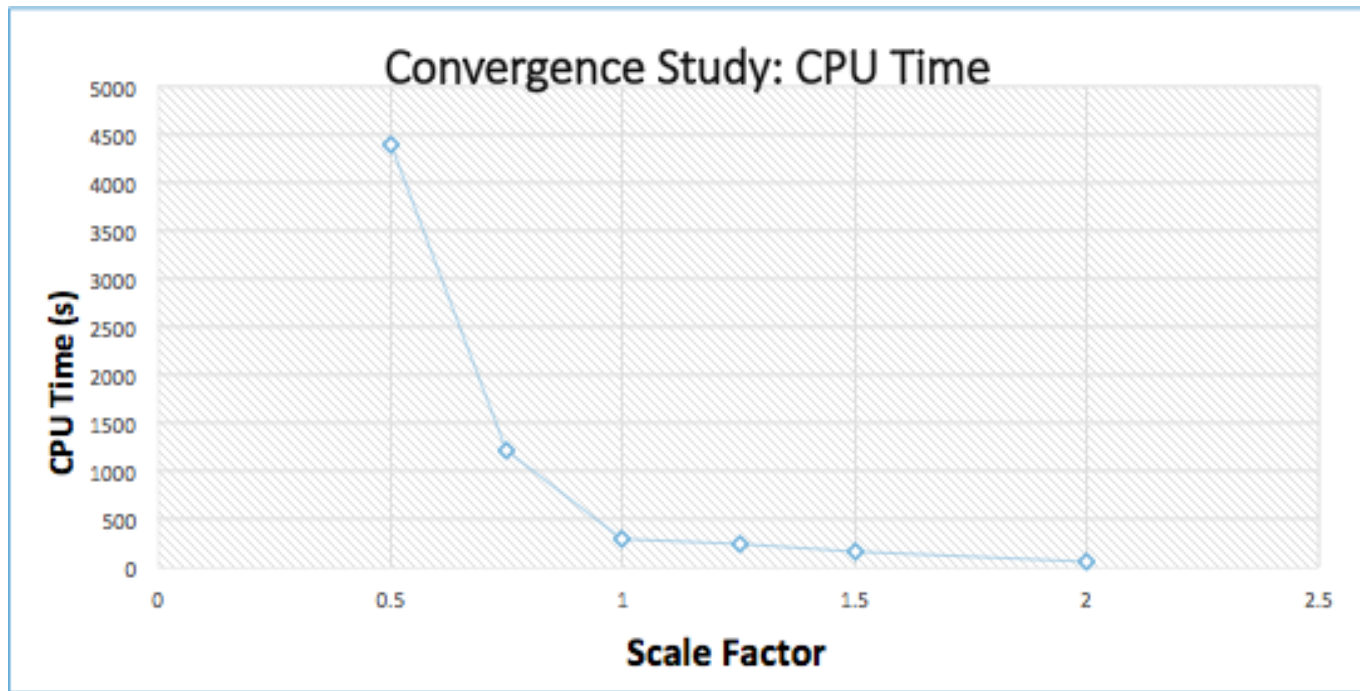


Figure 49: Convergence study CPU time.

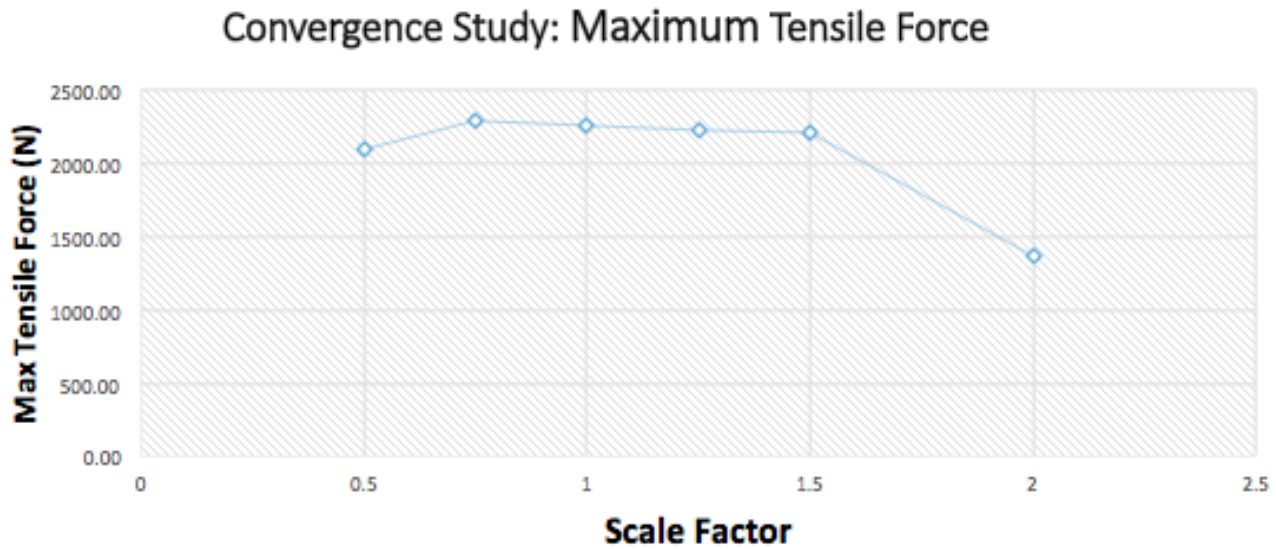


Figure 50: Convergence study maximum tensile force.

It can be readily seen in Figure 49 that the CPU time exponentially decreases as the scaling increases. Once the scaling reaches 1.00, the CPU time bottoms out. It can also be readily seen in Figure 50 that the maximum tensile force at a scale factor of 2.00 is almost half as large as the maximum force at the other scale factors. The dip in maximum force with the 0.50 scale factor is alarming as one would expect this value not to be so different from the other smaller scaled element sizes. Further investigation should be done in order to find the cause of this dip. It should also be noted that the scale factor of 0.50 was the smallest that LS-PrePost could mesh without crashing. It was hypothesized that this crashing was due to the inability of the program to meet the high computing demands. However, with the aforementioned trends considered, an element scale factor of 1.00 was selected as the most logical convergence of minimizing CPU time and returning accurate maximum tensile force measurements.

c. Final Testing Methods

When testing the final model, it was first run through all of the cfiles provided to load the file, to create a surface mesh, to transform that into a tetrahedral mesh, and then to assign section and material properties. These final cfiles can be found in Appendix E. Additionally the numbering system for a model with 13 parts described in the Methods section was used to prevent LS-PrePost from crashing due to numbering overlap. Furthermore, the Sections and Materials cfile had to be split into separate files as described in the Methods section as they caused LS Prepost to crash when they were run on a model with 13 parts. Additionally, even after they were split it was often necessary to slowly step through the files to prevent overloading the software and causing it to crash. When these meshes were created, an element size of 4.5 mm

was used for all deformable bodies (elform=10). This element size was identified as ideal by the convergence study because it allowed for accurate results while maintaining a reasonable computation time. The only deformable body to not have this element size was the thin bumper. It was too narrow to mesh at that size so an element size of 2 mm was used exclusively for that piece. For all rigid bodies (elform=1) except the base and top plate, an element size of 6 mm was used. Note that they are defined as rigid so the element size does not affect their behavior. For these two pieces, the element size was set to 3 mm. This is because they incorporate the screw holes to attach the neck to the rest of the H-III six-year old dummy. LS-PrePost was unable to mesh these parts accurately unless the element size was reduced to this level.

The next step was to constrain the different portions of the model that would be attached during testing. For attaching rigid bodies to deformable bodies, the Extra_Nodes_Set constraint type was used. Four node sets were created for this purpose: the tops of the outer rods, the bottoms of all rods, the back of the spring, and the front of the spring. The nodes making up the top of the six outer rods were attached to the top plate, the bottom of all 7 rods were attached to the bottom plate, the front of the ABR rubber spring was attached to the slider nub, and the back of the spring was attached to the base. The only other constraint that was incorporated into the model was a Rigid_Bodies attachment between the base plate and the slider nub to ensure that they stay connected during testing. This gave a total of five constraints in the final model.

After the model was fully constrained, the next step was to define contacts between solid parts that may hit each other during the various tests. This was done by adding Automatic_Surface_to_Surface contacts in the keyword file. For all of the contacts defined in this section, they are between two parts, and the friction coefficients are taken from the materials database. The first contact was between the center rod and the top plate, as they are not attached to provide different stiffnesses in tension and compression. Then, contacts were defined between the center rod and each of the outer rods (6 total) because the center rod may come into contact with them during the bending or compression tests. However, contacts were not defined among the outer rods. It was verified by viewing the D3Plots that LS-DYNA created that there was no contact among these rods in any of the loading modes. Finally, a contact was defined between the thin bumper and the slider nub and between the thin bumper and the slider base. This contact simply allowed the thin bumper to perform its function by damping some of the movement in the slider and preventing rigid body contact, which can cause problems in LS-DYNA.

The final attachment that needed to be defined was the interaction between the slider nub and the slider base, both rigid bodies. This was accomplished using the “jointsV2” excel file provided by Dr. Nightingale, which allowed the two parts to interact as a frictionless joint with only one direction of movement. This process involved entering the coordinates of one node on the moving piece (slider nub), the part IDs of both rigid bodies involved, the vector for the direction of translation, and an orthogonal vector. Once this was completed the Excel file would provide a block of code that could be copied and pasted onto the end of the kfile in Notepad++.

At this point the keyword file was complete and could be exported to MATLAB for testing. The testing was performed using the `neck_sim_batch.m` script, which loaded the keyword file and ran it through tension, compression, NBDL, CHOP, extension, and validation testing in LS-Dyna [11, 12]. However, only the tension, compression, and high speed frontal impact data sets were used to evaluate the model.

d. Final Testing Results

The final neck model was subjected to the same FEA simulations and statistical tests as the rest of the design iterations. Using MATLAB to run the simulations, the model underwent tension, compression, and high-velocity frontal impact tests. The results of the simulations relative to the tension, compression, head lag, head CG, x-displacement timing, and z-displacement timing performance specification corridors can be found in Figures 51-56, respectively.

Please note that the IARVs for tension and compression were determined to be 1490 N and -1820 N, respectively, and that the corridors and responses were cut off at these points during the data analysis. For the fit metric and for the qualitative analyses, the corridors were cut off once the middle lines in the corridors reached their respective IARVs. Please note that the simulations plotted response values for stresses greater than the IARVs in both tension and compression.

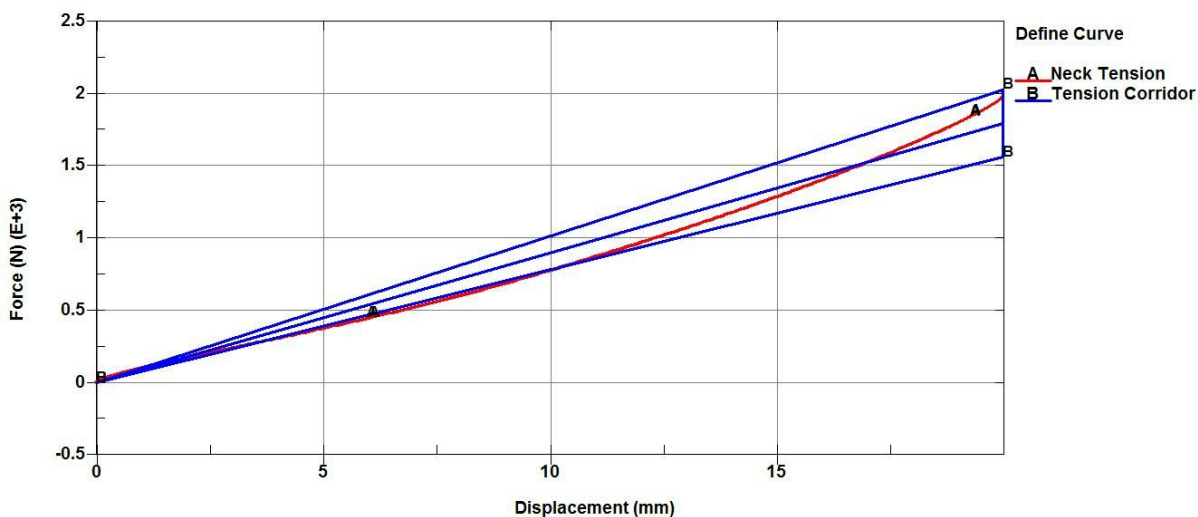


Figure 51: The tension response for the final model relative to the tension corridor.

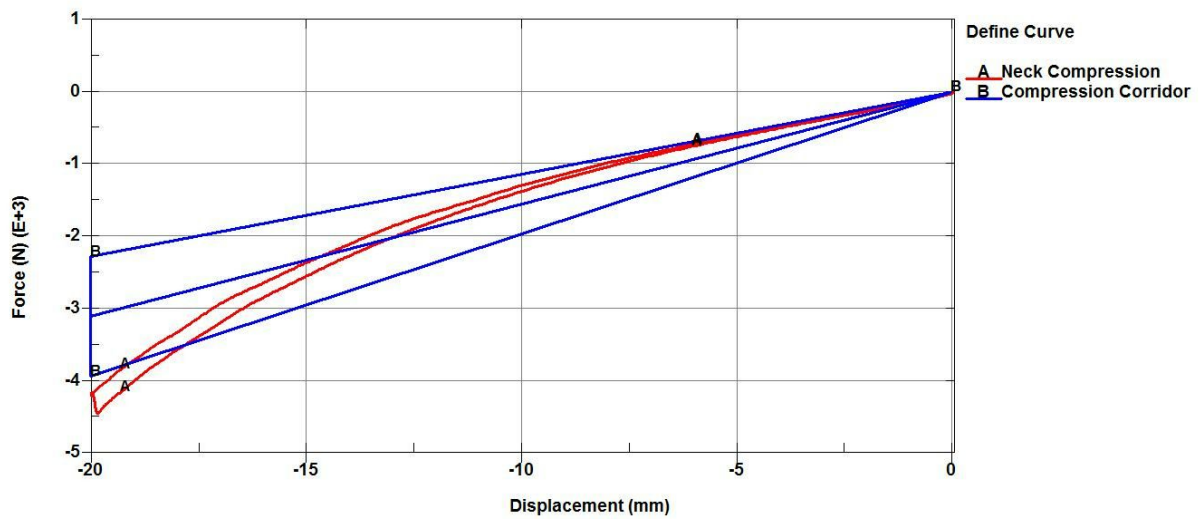


Figure 52: The compression response for the final model relative to the compression corridor.

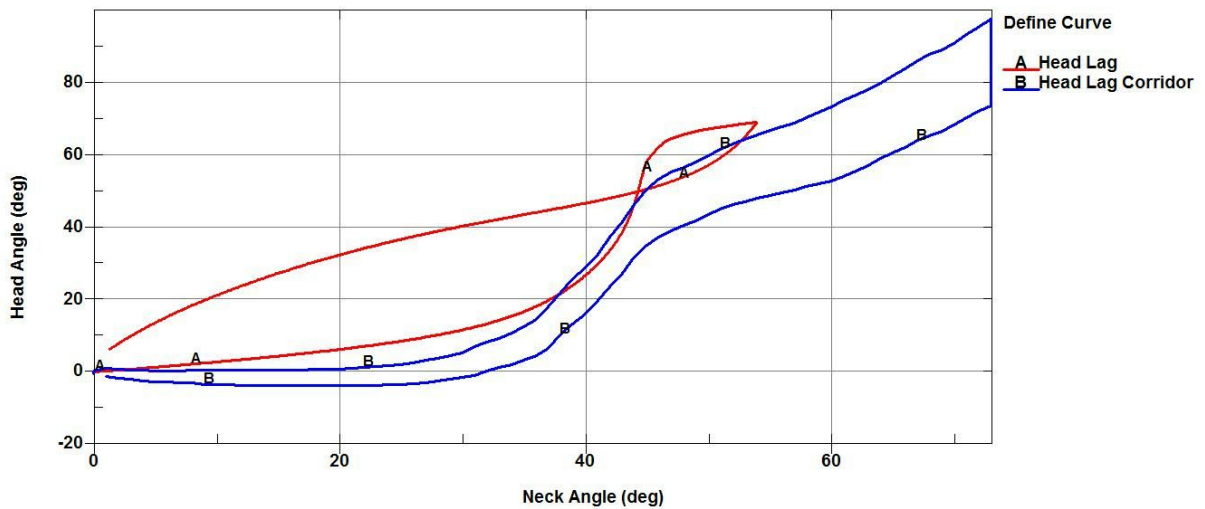


Figure 53: The head lag response for the final model relative to the head lag corridor.

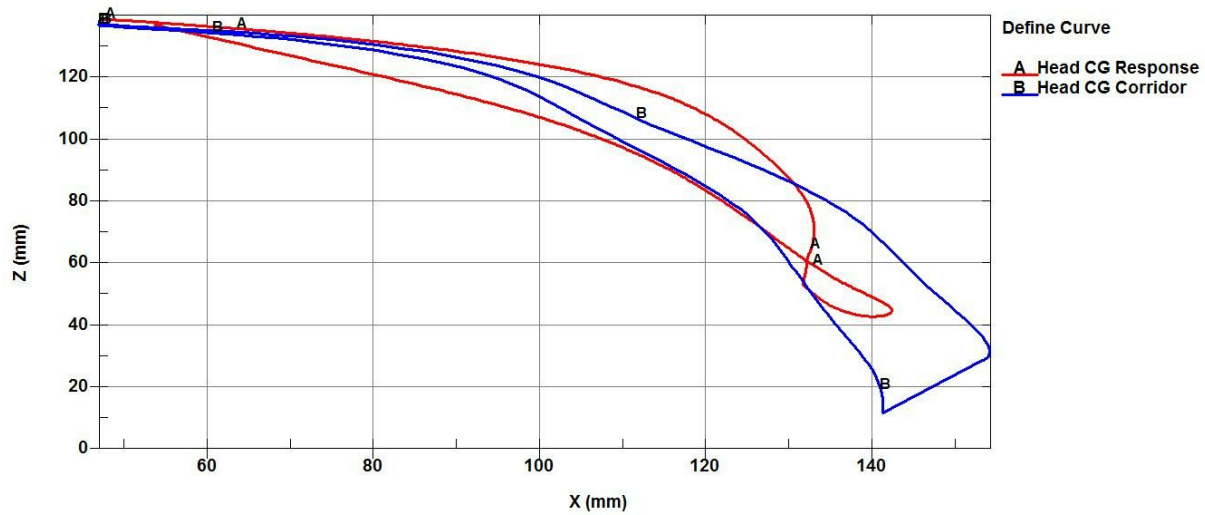


Figure 54: The head CG response for the final model relative to the head CG corridor.

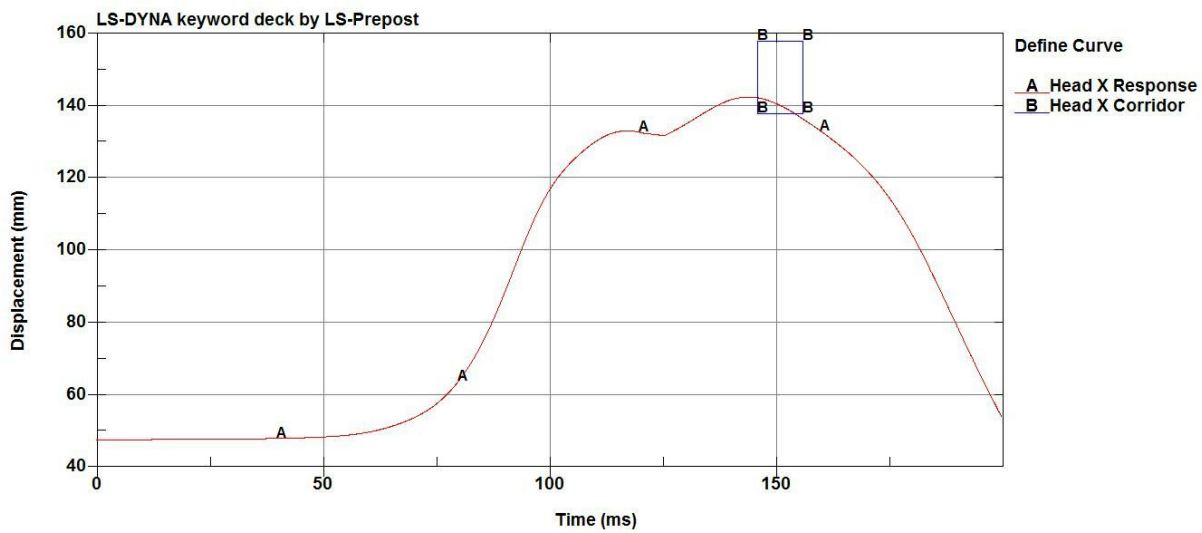


Figure 55: The x-displacement timing response for the final model relative to the x-displacement timing response corridor.

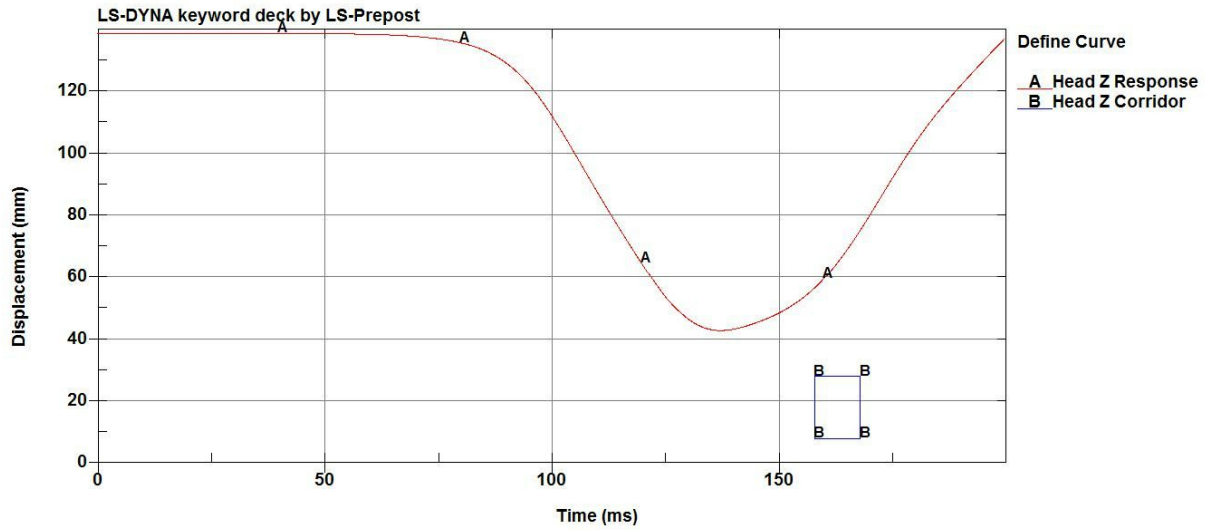


Figure 56: The z-displacement timing response for the final model relative to the z-displacement timing response corridor.

The FitMetric program in MATLAB was used to perform a statistical analysis on the results presented in Figures 51-56. The scoring results from these statistical analyses can be found in Table 6. Additionally, the fit metric scores for the final model relative to the rest of the design iterations can be found in Table D.1 in Appendix D. The fit metric plots for the tension, compression, head lag, and head CG analyses for the final model can be found in Figures D.1-D.4, also in Appendix D.

Table 7: The fit metric scores for each simulation obtained by using the FitMetric program

Simulation	Fit Metric Score (out of 100)
Tension	71.4
Compression	70.3
Head Lag	5.8
Head CG	16.9
X-Displacement Timing	91.2
Z-Displacement Timing	64.2
Total Score (out of 100)	53.3

The plots in Figures 51-56 and the fit metric scores in Table 7 indicate the best combined overall results obtained over the course of the entire design process. An important observation

that needs to be made is that the fit metric scores for the final design are not the highest scores obtained over the course of the semester. Table D.1 in Appendix D clearly demonstrates that some of the previous designs had scores that exceeded the overall fit metric score for the final design. Specifically, the FB8 model had the highest overall combined fit metric score.

The reason the FB8 design was not selected as the final design is because the stress analysis, which was performed late in the design process, revealed that the FB8 model had a fatal flaw. The analysis demonstrated that the stresses in the rods and slider spring exceeded the ultimate tensile stresses of the materials used to make them. Therefore, it was determined that the FB8 model was not physically possible given the materials being used, and that design changes needed to be made to lower the stress values experienced by the failing components.

Only a few additional design iterations could be made in the amount of time that was left after performing the revealing stress analysis. As such, a compromise was reached. Changes were made to lower the stresses in the at-risk components, and the fit metric score decreased as a result. Unfortunately, the few design iterations that were made did not succeed in completely lowering the experienced stresses below the ultimate tensile stresses of the materials. However, the stresses are much more manageable in the final model than in the FB8 model.

The fit metric scores for the final model, although lower than other previous models, are considered the best because they have the lowest relative stresses experienced by the at-risk components, and is therefore the design that will need to be improved upon to yield a model that does not exceed the ultimate tensile stresses of its materials. With this knowledge in mind, the results presented for the final model can be appreciated better compared to the results from the other design iterations.

The tension and compression responses in Figures 51 and 52, respectively, fit within the corridors very well, especially when the IARV cutoffs are taken into consideration. When the responses are cut off at the IARVs, almost the entire tension and compression responses reside within the corridors. The reason the scores for both simulations are in the 70s is because the nonlinearity of the chloroprene rubber causes the responses to have a degree of curvature, resulting in a lower regression score. As such, all of the design iterations had tension and compression responses that were nonlinear to some degree, and the fit metric scores for the final model were the highest out of all of the iterations. Additionally, please note that two lines are visible in the compression response due to slight movement of the slider during high compressive strains.

The head lag response in Figure 53 demonstrates the effectiveness of the slider component of the final model. As can be seen in the plot, the head angle remained relatively constant as the neck angle increased from 0 to approximately 30 degrees. At this point, the head angle increased sharply as the head rotated down towards the chest. Then, after this sharp increase, in the final model simulation, the head contacted the chest, resulting in an increase in the neck angle but not in the head angle.

While the plot in Figure 53 demonstrates the advantages of the slider system, it also demonstrates one of the major drawbacks of the design; insufficient head extension out from the body. The response plot stops at approximately 69 degrees of head rotation and 54 degrees of neck rotation, even though the corridor extends to a head angle of 80 degrees and a neck angle of 75 degrees. If the neck was extended further out from the chest than in the final model, then both the head and the neck would be able to rotate more, and the response would continue to the end of the corridor.

The head lag response for the final model closely resembles the corridor up until a certain point. Past that point, the model fails to satisfy the head lag performance specification corridor. It is also important to note that the fit metric score of 5.8 for the head lag of the final model is low compared to many of the other design iterations. This is due to the fact that after the stress analysis, the spring in the slider system was changed significantly to reduce the stress it experienced during a frontal impact. This change, although it preserved the shape of the lag response, shifted the response up slightly, to the point where most of the response was outside of the corridor. As a result, even though the shape of the head lag response was very accurate, its positioning due to the new spring resulted in a lower fit metric score.

When examining the head lag response curve in Figure 53, please note that both the loading and unloading phases are present in the plot. The nearly straight line that is significantly outside of the corridor represents the unloading phase, which was not designed for and was ignored in the data analysis.

The head CG response in Figure 54 again demonstrates the effects of the slider assembly, as well as the extension drawback of the final model. Please note that the top red line represents the loading phase of the response to a high velocity frontal impact, and the lower line represents the unloading phase, which was ignored during data analysis. The response closely follows the shape of the head CG corridor initially, but then rises above the corridor due to the presence of the slider. Some of the previous design iterations had head CG responses within the corridor for a majority of the time, but again, they could not be used after the stress analysis. Additionally, in order to get the response curve within the head CG corridor, the dynamics of the slider system would need to be altered, thereby adversely affecting the head lag response. The lag and CG responses in the final model represent a balance between designing for the two constraints.

As with the head lag response, the head CG response is meant to continue to the end of the corridor. However, due to the fact that the final model did not extend the head far enough away from the body to allow for increased rotation and downward movement in the z-direction, the response curve stopped before it reached the end of the corridor. Additionally, a loop can be seen at the lower right end of the response curve. This loop is due to the premature contact of the chin with the chest, resulting in a stop of the downward z movement and an increase in the forward x movement at the end of the response. With a design that allowed for better extension

of the head away from the body, it is hypothesized that the head CG response would continue to the end of the corridor.

Figure 55 shows the x-displacement timing response for the final model. The final model actually exhibited the highest ranking fit metric score for this parameter compared to the rest of the design iterations. The peak value was within the range of the corridor, and the time of that peak value was right on the edge of the corridor. Therefore, the final design yielded excellent x-displacement timing results. One thing to note is that the notch just prior to the peak is when the chin contacted the chest. After examining the effects of the chin-chest contact on the head CG response, this contact likely artificially shifted the magnitude of the peak up and the timing of the peak to the right. In fact, the notch just before the peak shows that the x-displacement was beginning to decrease prior to the chin-chest contact. As a result, if this chin-chest contact was avoided, the peak would have been where the notch was. Therefore, the chin-chest contact artificially yielded better results, but this contact was common throughout all of the designs. A model with improved head extension from the body would require additional tweaking to better fit the x-displacement timing corridor.

The plot in Figure 56 indicates that the z-displacement timing peak was not close to the corridor. The magnitude of the z-displacement was too small, and the peak displacement occurred too quickly. Interestingly, the chin-chest contact was not evident on the z-displacement plot, likely because this contact had a smaller effect on the z-displacement than it did on the x-displacement. The magnitude issue of the z-displacement would be solved by a model with better head extension outward from the body, and the time of the peak could be shifted by altering the slider system response to a frontal impact.

As mentioned previously, the final model does not rank the best in the fit metric scores for both the individual and total scores. The rankings for each score can be found in Table 8. The reason for this is because of the design changes that had to be made to reduce stress values compromised the fit metric scores. Given more time, the new, lower-stress model could have been improved upon to yield fit metric scores with higher rankings across the board, thereby providing more objective reasons to choose this model. However, the lower-stress design was improved as much as possible to yield the highest fit metric scores possible in the given amount of time.

Table 8: The ranking of the final model's fit metric scores relative to the other 15 design iterations tested with the FitMetric MATLAB program

Fit Metric	Final Model Overall Rank (out of 15)
Tension	6th
Compression	5th
Head Lag	11th
Head CG	1st
X-Displacement Timing	1st
Z-Displacement Timing	8th
Overall Score	5th

Unfortunately, the FitMetric MATLAB program was not developed until approximately halfway through the design process during the semester. Furthermore, it was not finalized and made robust until near the end of the process. As a result, the fit metric was not applied to every iteration along the way. Rather, the fit metric analysis was performed on a majority of the data after the fact. This is why the results do not consistently show an improvement in the fit metric score for each design iteration.

If the design process were to continue, the fit metric would be used for each iteration to allow for more informed design alterations. Additionally, an objective score would be determined and set by the team, such that if that score was exceeded, the design process would be stopped. Without doing this, the design process would continue indefinitely, with each iteration attempting to reach perfection. The design team has recognized the value of a fit metric statistical analysis, and acknowledges that its continued use throughout the semester likely would have resulted in more verification tests throughout the process. This may have enabled the team to discover the stress issues earlier in the design process, which would have allowed more lower-stress design iterations to be performed before the end of the semester.

The final model was selected because it had the highest overall fit metric value, which was comparable to other high-ranking models, out of all of the lower-stress design iterations. The reason design was halted at this model was because the team ran out of time, and was forced to decide upon a model that displayed the best fit metric scores while demonstrating more realistic stress values in the components.

e. Stress Failure

As previously mentioned, while Team SQUAD's final model did not fail the stress analysis test in tension or compression, one of the group's most prevalent obstacles was avoiding the failure stress during the frontal impact testing. The team got to a point where they were satisfied with the responses, but the stresses on the spring and the back rod for NBDL exceeded the ultimate tensile stress of their materials (failure stress of both chloroprene rubber and ABR rubber is about 15 MPa). Changing the spring to a stiffer material and/or a larger surface area not only worsened the CG and lag responses that previously hit the corridors, but it also increased the amount of stress on the back rod, so failure still would have occurred. The group determined specifically which node within both the spring and the back rod endured the greatest amount of stress and plotted this with respect to time, which gives some idea of where in the simulation this failure would occur.

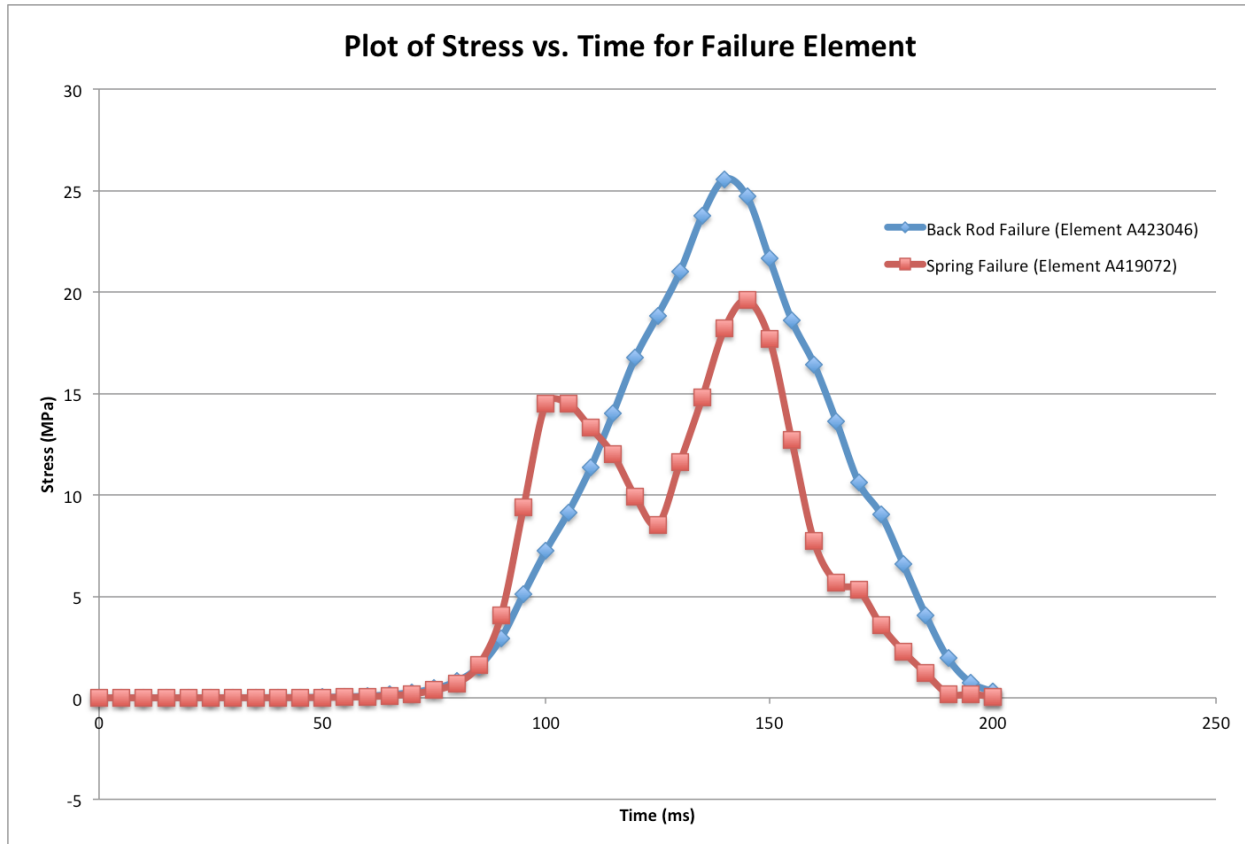


Figure 57: Plot of stress vs. time for the two most failure-prone parts of final model.

f. Ethical Concerns

As a conscientious engineering group, Team SQUAD is aware of the present, but mostly innocuous, ethical concerns surrounding the production of our neck model. Namely, manufacturers of the model should know that transportation of uninhibited chloroprene has been banned in the United States by the US Department of Transportation, and that stabilized chloroprene is in hazard class 3, a flammable liquid [24].

In addition to the chemical hazard ethical concerns, Team SQUAD would like to issue a disclaimer that it did not fabricate any data during the design process. It would be unethical to release a model that did not mimic a six-year old neck to a reasonable degree. This is because human lives depend on appropriate vehicle safety design.

Conclusion

a. Limitations

From the beginning of this course when the class was given the charge and description of the design challenge, Team SQUAD realized that there would be a number of challenges to overcome at nearly every phase of the process. When creating the performance specification proposals, a rather significant limitation was the lack of data on the mechanical properties of the six-year old neck. As previously discussed, this is to be expected for a number of reasons. However, this lack of data makes the group's estimates and methods of deduction much less reliable. Many other groups were forced to make drastic assumptions and potentially illegitimate mathematical correlations in an effort to reach some plausible conclusion of the reality of this understudied mechanical behavior. From a design and iterative perspective, Team SQUAD was also limited by using a computer program that seemed to crash unexpectedly, which made it very difficult to move forward in an efficient manner.

b. Next Steps and Final Remarks

Unfortunately, this semester came and went very quickly, so quickly that Team SQUAD was not able to complete all of the analysis that they would have liked in order to create a better model. As a result, given more time to complete this project, there are a number of things that the group could do differently. First, it would have been helpful to receive the prioritization of performance specifications earlier in the design process. One of the most difficult challenges the team faced during the iteration phase was stepping through performance specifications not knowing which to prioritize. Weeks into the design process, the class was informed that an additional specification, timing, was not only required, but it was also the number one priority of all of the performance specifications. This prioritization makes sense from a mechanical and biofidelic standpoint, but because the class was not initially aware of this requirement, Team SQUAD's design, even from the brainstorming stage, did not account for this. Unless a group's design turned out lucky, being midway through the design process and then needing to redirect focus

can either require a completely new beginning or some sharp innovation. Challenges are indeed what push engineers to think outside of the box, but this was nonetheless one aspect that Team SQUAD would have changed, so that the group's focus could have been on the correct goals.

Team SQUAD was overall satisfied with the final results from the specifications standpoint, but there is always room for improvement. Specifically, the next steps would be to correct for the two most significant issues that the group could not seem to correct for during the past few weeks as the deadline approached. The first issue concerned the z-displacement timing response. Every trial fell short of the mark that the team was aiming for: the head needed to drop down further and reach its maximum displacement later in the impact. The second issue was failure analysis. In both tension and compression, the activated rods stayed well underneath the ultimate failure stress threshold. However, for the frontal impact test, both the spring and the rods exceeded their ultimate stress value. Team SQUAD needed the spring and the rods to be made of compliant materials for specific reasons: the spring, so that the frontal impact loading would allow the head to sufficiently translate forward before rotating downwards, and the rods to help the head bend downwards. However, the material could not be so compliant that the range of motion caused the material to rupture. If given more time, Team SQUAD's next step would be to search more thoroughly in various material databases and to experiment with materials that fulfilled these needs with more success.

References

- [1] Nightingale, R. 2015, "BME432: Lecture 2: History and Charge."
- [2] Nightingale, R. 2015, "BME432: Lecture 7: 6 Year Old Design and Performance Specifications, and Injury Assessment Reference Values,".
- [3] Nightingale, R., McElhaney, J., Camacho, D., Kleinberger, M. et al., "The Dynamic Responses of the Cervical Spine: Buckling, End Conditions, and Tolerance in Compressive Impacts," SAE Technical Paper 973344, 1997, doi:10.4271/973344.
- [4] Nuckley, David J., David R. Linders, and Randal P. Ching. "Developmental biomechanics of the human cervical spine." *Journal of Biomechanics* 46.6 (2013): 1147-54. Print.
- [5] Nightingale, R., Doherty, B., Myers, B., McElhaney, J. et al., "The Influence of End Condition on Human Cervical Spine Injury Mechanisms," SAE Technical Paper 912915, 1991, doi:10.4271/912915.
- [6] Dibb, Alan Thomas. "Pediatric Head and Neck Dynamic Response: A Computational Study." Diss. Duke U, 2011. Print.
- [7] Chancey, Valeta Carol, et al. "Improved Estimation of Human Neck Tensile Tolerance: Reducing the range of reported tolerance using anthropometrically correct muscles and optimized physiologic initial conditions." *Stapp Car Crash Journal* 47 (2003): n. pag. Print.
- [8] Irwin, A. and Mertz, H., "Biomechanical Basis for the CRABI and Hybrid III Child Dummies," SAE Technical Paper 973317, 1997, doi:10.4271/973317.
- [9] Luck, Jason F., et al. "Tensile Failure Properties of the Perinatal, Neonatal, and Pediatric Cadaveric Cervical Spine." *SPINE* 38.1 (2013): E1-E12. Print.
- [11] Thunnissen, J., Wismans, J., Ewing, C., and Thomas, D., "Human Volunteer Head-Neck Response in Frontal Flexion: A New Analysis," SAE Technical Paper 952721, 1995, doi:10.4271/952721.
- [12] Arbogast, Kristy B., et al. "Comparison of Kinematic Responses of the Head and Spine for Children and Adults in Low-Speed Frontal Sled Tests." *Stapp Car Crash Journal* 59 (2009): 329-72. Print.
- [13] Seacrist, Thomas, Kristy B. Arbogast, and Matthew R. Maltese. "Kinetics of the cervical spine in pediatric and adult volunteers during low speed frontal impacts." *Journal of Biomechanics* 45 (2011): 99-106. Print.

[14] Dibb, Alan T., et al. "Tension and Combined Tension-Extension Structural Response and Tolerance Properties of the Human Male Ligamentous Cervical Spine." *Journal of Biomechanical Engineering* 131 (2009): n. pag. Print.

[16] "Nat'l Highway Traffic Safety Admin., DOT : 571.208 Standard No. 208; Occupant Crash Protection." Web. 4 Dec. 2015.

[17] "Nat'l Highway Traffic Safety Admin., DOT : 571.213 Standard No. 213; Child Restraint Systems." Web. 4 Dec. 2015

[18] Multipurpose 6061 Aluminum, 1" Thick x 4" Width.
<<http://www.mcmaster.com/#8975k242/=103d40y>>

[19] Multipurpose 6061 Aluminum, 5/8" Thick x 2" Width.
<<http://www.mcmaster.com/#8975k77/=103d53s>>

[20] Multipurpose 6061 Aluminum Rod, 2-¾" Diameter.
<<http://www.mcmaster.com/#8974k51/=103d615>>

[21] Multipurpose 6061 Aluminum Rod, 3-½" Diameter.
<<http://www.mcmaster.com/#8974k88/=103d6kx>>

[22] CR rubber 232/244/ DCR213 Chloroprene rubber.
<http://www.alibaba.com/product-detail/CR-rubber-232-244-DCR213-Chloroprene_60360295367.html?spm=a2700.7724857.29.1.Wr1aNi&s=p>

[23] COMMERCIAL GRADE SBR, MAXIMUM CONTINUOUS LENGTH 50 FEET .500 X 1.00" X LINEAR F. <<http://store20.prestostore.com/catalog.php/rsrstore/pd2174882>>

[24] Wikipedia contributors. "Chloroprene." *Wikipedia, The Free Encyclopedia*. Wikipedia, The Free Encyclopedia, 16 Nov. 2015. Web. 3 Dec. 2015.

[25] FAQs, REX Plastics. <<http://rexplastics.com/faqs>>

Appendix A - Engineering Drawings

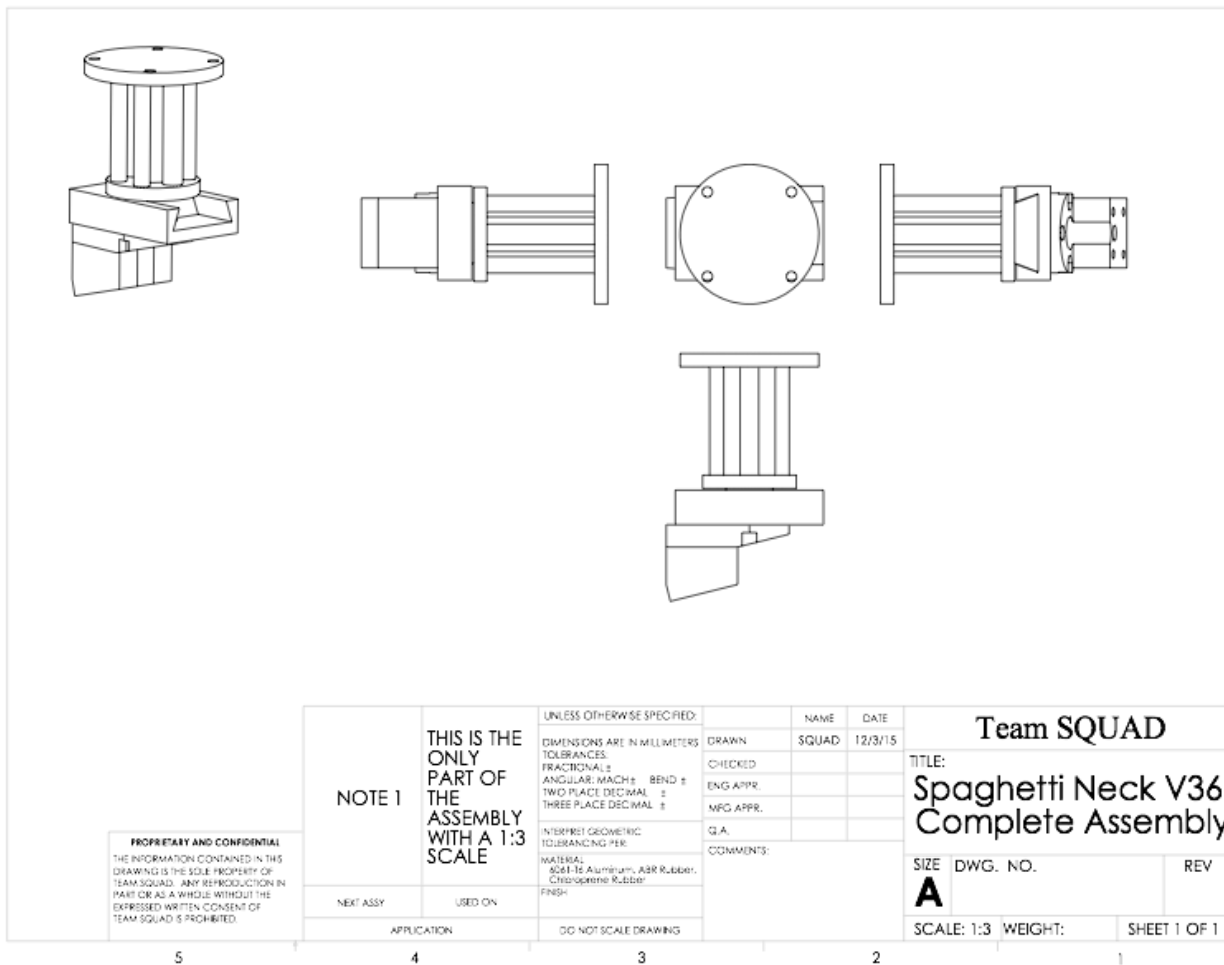


Figure A.1: Engineering drawing of Spaghetti Neck V36 full assembly (including neck bracket).

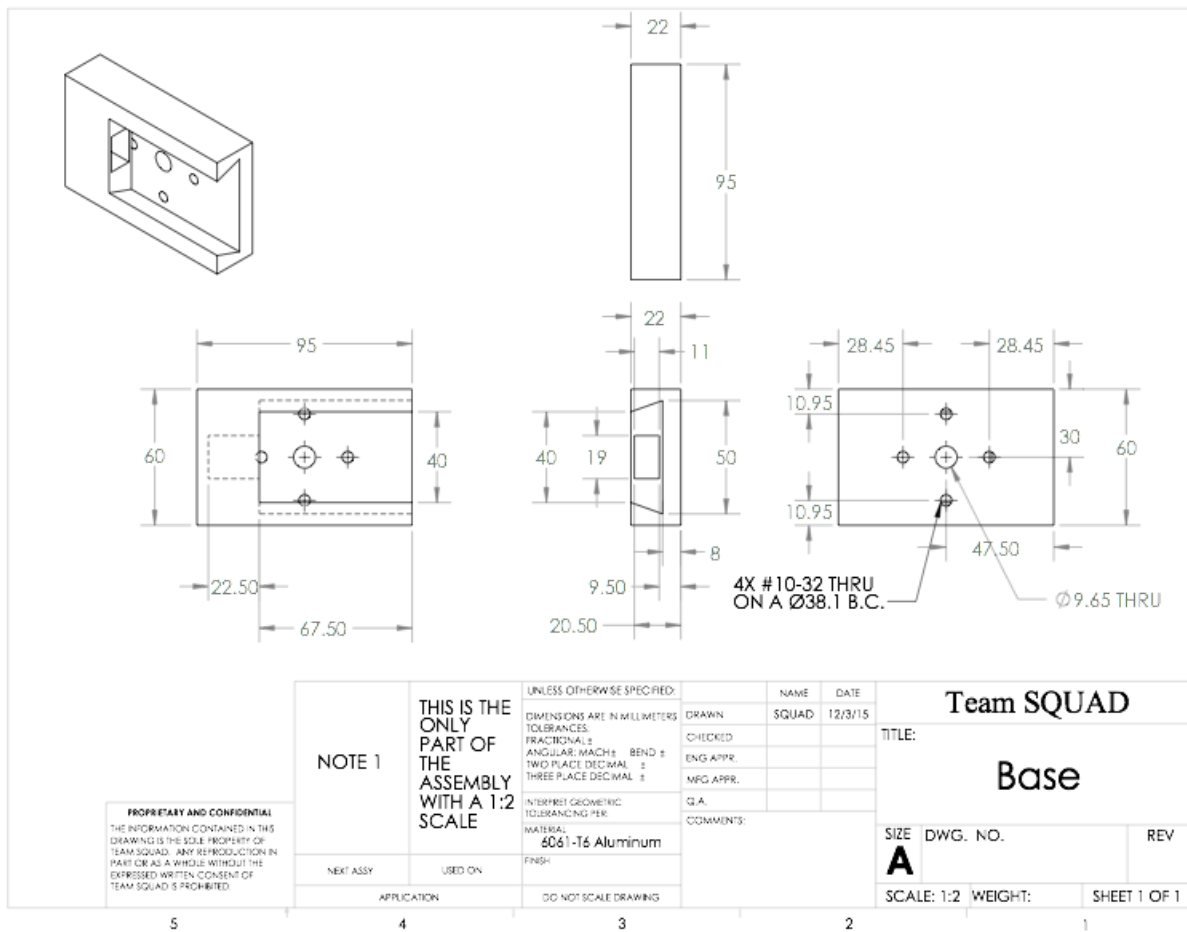


Figure A.2: Engineering drawing of base (also referred to as slider base).

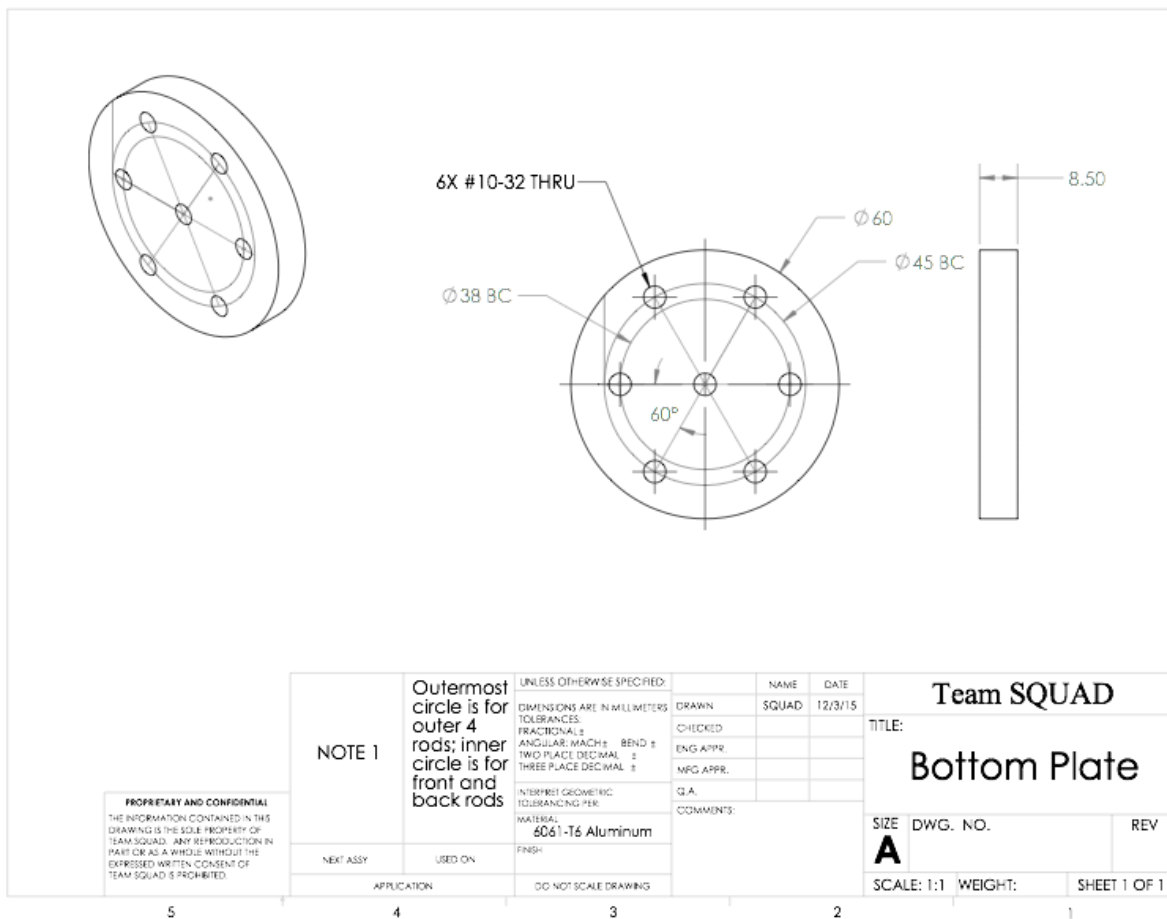


Figure A.3: Engineering drawing of bottom plate.

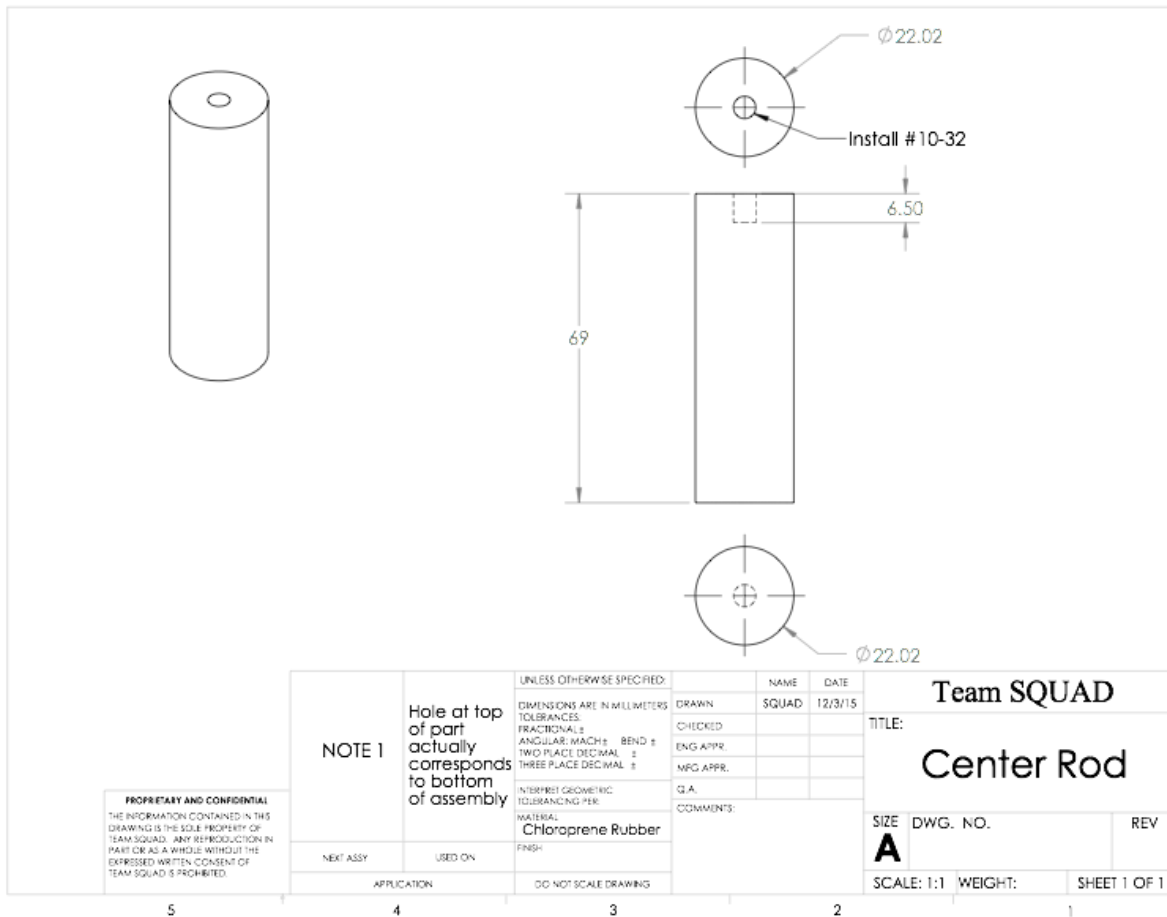


Figure A.4: Engineering drawing of center rod.

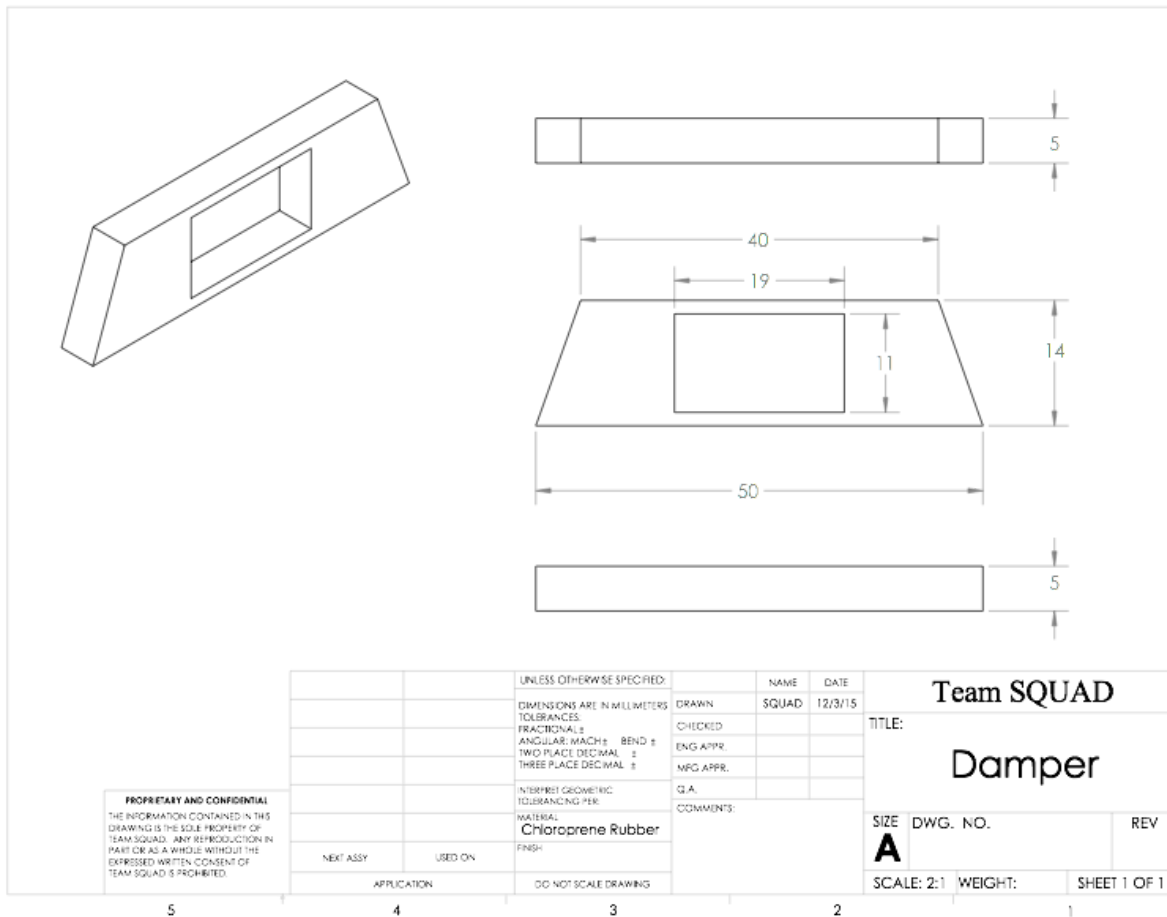


Figure A.5: Engineering drawing of damper (also referred to as thin bumper).

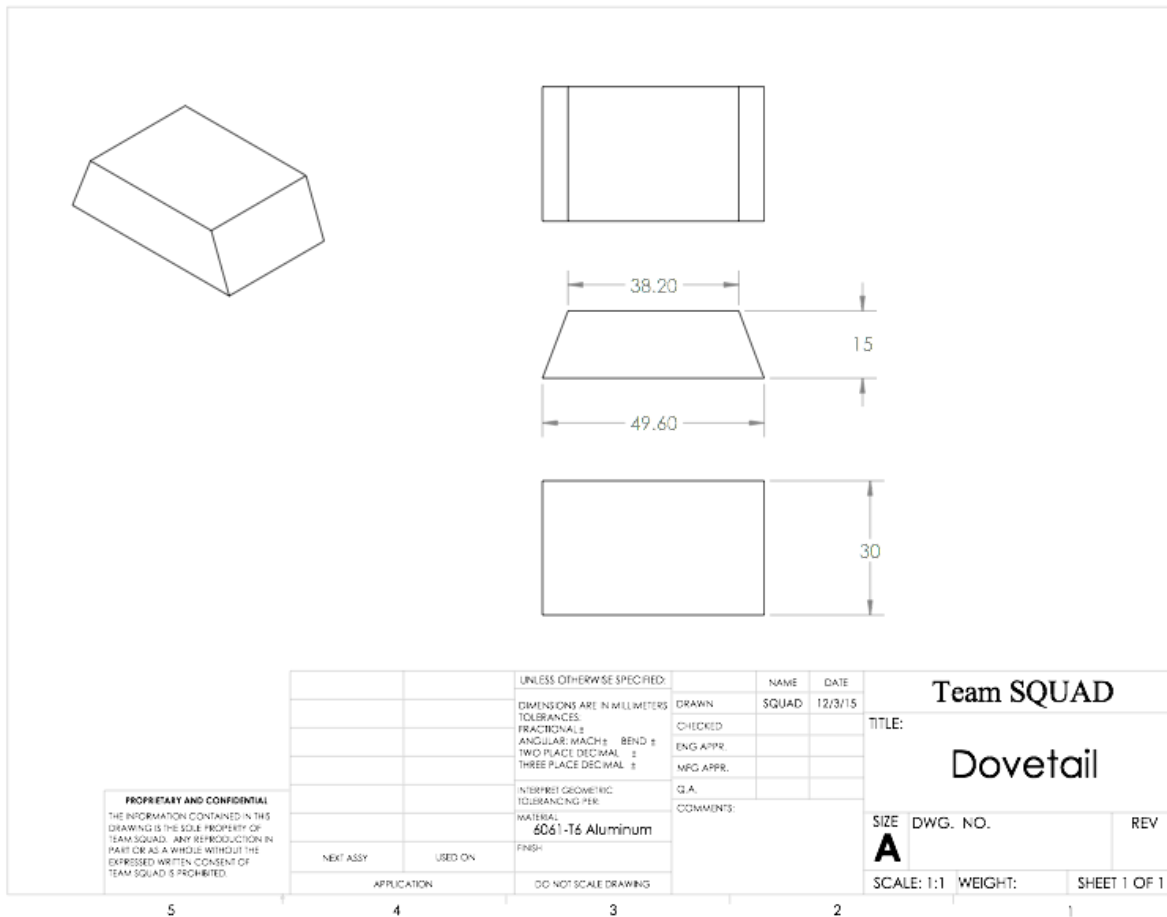


Figure A.6: Engineering drawing of dovetail (also referred to as slider nub).

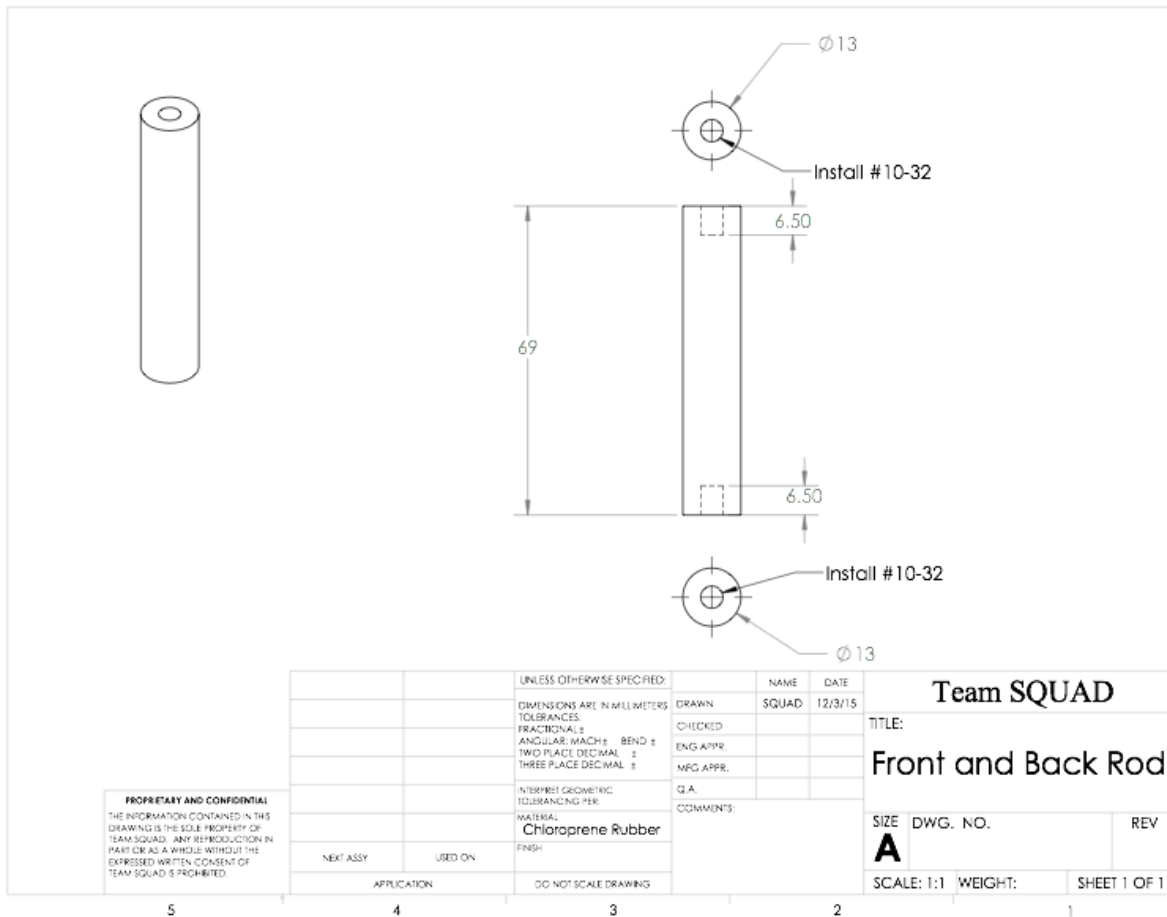


Figure A.7: Engineering drawing of front and back rods.

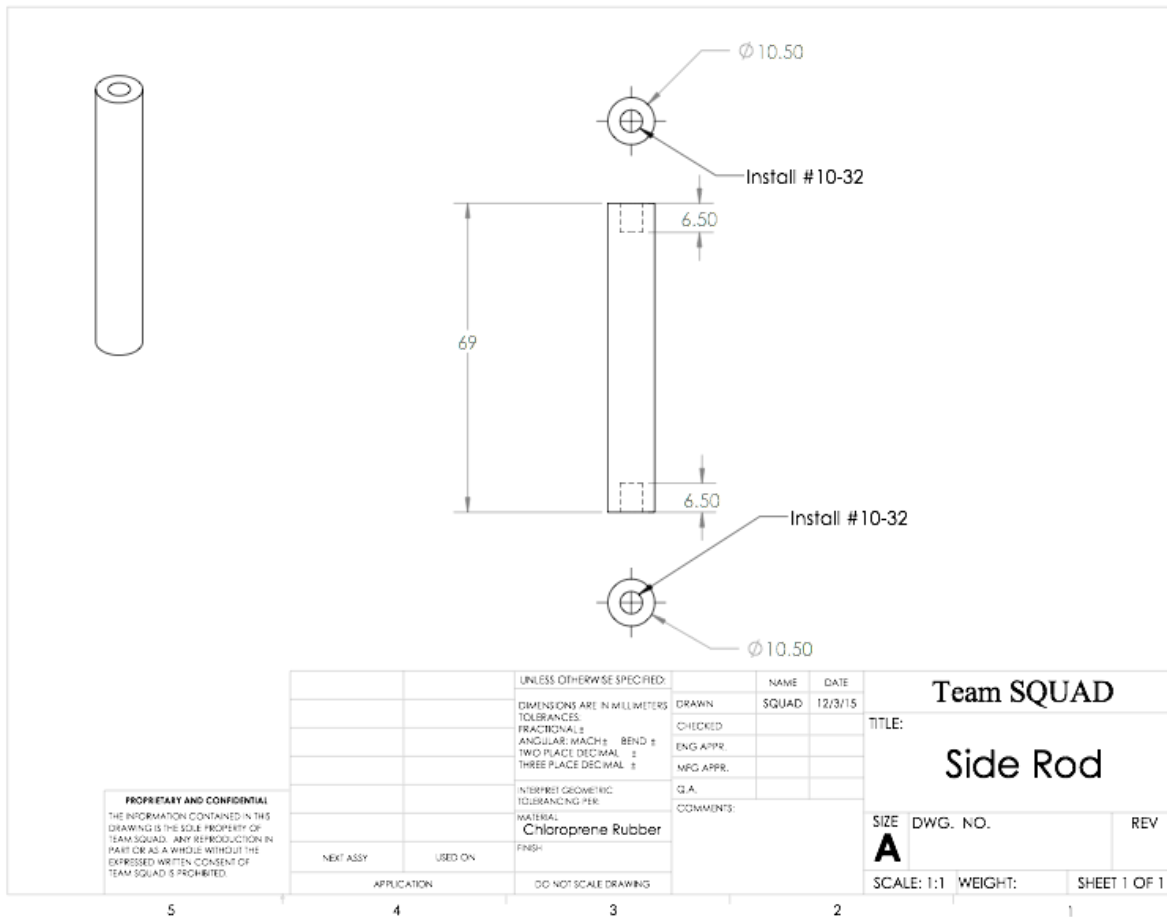


Figure A.8: Engineering drawing of the side rods (x4).

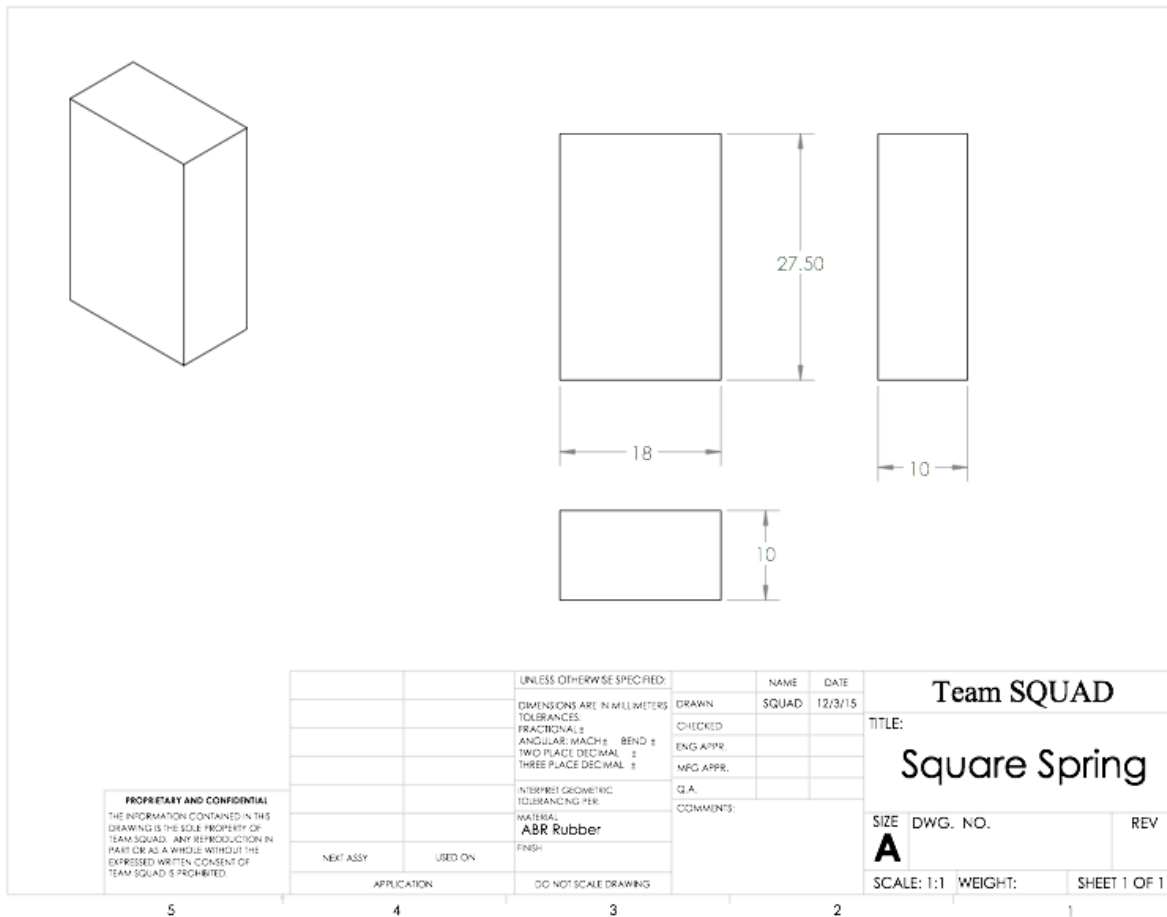


Figure A.9: Engineering drawing of square spring.

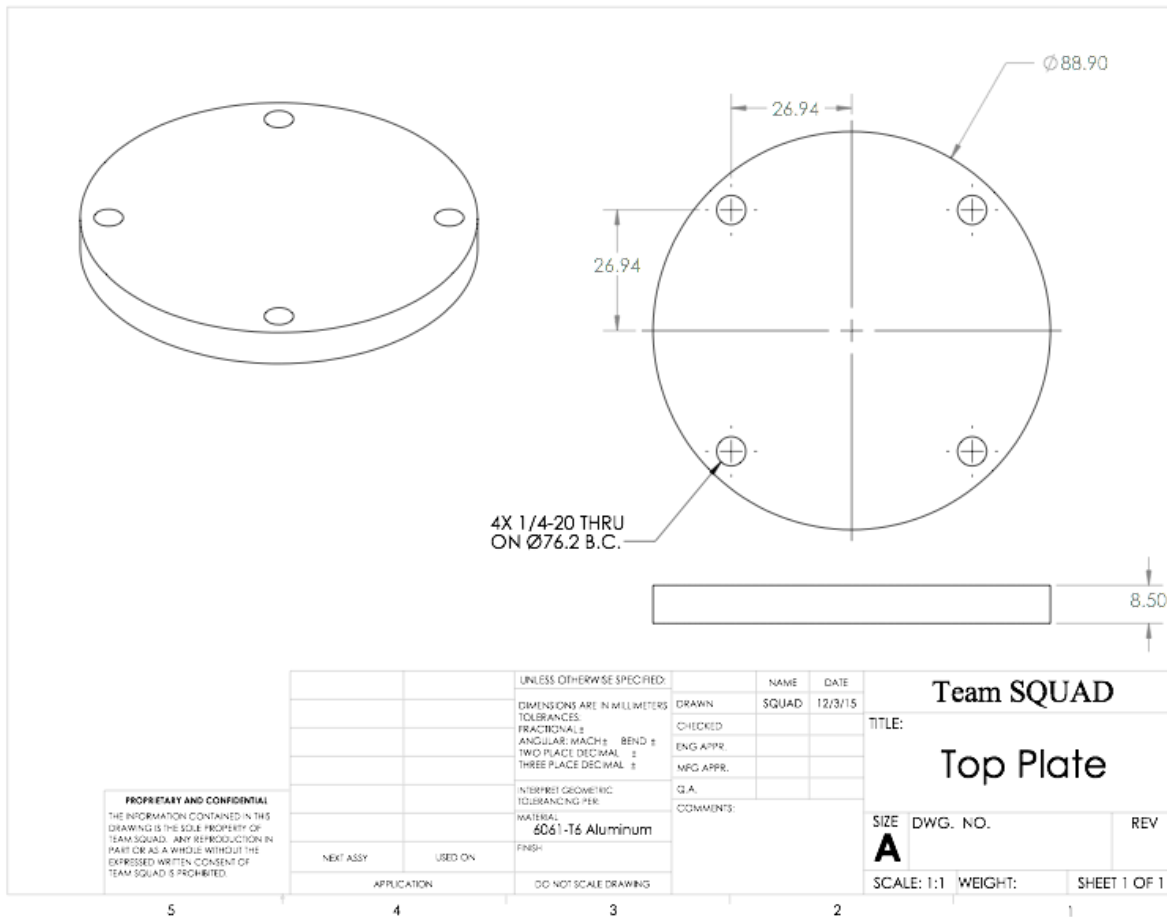


Figure A.10: Engineering drawing of top plate.

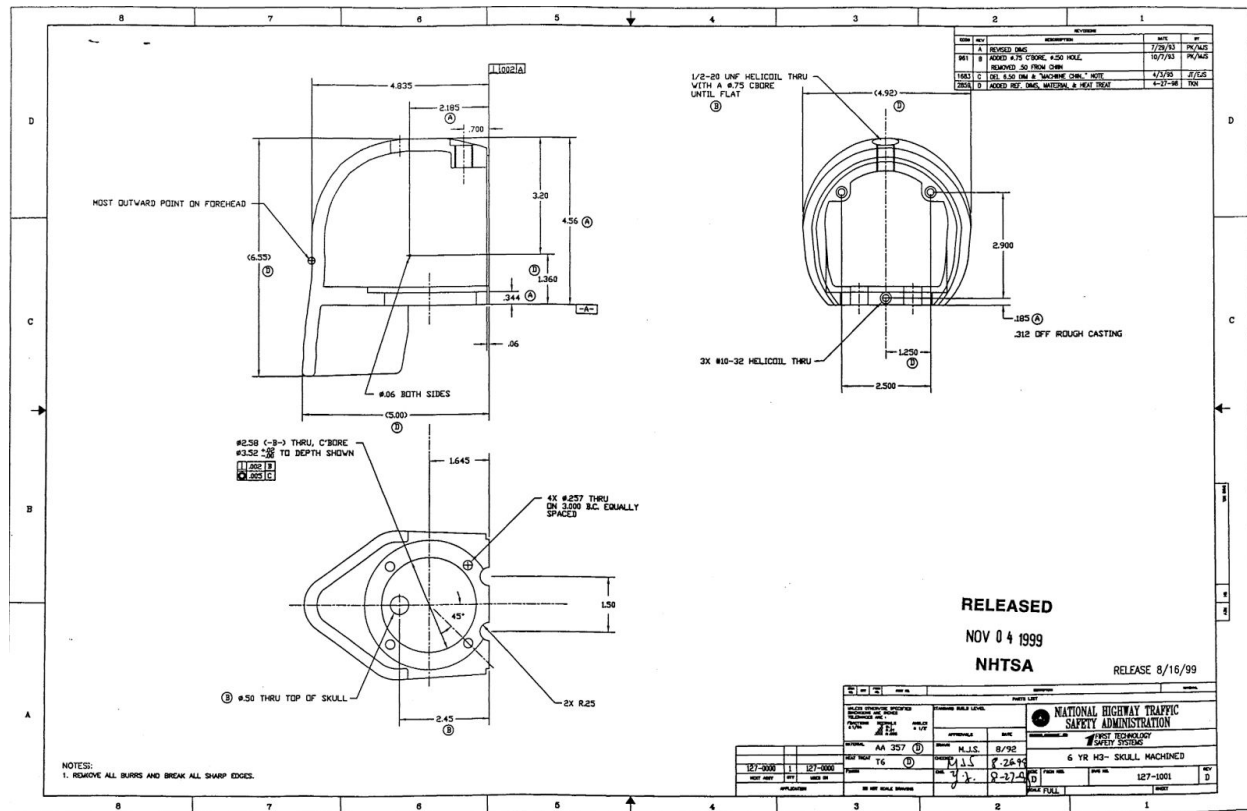


Figure A.11: Engineering drawing of the H-III Head Base.

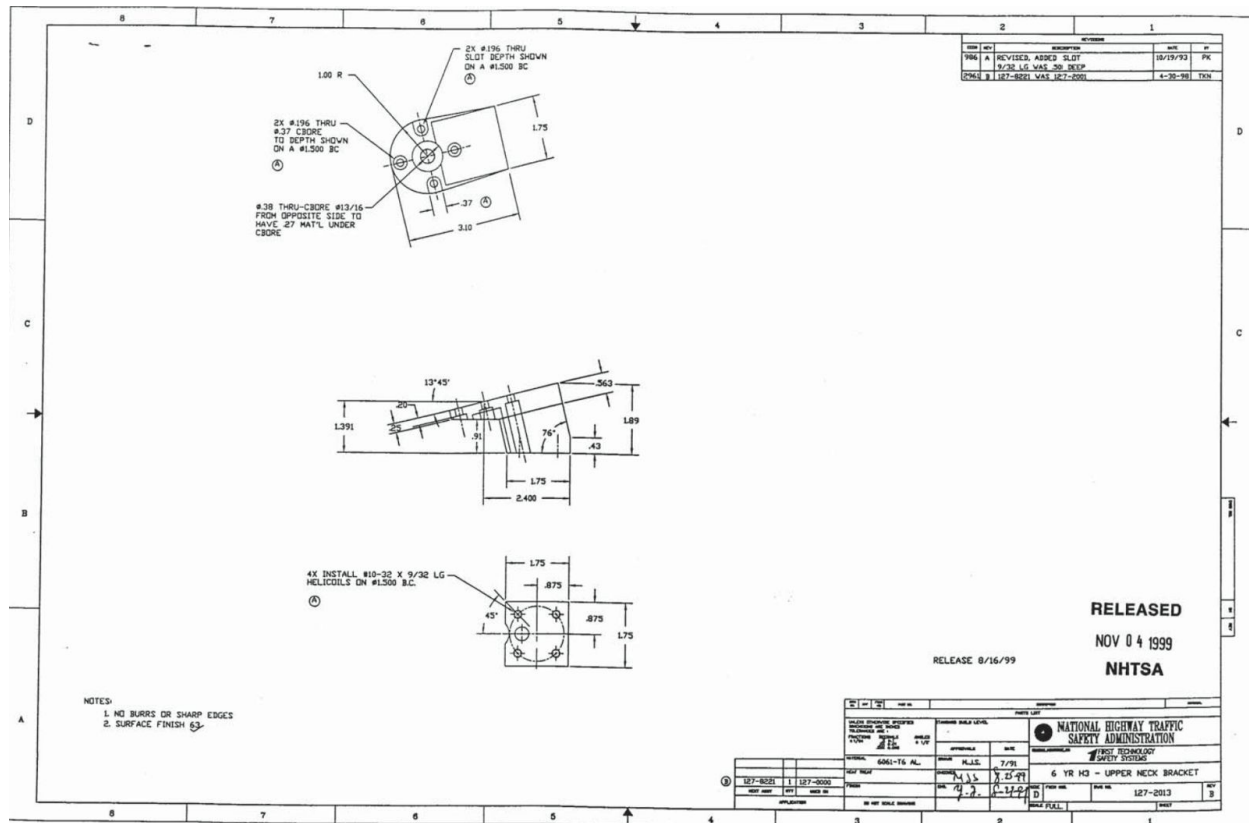


Figure A.12: Engineering drawing of the lower neck bracket.

Appendix B - Convergence Study

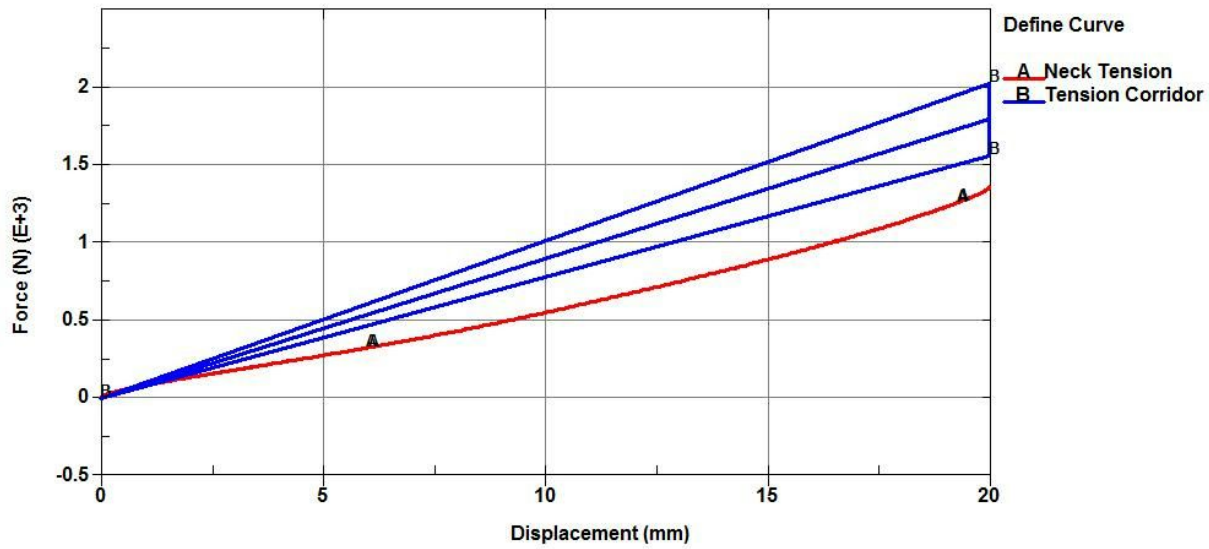


Figure B.1: Tensile response of the neck model at an element scale of 2.00.

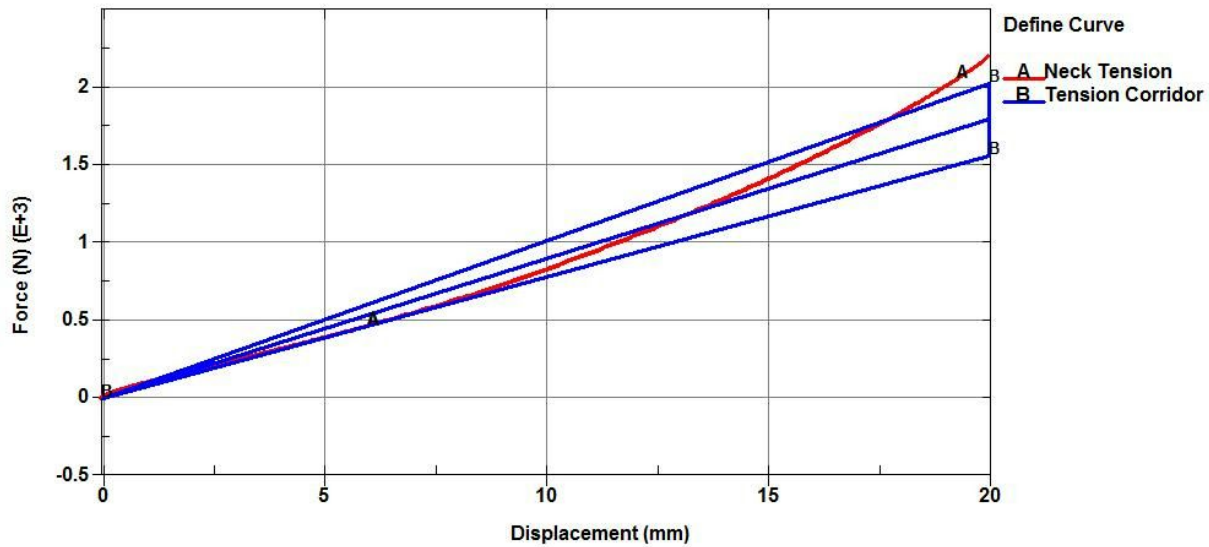


Figure B.2: Tensile response of the neck model at an element scale of 1.50.

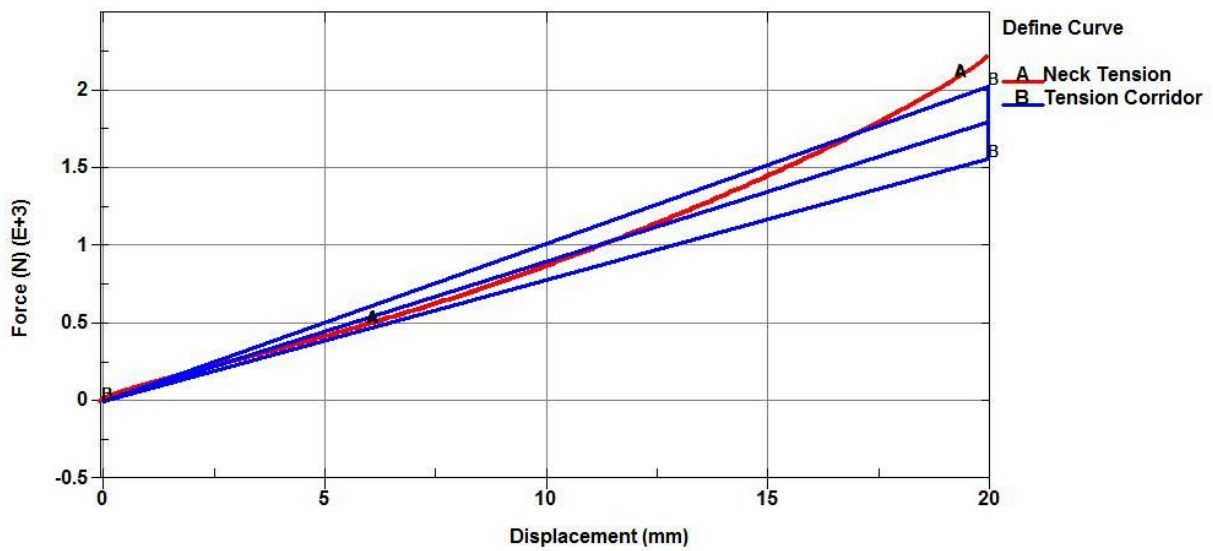


Figure B.3: Tensile response of the neck model at an element scale of 1.25.

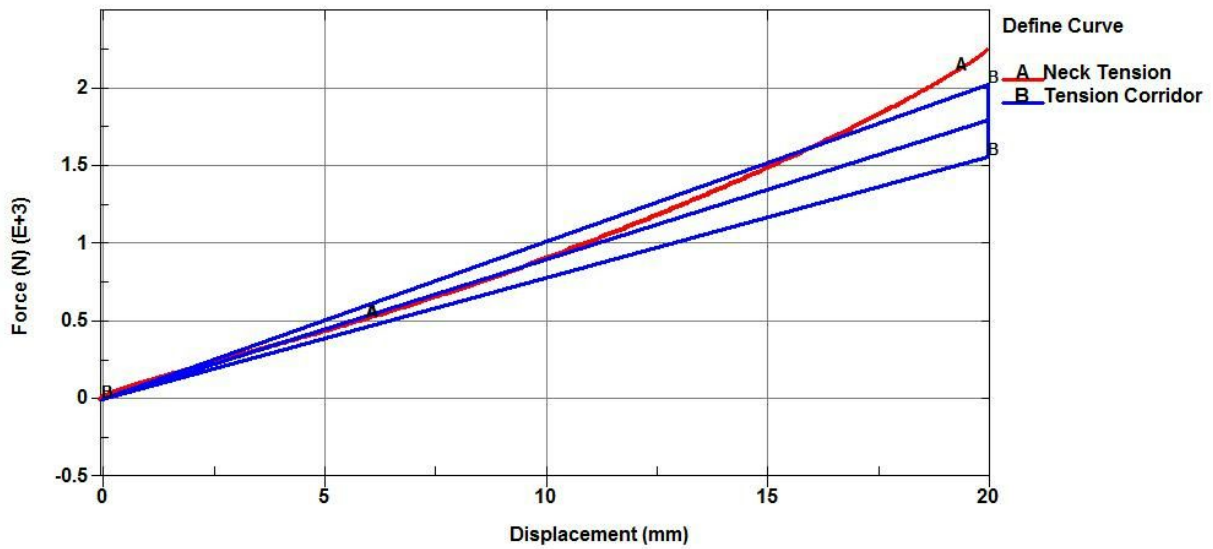


Figure B.4: Tensile response of the neck model at an element scale of 1.00.

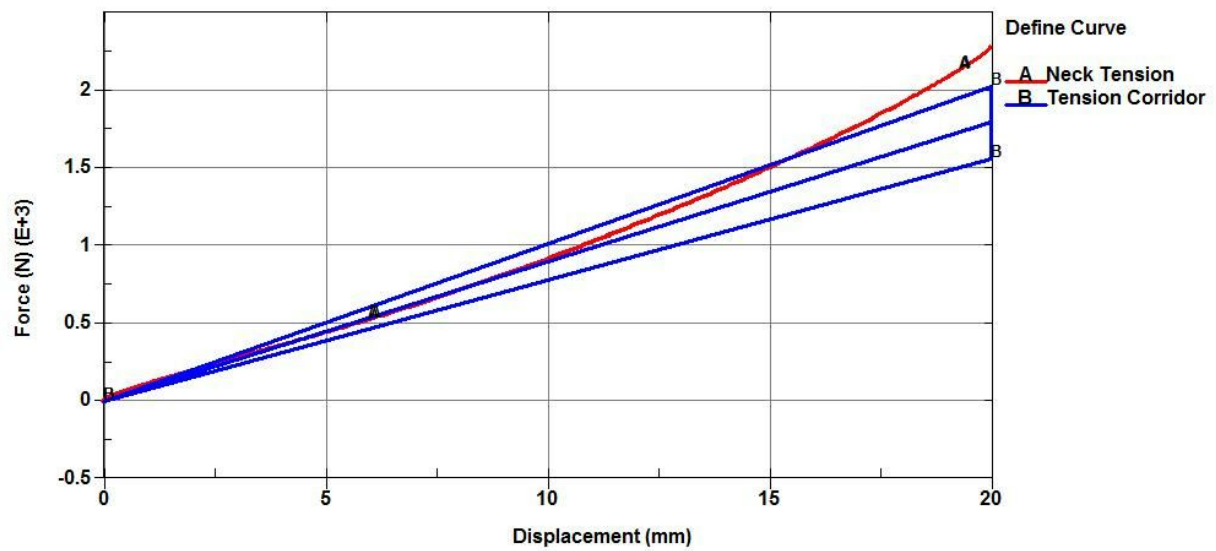


Figure B.5: Tensile response of the neck model at an element scale of 0.75.

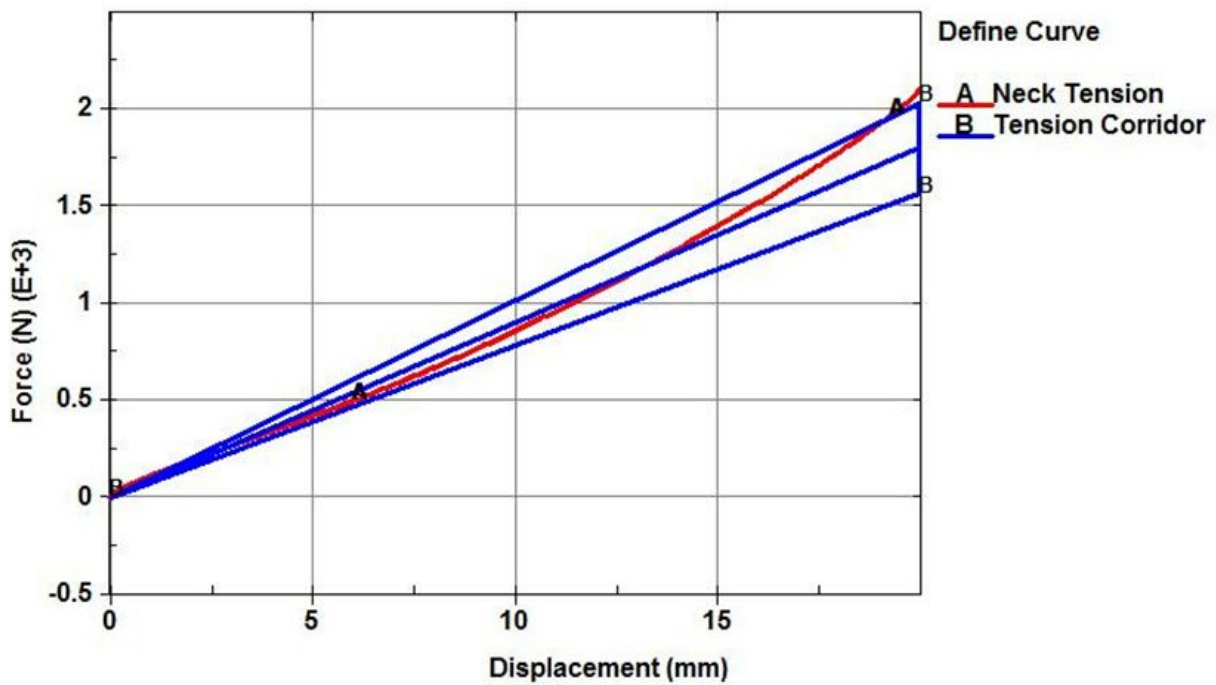


Figure B.6: Tensile response of the neck model at an element scale of 0.50.

Appendix C - FitMetric MATLAB Code

```
% This script will enable a user to input file names from a specific
% test of the neck and receive two "goodness of fit" values on a scale
% from 1-100 for both the goodness of fit of being within the corridor and
% the goodness of fit of being close to the center line of the corridor
% (this only applies for tension and compression). This is an automated
% script, but requires manual input of the file names in Excel format in
% order to work.

% This script is a collaborative effort by Team Squad (Sutton, Ruprecht,
% Freyburger, and Method) and was written by Method for the sole use by
% Team Squad.

% Original preparation date: November 11, 2015

%% Initialize the workspace

% Type the Excel filename without the .xls extension
filename = 'Z_Timing_3';

data = xlsread(filename);
list = {'Tension','Compression','CG','Lag','X_Timing','Z_Timing'};

x = strncmp(filename,list,2);

if x(1) == 1
    corridor = 'Tension';
elseif x(2) == 1
    corridor = 'Compression';
elseif x(3) == 1
    corridor = 'CG';
elseif x(4) == 1
    corridor = 'Lag';
elseif x(5) == 1
    corridor = 'X';
elseif x(6) == 1
    corridor = 'Z';
end

%
% Begin the case for "Tension"
```

```

%
if strcmp(corridor,'Tension') == 1
    % Sort the imported data
    middle = 90.*data(:,1);
    q = find(middle>=1490,1,'first');
    xval = data(1:q,1); % Displacement data
    yval = data(1:q,2); % Force data

    % Establish the tension corridor
    lower = 78.*xval;
    middle = 90.*xval;
    upper = 101.5.*xval;

fit = 0;
% The total length of the corridor is approx 17.6mm, meaning that each
% section is approx 4.4mm
a1 = find(xval>=xval(end)*.25,1,'first');
a2 = find(xval>=xval(end)*.5,1,'first');
a3 = find(xval>=xval(end)*.75,1,'first');
a4 = find(xval==xval(end));

% Determine the score for how much the curve is within the corridor
for i = 1:length(xval)
    if (yval(i)/lower(i))>=1 && (yval(i)/upper(i))<=1
        if i>a1 && i<=a2
            fit = fit + .1; % Adds a score of .1 for being within the second quarter of the corridor
        elseif i>a2 && i<=a3
            fit = fit + .15; % Adds a score of .15 for being within the third quarter of the corridor
        elseif i>a3 && i<=a4
            fit = fit + .75; % Adds a score of .7 for being within the fourth quarter of the corridor
        end
    end
end

% A score of totpot is possible
totpot = ((a2-a1).*1)+((a3-a2).*15)+((a4-a3).*75);
corrscor = fit./totpot;
corrscor = corrscor.*100;

% Determine the score for how close the curve is to the center line
% aka, find the R^2 value of fitting the curve with the center line
yresid = yval - middle;
SSresid = sum(yresid.^2);

```

```

SStotal = (length(yval)-1).*var(yval);
rsq = 1 - SSresid/SStotal;
rscore = 1/(1-rsq);
% Determine the score by calculating the inverse of 1-rsq
% A score of 100 is possible
if rscore >= 100
    rscore = 100;
end

% Total the two scores to combine into one fit metric
% A TOTAL score of 300 is possible
total = 2*corrsscore + rscore; % Weight the corridor higher than the regression
finalscore = total/300;
finalscore = finalscore*100;

% Print the table with the results
fprintf("\n Corridor Score = %2.4g/100 \n", corrsscore);
fprintf("\n Regression Score = %2.4g/100 \n", rscore);
fprintf("\n Total Score = %2.4g/100 \n", finalscore);

figure(1);clf;
plot(xval,yval,'k-',xval,lower,'b-',xval,middle,'r-',xval,upper,'b-')
title('Tension Response')
%
% End of the tension case
%
%
% Begin the compression case
%
elseif strcmp(corridor,'Compression') == 1
    % Sort the imported data
    middle = 155.4.*data(:,1);
    q = find(middle<=-1820,1,'first');
    xval = data(1:q,1); % Displacement data
    yval = data(1:q,2); % Force data

    % Establish the compression corridor
    lower = 196.9.*xval;
    middle = 155.4.*xval;
    upper = 113.9.*xval;

fit = 0;

```

```

% The total length of the corridor is approx 17.6mm, meaning that each
% section is approx 4.4mm
a1 = find(xval<=xval(end)*.25,1,'first');
a2 = find(xval<=xval(end)*.5,1,'first');
a3 = find(xval<=xval(end)*.75,1,'first');
a4 = find(xval==xval(end));

% Determine the score for how much the curve is within the corridor
for i = 1:length(xval)
    if (yval(i)/lower(i))<=1 && (yval(i)/upper(i))>=1
        if i>a1 && i<=a2
            fit = fit + .1; % Adds a score of .1 for being within the second quarter of the corridor
        elseif i>a2 && i<=a3
            fit = fit + .15; % Adds a score of .15 for being within the third quarter of the corridor
        elseif i>a3 && i<=a4
            fit = fit + .75; % Adds a score of .7 for being within the fourth quarter of the corridor
        end
    end
end

% A score of q/4 is possible (4 segments, each segment with a maximum
% percentage of q/4)
totpot = ((a2-a1).*1)+((a3-a2).*15)+((a4-a3).*75);
corrscor = fit./totpot;
corrscor = corrscor.*100;

% Determine the score for how close the curve is to the center line
% aka, find the R^2 value of fitting the curve with the center line
yresid = yval - middle;
SSresid = sum(yresid.^2);
SStotal = (length(yval)-1).*var(yval);
rsq = 1 - SSresid/SStotal;
rscore = 1/(1-rsq);

% Determine the score by calculating the inverse of 1-rsq
% A score of 100 is possible
if rscore >= 100
    rscore = 100;
end

% Total the two scores to combine into one fit metric
% A TOTAL score of 300 is possible
total = 2*corrscor + rscore; % Weight the corridor higher than the regression

```

```

finalscore = total/300;
finalscore = finalscore*100;

% Print the table with the results
fprintf("\n Corridor Score = %2.4g/100 \n", corrscore);
fprintf("\n Regression Score = %2.4g/100 \n", rscore);
fprintf("\n Total Score = %2.4g/100 \n", finalscore);

figure(1);clf;
plot(xval,yval,'k-',xval,lower,'b-',xval,middle,'r-',xval,upper,'b-')
title('Compression Response')

%
% End of the compression case
%

%
% Begin the head lag case
%
elseif strcmp(corridor,'Lag') == 1
    % Sort the imported data
    xval = data(:,1); % Displacement data
    yval = data(:,2); % Force data

    % Trim the data so it's just the first portion
    maxxval = find(xval==max(xval));
    xval = xval(1:maxxval);
    yval = yval(1:maxxval);

    % Establish the head lag corridor
    a = 1;
    b = find(xval>=29,1,'first');
    c = find(xval>=37,1,'first');
    d = find(xval>=48,1,'first');
    if isempty(d) == 1
        d = find(xval == max(xval)) - 5;
    end
    ef = find(xval == max(xval));
    g = d;
    h = c;
    i = b;

    AB = (-1.99/29).*xval(a:b);

```

```

BC = (6.47+1.99)/(37-29).*xval(b:c) - 32.6575;
CD = (40.6-6.47)/(48-37).*xval(c:d) - 108.3309;
DE = (73.8-40.6)/(73-48).*xval(d:ef) - 23.144;
AI = (4.51/29).*xval(a:i);
IH = (18-4.51)/(37-29).*xval(i:h) - 44.3912;
HG = (56.7-18)/(48-37).*xval(h:g) - 112.1727;
GF = (97.8-56.7)/(73-48).*xval(g:ef) - 22.2120;

fit = 0;
% Determine how long the curve is within the corridor
for j = 1:length(xval)
if j>=1 && j<=b
if yval(j)/AB(j)>=1 && yval(j)/AI(j)<=1
    fit = fit + 1;
end
elseif j>b && j<=c
if yval(j)/BC(j-b)>=1 && yval(j)/IH(j-b)<=1
    fit = fit + 1;
end
elseif j>c && j<=d
if yval(j)/CD(j-c)>=1 && yval(j)/HG(j-c)<=1
    fit = fit + 1;
end
elseif j>d && j<=ef
if yval(j)/DE(j-d)>=1 && yval(j)/GF(j-d)<=1
    fit = fit + 1;
end
end
end
totalscore = length(xval);
lagscore = fit/totalscore;
lagscore = lagscore*100;
fprintf('\n Lag Corridor Score = %2.4g/100 \n', lagscore);
figure(1);clf;
plot(xval,yval,'r-')
hold on
plot(xval(a:b),AB,'k-');plot(xval(b:c),BC,'k-');plot(xval(c:d),CD,'k-');
plot(xval(d:ef),DE,'k-');plot(xval(a:i),AI,'k-');plot(xval(i:h),IH,'k-');
plot(xval(h:g),HG,'k-');plot(xval(g:ef),GF,'k-');
hold off
title('Lag Response')
%
% End of head lag case

```

```

%
%
% Begin the head CG case
%
elseif strcmp(corridor,'CG') == 1
    % Sort the imported data
    xval = data(:,1); % Displacement data
    yval = data(:,2); % Force data

    % Trim the data so it's just the first portion
    maxxval = find(xval==max(xval));
    xval = xval(1:maxxval);
    yval = yval(1:maxxval);

    % Establish the head lag corridor
    a = 1;
    b = find(xval>=97.1,1,'first');
    c = find(xval>=133,1,'first');
    if isempty(c)==1
        c = find(xval==max(xval))-1;
    end
    de = find(xval == max(xval));
    f = find(xval>=126,1,'first');
    g = find(xval>=98.6,1,'first');

    b = floor(mean([b g]));
    g = b;
    c = floor(mean([c f]));
    f = c;

    AB = (123-137)/(97.1-47).*xval(a:b) + 150.1337;
    BC = (82.4-123)/(133-97.1).*xval(b:c) + 232.8123;
    CD = (29-82.4)/(154-133).*xval(c:de) + 414.8738;
    AG = (116-137)/(98.6-47).*xval(a:g) + 156.1279;
    GF = (73-116)/(126-98.6).*xval(g:f) + 270.7372;
    FE = (15.2-73)/(141-126).*xval(f:de) + 565.2451;

    fit = 0;
    % Determine how long the curve is within the corridor
    for j = 1:length(xval)
        if j>=1 && j<=b
            if yval(j)/AB(j)<=1 && yval(j)/AG(j)>=1

```

```

        fit = fit + 1;
    end
    elseif j>b && j<=c
        if yval(j)/BC(j-b)<=1 && yval(j)/GF(j-g)>=1
            fit = fit + 1;
        end
        elseif j>c && j<=de
            if yval(j)/CD(j-c)<=1 && yval(j)/FE(j-f)>=1
                fit = fit + 1;
            end
        end
        totalscore = length(xval);
        cgsscore = fit/totalscore;
        cgsscore = cgsscore*100;
        fprintf('\n CG Corridor Score = %2.4g/100 \n', cgsscore);

figure(1);clf;
plot(xval,yval,'r-')
hold on
plot(xval(a:b),AB,'k-');plot(xval(b:c),BC,'k-');plot(xval(c:de),CD,'k-');
plot(xval(a:g),AG,'k-');plot(xval(g:f),GF,'k-');plot(xval(f:de),FE,'k-');
hold off
title('CG Response')
%
% End the CG case
%
%
% Begin the x timing case
%
elseif strcmp(corridor,'X') == 1
    % Sort the imported data
    xval = data(:,1); % Displacement data
    yval = data(:,2); % Force data

    % Establish center of the timing box
    timexx = 151;
    timexy = 148;

    % Determine the maximum and the coordinate of the maximum from the data
    maxpoint = max(yval);
    index = find(yval==max(yval));

```

```

maxindex = xval(index);

% Determine the distance away from the center of the corridor
distance = sqrt((maxpoint-timexy).^2+(maxindex-timexx).^2);
score = (100-distance);
if score < 0
score = 0;
end

fprintf('\n X Timing Score = %2.4g/100 \n', score);

%
% End the x timing case
%

%
% Begin the z timing case
%
elseif strcmp(corridor,'Z') == 1
    % Sort the imported data
    xval = data(:,1); % Displacement data
    yval = data(:,2); % Force data

    % Establish center of the timing box
    timezx = 163;
    timezy = 18;

    % Determine the minimum and the coordinate of the minimum from the data
    minpoint = min(yval);
    index = find(yval==min(yval));
    minindex = xval(index);

    % Determine the distance away from the center of the corridor
    distance = sqrt((minpoint-timezy).^2+(minindex-timezx).^2);
    score = (100-distance);
    if score < 0
    score = 0;
    end

    fprintf('\n Z Timing Score = %2.4g/100 \n', score);
end

```

Appendix D - Final FitMetric Results

Table D.1: The FitMetric results for many of the design iterations.

Name	Compression	Tension	CG	Lag	X	Z	Total	NBDL Only
Final Assembly	70.3	71.36	16.92	5.816	91.19	64.17	53.29267	44.524
SquareSpringAssembly5	72.31	64.52	4.381	0	72.55	51.81	44.26183	32.18525
SquareSpringAssembly4	70.49	64.58	4.125	17.31	86.7	67.01	51.7025	43.78625
SquareSpringAssembly1	69.81	61.62	0	0	0	0	21.905	0
DovetailAssembly1ABR	0	0	4.301	0	70.88	50.51	20.9485	31.42275
DovetailAssembly1Chloro	0	0	8.65	10.14	73.27	59.21	25.21167	37.8175
ChloroRub_Slider_6rods_Stopper_FB11	70.18	20.91	0	2.066	0	0	15.526	0.5165
ChloroRub_Slider_6rods_Stopper_FB10	70.66	98.63	13.44	9.821	87.66	60.63	56.80683	42.88775
ChloroRub_Slider_6rods_Stopper_FB9	70.05	68.99	9.456	10.34	84.56	62.1	50.916	41.614
ChloroRub_Slider_6rods_Stopper_FB8	65.54	100	15.83	11.23	87.33	69.45	58.23	45.96
ChloroRub_Slider_6rods_Stopper_FB7	31	100	10.42	25.04	80.83	74.98	53.71167	47.8175
ChloroRub_Slider_6rods_Stopper_FB5	29.34	51.55	8.333	26.32	81.46	77.23	45.7055	48.33575
ChloroRub_Assembly_Slider_6rods_Stopper_3	24.05	97.53	7.53	18.21	79.99	74.46	50.295	45.0475
Chloro_Neck5	72.41	100	11.58	6.571	76.03	65.75	55.39017	39.98275
Chloro_Neck3withcontacts	0.7096	0.7649	12.88	23.26	78.91	70.85	31.22908	46.475

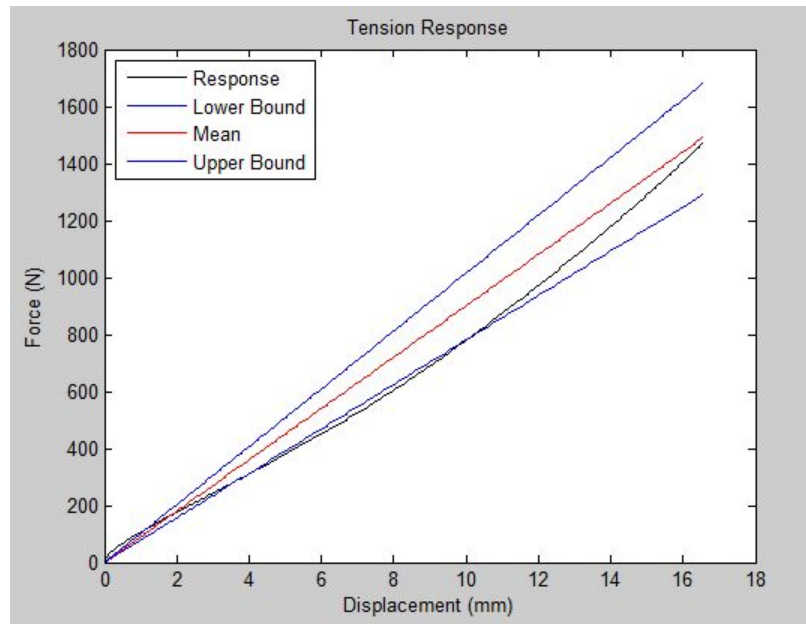


Figure D.1: The FitMetric tension response MATLAB plot.

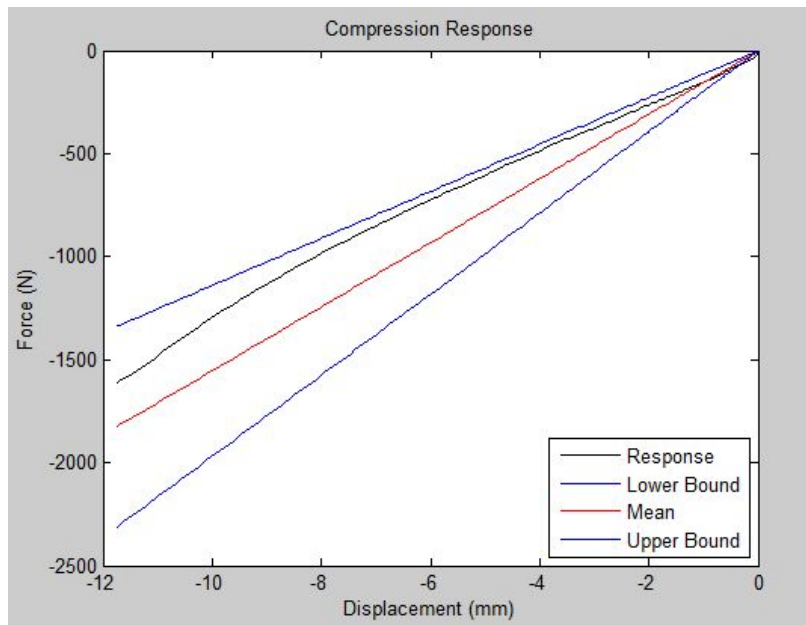


Figure D.2: The FitMetric compression response MATLAB plot.

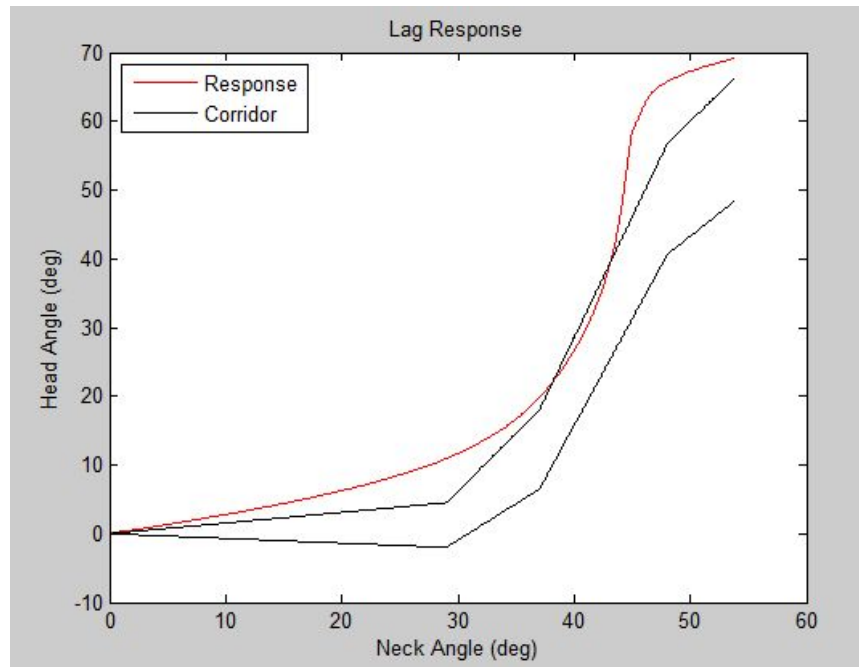


Figure D.3: The FitMetric head lag response MATLAB plot.

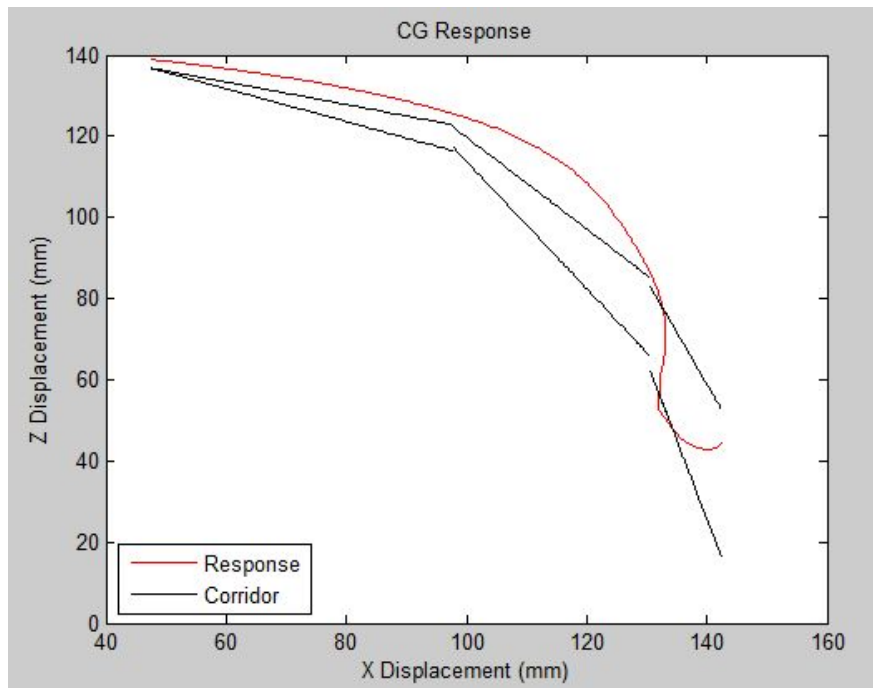


Figure D.4: The FitMetric head CG response MATLAB plot.

Appendix E - CFiles

SurfaceImportAndShells20_13parts.cfile:

```
#$ LS-PrePost command file created by LS-PrePost 4.2 (Beta) - 15Oct2014(08:00)
-64bit-Window
#$ Created on Oct-01-2015 (14:47:32)
$#
$# Modified to use the commands for the new GUI interface
$#
$# Start by exporting an IGS assembly with all parts from Solidworks
$#
open iges "C:\Users\team5\AutomationTests\SquareSpringAssembly4.IGS"
ac
rx 10
ry 10
rz 10
$#
$# Mesh Part 1
component off all
component on all 1
ac
selectpart select 0
geselect target occobject
occfilter clear
occfilter add Face
geselect allvis
occmesh mesh 0, 1 1 1 3 0
occmesh accept 1 0.0001 0 1
$#
$# Mesh Part 2
component off all
component on all 2
ac
selectpart select 0
geselect target occobject
occfilter clear
occfilter add Face
geselect allvis
occmesh mesh 0, 1 1 1 6 0
occmesh accept 1 0.0001 0 1
$#
$# Mesh Part 3
```

```
component off all
component on all 3
ac
selectpart select 0
geselect target occobject
occfilter clear
occfilter add Face
geselect allvis
occmesh mesh 0, 1 1 1 4.5 0
occmesh accept 1 0.0001 0 1
$#
$# Mesh Part 4
component off all
component on all 4
ac
selectpart select 0
geselect target occobject
occfilter clear
occfilter add Face
geselect allvis
occmesh mesh 0, 1 1 1 6 0
occmesh accept 1 0.0001 0 1
$#
$# Mesh Part 5
component off all
component on all 5
ac
selectpart select 0
geselect target occobject
occfilter clear
occfilter add Face
geselect allvis
occmesh mesh 0, 1 1 1 4.5 0
occmesh accept 1 0.0001 0 1
$#
$# Mesh Part 6
component off all
component on all 6
ac
selectpart select 0
geselect target occobject
occfilter clear
occfilter add Face
```

```
geselect allvis
occmesh mesh 0, 1 1 1 4.5 0
occmesh accept 1 0.0001 0 1
$#
$# Mesh Part 7
component off all
component on all 7
ac
selectpart select 0
geselect target occobject
occfilter clear
occfilter add Face
geselect allvis
occmesh mesh 0, 1 1 1 4.5 0
occmesh accept 1 0.0001 0 1
$#
$# Mesh Part 8
component off all
component on all 8
ac
selectpart select 0
geselect target occobject
occfilter clear
occfilter add Face
geselect allvis
occmesh mesh 0, 1 1 1 4.5 0
occmesh accept 1 0.0001 0 1
$#
$# Mesh Part 9
component off all
component on all 9
ac
selectpart select 0
geselect target occobject
occfilter clear
occfilter add Face
geselect allvis
occmesh mesh 0, 1 1 1 4.5 0
occmesh accept 1 0.0001 0 1
$#
$# Mesh Part 10
component off all
component on all 10
```

```
ac
selectpart select 0
geselect target occobject
occfilter clear
occfilter add Face
geselect allvis
occmesh mesh 0, 1 1 1 4.5 0
occmesh accept 1 0.0001 0 1
$#
$# Mesh Part 11
component off all
component on all 11
ac
selectpart select 0
geselect target occobject
occfilter clear
occfilter add Face
geselect allvis
occmesh mesh 0, 1 1 1 4.5 0
occmesh accept 1 0.0001 0 1
$# Top Plate
$# Mesh Part 12
component off all
component on all 12
ac
selectpart select 0
geselect target occobject
occfilter clear
occfilter add Face
geselect allvis
occmesh mesh 0, 1 1 1 3 0
occmesh accept 1 0.0001 0 1
$# Add more parts as needed
$#
component on all
component off geom all
$#
$# Mesh Part 13
component off all
component on all 13
ac
selectpart select 0
geselect target occobject
```

```

occfilter clear
occfilter add Face
geselect allvis
occmesh mesh 0, 1 1 1 2 0
occmesh accept 1 0.0001 0 1
## Add more parts as needed
##
component on all
component off geom all
ac

```

NormalsAndTests20_13parts.cfile:

```

## LS-PrePost command file created by LS-PrePost 4.1 (Beta) - 21Jan2014(01:00)
-64bit-Window
## Created on Oct-16-2014 (09:33:21)
##
## Now we renumber parts, reverse normals and make tetmeshes
##
## Part 1
##
component off all
component on fem 1
ac
geselect target part
geselect part add part 1/0
renumber renumkind 270
renumber renumkind 170
renumber renumkind 134
renumber setbypart 100000 100000 100000 1
renumber keyword 1
renumber clearbypart
geselect clear
geselect target shell
geselect shell add shell 100001
normal autoreverse 100001
tetmesh skin 100000 0 0 0
tetmesh mesh
tetmesh accept 100001 0
partdata delete 100000
delement accept
rx 10
rx -10
##

```

```
$# Part 2
$#
component on fem 2
ac
geselect target part
geselect part add part 2/0
renumber renumkind 270
renumber renumkind 170
renumber renumkind 134
renumber setbypart 200000 200000 200000 2
renumber keyword 1
renumber clearbypart
geselect clear
geselect target shell
geselect shell add shell 200001
normal autoreverse 200001
tetmesh skin 200000 0 0 0
tetmesh mesh
tetmesh accept 200001 0
partdata delete 200000
delement accept
rx 10
rx -10
$#
$# Part 3
$#
component on fem 3
ac
geselect target part
geselect part add part 3/0
renumber renumkind 270
renumber renumkind 170
renumber renumkind 134
renumber setbypart 300000 300000 300000 3
renumber keyword 1
renumber clearbypart
geselect clear
geselect target shell
geselect shell add shell 300001
normal autoreverse 300001
tetmesh skin 300000 0 0 0
tetmesh mesh
tetmesh accept 300001 0
```

```
partdata delete 300000
delement accept
rx 10
rx -10
$#
$# Part 4
$#
component on fem 4
ac
geselect target part
geselect part add part 4/0
renumber renumkind 270
renumber renumkind 170
renumber renumkind 134
renumber setbypart 400000 400000 400000 4
renumber keyword 1
renumber clearbypart
geselect clear
geselect target shell
geselect shell add shell 400001
normal autoreverse 400001
tetmesh skin 400000 0 0 0
tetmesh mesh
tetmesh accept 400001 0
partdata delete 400000
delement accept
rx 10
rx -10
$#
$# Part 5
$#
component on fem 5
ac
geselect target part
geselect part add part 5/0
renumber renumkind 270
renumber renumkind 170
renumber renumkind 134
renumber setbypart 500000 500000 500000 5
renumber keyword 1
renumber clearbypart
geselect clear
geselect target shell
```

```
geselect shell add shell 500001
normal autoreverse 500001
tetmesh skin 500000 0 0 0
tetmesh mesh
tetmesh accept 500001 0
partdata delete 500000
delement accept
rx 10
rx -10
$#
$#
$# Part 6
$#
component on fem 6
ac
geselect target part
geselect part add part 6/0
renumber renumkind 270
renumber renumkind 170
renumber renumkind 134
renumber setbypart 600000 600000 600000 6
renumber keyword 1
renumber clearbypart
geselect clear
geselect target shell
geselect shell add shell 600001
normal autoreverse 600001
tetmesh skin 600000 0 0 0
tetmesh mesh
tetmesh accept 600001 0
partdata delete 600000
delement accept
rx 10
rx -10
$#
$#
$# Part 7
$#
component on fem 7
ac
geselect target part
geselect part add part 7/0
renumber renumkind 270
renumber renumkind 170
renumber renumkind 134
```

```
renumber setbypart 700000 700000 700000 7
renumber keyword 1
renumber clearbypart
geselect clear
geselect target shell
geselect shell add shell 700001
normal autoreverse 700001
tetmesh skin 700000 0 0 0
tetmesh mesh
tetmesh accept 700001 0
partdata delete 700000
delement accept
rx 10
rx -10
$#
$# Part 8
$#
component on fem 8
ac
geselect target part
geselect part add part 8/0
renumber renumkind 270
renumber renumkind 170
renumber renumkind 134
renumber setbypart 800000 800000 800000 8
renumber keyword 1
renumber clearbypart
geselect clear
geselect target shell
geselect shell add shell 800001
normal autoreverse 800001
tetmesh skin 800000 0 0 0
tetmesh mesh
tetmesh accept 800001 0
partdata delete 800000
delement accept
rx 10
rx -10
$#
$# Part 9
$#
component on fem 9
ac
```

```
geselect target part
geselect part add part 9/0
renumber renumkind 270
renumber renumkind 170
renumber renumkind 134
renumber setbypart 900000 900000 900000 9
renumber keyword 1
renumber clearbypart
geselect clear
geselect target shell
geselect shell add shell 900001
normal autoreverse 900001
tetmesh skin 900000 0 0 0
tetmesh mesh
tetmesh accept 900001 0
partdata delete 900000
delement accept
rx 10
rx -10
$#
$# Part 10
$#
component on fem 10
ac
geselect target part
geselect part add part 10/0
renumber renumkind 270
renumber renumkind 170
renumber renumkind 134
renumber setbypart 20000 20000 20000 10
renumber keyword 1
renumber clearbypart
geselect clear
geselect target shell
geselect shell add shell 20001
normal autoreverse 20001
tetmesh skin 20000 0 0 0
tetmesh mesh
tetmesh accept 20001 0
partdata delete 20000
delement accept
rx 10
rx -10
```

```
$#
## Part 11
##
component on fem 11
ac
geselect target part
geselect part add part 11/0
renumber renumkind 270
renumber renumkind 170
renumber renumkind 134
renumber setbypart 30000 30000 30000 11
renumber keyword 1
renumber clearbypart
geselect clear
geselect target shell
geselect shell add shell 30001
normal autoreverse 30001
tetmesh skin 30000 0 0 0
tetmesh mesh
tetmesh accept 30001 0
partdata delete 30000
delement accept
rx 10
rx -10
##
## Part 12
##
component on fem 12
ac
geselect target part
geselect part add part 12/0
renumber renumkind 270
renumber renumkind 170
renumber renumkind 134
renumber setbypart 40000 40000 40000 12
renumber keyword 1
renumber clearbypart
geselect clear
geselect target shell
geselect shell add shell 40001
normal autoreverse 40001
tetmesh skin 40000 0 0 0
tetmesh mesh
```

```

tetmesh accept 40001 0
partdata delete 40000
delement accept
rx 10
rx -10
$#
$# Add more parts as needed
$#
$#
$# Part 13
$#
component on fem 13
ac
geselect target part
geselect part add part 13/0
renumber renumkind 270
renumber renumkind 170
renumber renumkind 134
renumber setbypart 50000 50000 50000 13
renumber keyword 1
renumber clearbypart
geselect clear
geselect target shell
geselect shell add shell 50001
normal autoreverse 50001
tetmesh skin 50000 0 0 0
tetmesh mesh
tetmesh accept 50001 0
partdata delete 50000
delement accept
rx 10
rx -10
$#
$# Add more parts as needed
$#
$#
component on fem all
component on fem all
ac

```

Sections20_13parts.cfile:

LS-PrePost command file created by LS-PrePost 4.2 (Beta) - 15Oct2014(08:00)
-64bit-Window

```
$# Created on Oct-17-2014 (08:42:21)
$#
## Renumber the parts
$#
geselect target part
geselect part add part 100002/0
renumber renumkind 270
renumber renumkind 170
renumber renumkind 134
renumber setbypart 98 1000000 1000000 100002
renumber keyword
renumber clearbypart
geselect clear
geselect target part
geselect part add part 200002/0
renumber renumkind 270
renumber renumkind 170
renumber renumkind 134
renumber setbypart 2000000 2000000 2000000 200002
renumber keyword
renumber clearbypart
geselect clear
geselect target part
geselect part add part 300002/0
renumber renumkind 270
renumber renumkind 170
renumber renumkind 134
renumber setbypart 3000000 3000000 3000000 300002
renumber keyword
renumber clearbypart
geselect clear
geselect target part
geselect part add part 400002/0
renumber renumkind 270
renumber renumkind 170
renumber renumkind 134
renumber setbypart 4000000 4000000 4000000 400002
renumber keyword
renumber clearbypart
geselect clear
geselect target part
geselect part add part 500002/0
renumber renumkind 270
```

```
renumber renumkind 170
renumber renumkind 134
renumber setbypart 5000000 5000000 5000000 500002
renumber keyword
renumber clearbypart
geselect clear
geselect target part
geselect part add part 600002/0
renumber renumkind 270
renumber renumkind 170
renumber renumkind 134
renumber setbypart 6000000 6000000 6000000 600002
renumber keyword
renumber clearbypart
geselect clear
geselect target part
geselect part add part 700002/0
renumber renumkind 270
renumber renumkind 170
renumber renumkind 134
renumber setbypart 7000000 7000000 7000000 700002
renumber keyword
renumber clearbypart
geselect clear
geselect target part
geselect part add part 800002/0
renumber renumkind 270
renumber renumkind 170
renumber renumkind 134
renumber setbypart 8000000 8000000 8000000 800002
renumber keyword
renumber clearbypart
geselect clear
geselect target part
geselect part add part 900002/0
renumber renumkind 270
renumber renumkind 170
renumber renumkind 134
renumber setbypart 9000000 9000000 9000000 900002
renumber keyword
renumber clearbypart
geselect clear
geselect target part
```

```

geselect part add part 20002/0
renumber renumkind 270
renumber renumkind 170
renumber renumkind 134
renumber setbypart 10000000 10000000 10000000 20002
renumber keyword
renumber clearbypart
geselect target part
geselect part add part 30002/0
renumber renumkind 270
renumber renumkind 170
renumber renumkind 134
renumber setbypart 11000000 11000000 11000000 30002
renumber keyword
renumber clearbypart
geselect clear
geselect target part
geselect part add part 40002/0
renumber renumkind 270
renumber renumkind 170
renumber renumkind 134
renumber setbypart 99 12000000 12000000 40002
renumber keyword
renumber clearbypart
geselect clear
geselect target part
geselect part add part 50002/0
renumber renumkind 270
renumber renumkind 170
renumber renumkind 134
renumber setbypart 13000000 13000000 13000000 50002
renumber keyword
renumber clearbypart
geselect clear
$#
$# Delete old parts
$#
partdata delete 100002 200002 300002 400002 500002 600002 700002 800002 900002 20002
30002 40002 50002
delement unrefn 0
*END

```

Materials20_13parts.cfile:

```
$# LS-PrePost command file created by LS-PrePost 4.2 (Beta) - 15Oct2014(08:00)
-64bit-Window
$# Created on Oct-17-2014 (08:42:21)
$#
$# DEfine Material Properties
$#
KEYWORD INPUT 98
*SECTION_SOLID_TITLE
Rigid Solid
$# secid elform aet
98 1 0
*END
keyword updatekind
SECTION_SOLID
KEYWORD INPUT 2000000
*SECTION_SOLID_TITLE
Rigid Solid
$# secid elform aet
2000000 1 0
*END
keyword updatekind
SECTION_SOLID
KEYWORD INPUT 3000000
*SECTION_SOLID_TITLE
Deformable Solid
$# secid elform aet
3000000 10 0
*END
keyword updatekind
SECTION_SOLID
KEYWORD INPUT 4000000
*SECTION_SOLID_TITLE
Rigid Solid
$# secid elform aet
4000000 1 0
*END
keyword updatekind
SECTION_SOLID
KEYWORD INPUT 5000000
*SECTION_SOLID_TITLE
Deformable Solid
$# secid elform aet
5000000 10 0
```

```
*END
keyword updatekind
SECTION_SOLID
KEYWORD INPUT 6000000
*SECTION_SOLID_TITLE
Deformable Solid
$# secid elform aet
 6000000 10 0
*END
keyword updatekind
SECTION_SOLID
KEYWORD INPUT 7000000
*SECTION_SOLID_TITLE
Deformable Solid
$# secid elform aet
 7000000 10 0
*END
keyword updatekind
SECTION_SOLID
KEYWORD INPUT 8000000
*SECTION_SOLID_TITLE
Deformable Solid
$# secid elform aet
 8000000 10 0
*END
keyword updatekind
SECTION_SOLID
KEYWORD INPUT 9000000
*SECTION_SOLID_TITLE
Deformable Solid
$# secid elform aet
 9000000 10 0
*END
keyword updatekind
SECTION_SOLID
KEYWORD INPUT 10000000
*SECTION_SOLID_TITLE
Deformable Solid
$# secid elform aet
 10000000 10 0
*END
keyword updatekind
SECTION_SOLID
```

```

KEYWORD INPUT 11000000
*SECTION_SOLID_TITLE
Deformable Solid
$# secid elform aet
 11000000 10 0
*END
keyword updatekind
SECTION_SOLID
KEYWORD INPUT 99
*SECTION_SOLID_TITLE
Rigid Solid
$# secid elform aet
 99 1 0
*END
keyword updatekind
SECTION_SOLID
KEYWORD INPUT 13000000
*SECTION_SOLID_TITLE
Deformable Solid
$# secid elform aet
 13000000 10 0
*END
keyword updatekind
SECTION_SOLID
$#
$# Import the materials database
$#
matdatabase readfile "C:\Users\team5\AutomationTests\BME432_matDB2014.k"
matdatabase get 2
matdatabase get 27
matdatabase get 29
matdatabase get 25
matdatabase get 24
matdatabase get 11
matdatabase get 23
KEYWORD INPUT 98
*PART
$# title
Slider Base
$# pid secid mid eosid hgid grav adpopt tmid
 98 98 1 0 0 0 0 0
*SECTION_SOLID_TITLE
Rigid Solid

```

```

$# secid elform aet
 98 1 0
*MAT_RIGID_TITLE
Aluminum (Rigid)
$# mid ro e pr n couple m alias
 1 2.7100E-3 70000.000 0.330000 0.000 0.000 0.000
$# cmo con1 con2
 0.000 0. 0.
$#lco or a1 a2 a3 v1 v2 v3
 0.000 0.000 0.000 0.000 0.000 0.000
*END
keyword updatekind
PART_PART
KEYWORD INPUT 2000000
*PART
$# title
Slider Nub
$# pid secid mid eosid hgid grav adpopt tmid
 2000000 2000000 1 0 0 0 0 0
*SECTION_SOLID_TITLE
Rigid Solid
$# secid elform aet
 2000000 1 0
*MAT_RIGID_TITLE
Aluminum (Rigid)
$# mid ro e pr n couple m alias
 1 2.7100E-3 70000.000 0.330000 0.000 0.000 0.000
$# cmo con1 con2
 0.000 0. 0.
$#lco or a1 a2 a3 v1 v2 v3
 0.000 0.000 0.000 0.000 0.000 0.000
*END
keyword updatekind
PART_PART
KEYWORD INPUT 3000000
*PART
$# title
Slider Spring
$# pid secid mid eosid hgid grav adpopt tmid
 3000000 3000000 7 0 0 0 0 0
*SECTION_SOLID_TITLE
Deformable Solid
$# secid elform aet

```

```

3000000      10      0
*MAT_OGDEN_RUBBER_TITLE
ABR Rubber (Visco)
$#  mid  ro   pr   n   nv   g   sigf
    7 0.0012500 0.499500      0      6  0.000  0.000
$#  mu1  mu2  mu3  mu4  mu5  mu6  mu7  mu8
0.6166000-0.0504300  0.000  0.000  0.000  0.000  0.000  0.000
$#  alpha1 alpha2 alpha3 alpha4 alpha5 alpha6 alpha7 alpha8
3.0197999-2.0293000  0.000  0.000  0.000  0.000  0.000  0.000
*END
keyword updatekind
PART_PART
KEYWORD INPUT 4000000
*PART
$#                               title
Bottom Plate
$#  pid  secid  mid  eosid  hgid  grav  adopt  tmid
  4000000 4000000      1      0      0      0      0      0
*SECTION_SOLID_TITLE
Rigid Solid
$#  secid  elform  aet
  4000000      1      0
*MAT_RIGID_TITLE
Aluminum (Rigid)
$#  mid  ro   e   pr   n   couple   m   alias
  1 2.7100E-3 70000.000 0.330000  0.000  0.000  0.000
$#  cmo  con1  con2
  0.000  0.  0.
$#lco or a1  a2  a3  v1  v2  v3
  0.000  0.000  0.000  0.000  0.000  0.000
*END
keyword updatekind
PART_PART
KEYWORD INPUT 5000000
*PART
$#                               title
Center Rod
$#  pid  secid  mid  eosid  hgid  grav  adopt  tmid
  5000000 5000000      5      0      0      0      0      0
*SECTION_SOLID_TITLE
Deformable Solid
$#  secid  elform  aet
  5000000      10      0

```

```

*MAT_OGDEN_RUBBER_TITLE
Chloroprene Rubber 25% Carbon (Visco)
$#  mid  ro   pr   n   nv   g   sigf
    5 0.0012500 0.499500    0    6  0.000  0.000
$#  mu1  mu2  mu3  mu4  mu5  mu6  mu7  mu8
  0.6143000  0.000  0.000  0.000  0.000  0.000  0.000  0.000
$#  alpha1 alpha2 alpha3 alpha4 alpha5 alpha6 alpha7 alpha8
  6.6901002  0.000  0.000  0.000  0.000  0.000  0.000  0.000
*END
keyword updatekind
PART_PART
KEYWORD INPUT 6000000
*PART
$#                               title
Rod 1
$#  pid  secid  mid  eosid  hgid  grav  adpopt  tmid
  6000000 6000000    5    0    0    0    0    0
*SECTION_SOLID_TITLE
Deformable Solid
$#  secid  elform  aet
  6000000    10    0
*MAT_OGDEN_RUBBER_TITLE
Chloroprene Rubber 25% Carbon (Visco)
$#  mid  ro   pr   n   nv   g   sigf
    5 0.0012500 0.499500    0    6  0.000  0.000
$#  mu1  mu2  mu3  mu4  mu5  mu6  mu7  mu8
  0.6143000  0.000  0.000  0.000  0.000  0.000  0.000  0.000
$#  alpha1 alpha2 alpha3 alpha4 alpha5 alpha6 alpha7 alpha8
  6.6901002  0.000  0.000  0.000  0.000  0.000  0.000  0.000
*END
keyword updatekind
PART_PART
KEYWORD INPUT 7000000
*PART
$#                               title
Rod 2
$#  pid  secid  mid  eosid  hgid  grav  adpopt  tmid
  7000000 7000000    5    0    0    0    0    0
*SECTION_SOLID_TITLE
Deformable Solid
$#  secid  elform  aet
  7000000    10    0
*MAT_OGDEN_RUBBER_TITLE

```

Chloroprene Rubber 25% Carbon (Visco)

\$#	mid	ro	pr	n	nv	g	sigf	
	5	0.0012500	0.499500	0	6	0.000	0.000	
\$#	mu1	mu2	mu3	mu4	mu5	mu6	mu7	mu8
	0.6143000	0.000	0.000	0.000	0.000	0.000	0.000	0.000
\$#	alpha1	alpha2	alpha3	alpha4	alpha5	alpha6	alpha7	alpha8
	6.6901002	0.000	0.000	0.000	0.000	0.000	0.000	0.000

*END

keyword updatekind

PART_PART

KEYWORD INPUT 8000000

*PART

\$#	title							
Rod 3								
\$#	pid	secid	mid	eosid	hgid	grav	adpopt	tmid
	8000000	8000000	5	0	0	0	0	0

*SECTION_SOLID_TITLE

Deformable Solid

\$#	secid	elform	aet	title						
	8000000	10	0							

*MAT_OGDEN_RUBBER_TITLE

Chloroprene Rubber 25% Carbon (Visco)

\$#	mid	ro	pr	n	nv	g	sigf	
	5	0.0012500	0.499500	0	6	0.000	0.000	
\$#	mu1	mu2	mu3	mu4	mu5	mu6	mu7	mu8
	0.6143000	0.000	0.000	0.000	0.000	0.000	0.000	0.000
\$#	alpha1	alpha2	alpha3	alpha4	alpha5	alpha6	alpha7	alpha8
	6.6901002	0.000	0.000	0.000	0.000	0.000	0.000	0.000

*END

keyword updatekind

PART_PART

KEYWORD INPUT 9000000

*PART

\$#	title							
Rod 4								
\$#	pid	secid	mid	eosid	hgid	grav	adpopt	tmid
	9000000	9000000	5	0	0	0	0	0

*SECTION_SOLID_TITLE

Deformable Solid

\$#	secid	elform	aet	title						
	9000000	10	0							

*MAT_OGDEN_RUBBER_TITLE

Chloroprene Rubber 25% Carbon (Visco)

```

$#  mid  ro   pr   n   nv   g   sigf
    5 0.0012500 0.499500    0    6  0.000  0.000
$#  mu1  mu2  mu3  mu4  mu5  mu6  mu7  mu8
  0.6143000  0.000  0.000  0.000  0.000  0.000  0.000  0.000
$# alpha1 alpha2 alpha3 alpha4 alpha5 alpha6 alpha7 alpha8
  6.6901002  0.000  0.000  0.000  0.000  0.000  0.000  0.000
*END
keyword updatekind
PART_PART
KEYWORD INPUT 10000000
*PART
$#                                     title
Rod 5
$#  pid  secid  mid  eosid  hgid  grav  adpopt  tmid
  10000000 10000000    5    0    0    0    0    0
*SECTION_SOLID_TITLE
Deformable Solid
$#  secid  elform  aet
  10000000    10    0
*MAT_OGDEN_RUBBER_TITLE
Chloroprene Rubber 25% Carbon (Visco)
$#  mid  ro   pr   n   nv   g   sigf
    5 0.0012500 0.499500    0    6  0.000  0.000
$#  mu1  mu2  mu3  mu4  mu5  mu6  mu7  mu8
  0.6143000  0.000  0.000  0.000  0.000  0.000  0.000  0.000
$# alpha1 alpha2 alpha3 alpha4 alpha5 alpha6 alpha7 alpha8
  6.6901002  0.000  0.000  0.000  0.000  0.000  0.000  0.000
*END
keyword updatekind
PART_PART
KEYWORD INPUT 11000000
*PART
$#                                     title
Rod 6
$#  pid  secid  mid  eosid  hgid  grav  adpopt  tmid
  11000000 11000000    5    0    0    0    0    0
*SECTION_SOLID_TITLE
Deformable Solid
$#  secid  elform  aet
  11000000    10    0
*MAT_OGDEN_RUBBER_TITLE
Chloroprene Rubber 25% Carbon (Visco)
$#  mid  ro   pr   n   nv   g   sigf

```

```

      5 0.0012500 0.499500      0      6  0.000  0.000
$#  mu1    mu2    mu3    mu4    mu5    mu6    mu7    mu8
  0.6143000  0.000  0.000  0.000  0.000  0.000  0.000  0.000
$#  alpha1  alpha2  alpha3  alpha4  alpha5  alpha6  alpha7  alpha8
  6.6901002  0.000  0.000  0.000  0.000  0.000  0.000  0.000
*END
keyword updatekind
PART_PART
KEYWORD INPUT 99
*PART
$#                               title
Top Plate
$#  pid    secid    mid    eosid    hgid    grav    adpopt    tmid
  99      99      1      0      0      0      0      0
*SECTION_SOLID_TITLE
Rigid Solid
$#  secid  elform  aet
  99      1      0
*MAT_RIGID_TITLE
Aluminum (Rigid)
$#  mid    ro     e     pr     n  couple      m  alias
  1 2.7100E-3 70000.000 0.330000  0.000  0.000  0.000
$#  cmo    con1    con2
  0.000  0.    0.
$#lco or a1    a2    a3    v1    v2    v3
  0.000  0.000  0.000  0.000  0.000  0.000
*END
keyword updatekind
PART_PART
KEYWORD INPUT 13000000
*PART
$#                               title
Thin Bumper
$#  pid    secid    mid    eosid    hgid    grav    adpopt    tmid
  13000000 13000000  5      0      0      0      0      0
*SECTION_SOLID_TITLE
Deformable Solid
$#  secid  elform  aet
  13000000  10      0
*MAT_OGDEN_RUBBER_TITLE
Chloroprene Rubber 25% Carbon (Visco)
$#  mid    ro     pr     n     nv    g     sigf
  5 0.0012500 0.499500      0      6  0.000  0.000

```

```
$# mu1 mu2 mu3 mu4 mu5 mu6 mu7 mu8
0.6143000 0.000 0.000 0.000 0.000 0.000 0.000 0.000
$# alpha1 alpha2 alpha3 alpha4 alpha5 alpha6 alpha7 alpha8
6.6901002 0.000 0.000 0.000 0.000 0.000 0.000 0.000
*END
```